

PREDICTION METHOD FOR GRASS EROSION  
ON LEVEES BY WAVE OVERTOPPING

*Linking models to experiments*

*MSc Thesis*  
P.M. VAN DIJK

Design: © Elma Hogeboom 2021 for GreenThesis ([www.greenthesis.nl](http://www.greenthesis.nl))  
Photo location: Vechtdijk experiments, January 2021.



Proudly printed on 100% recycled paper.  
A tree was planted for every printed copy of this thesis.

# Prediction method for grass erosion on levees by wave overtopping

## *Linking models to experiments*

By

Ing. P.M. van Dijk

in partial fulfilment of the requirements for the degree of

**Master of Science**

in Civil Engineering

at the Delft University of Technology,

to be defended publicly on Tuesday August 31, 2021 at 13:00.

Committee chair:	Dr. Ir. J.P. Aguilar-López,	TU Delft
Thesis committee:	Ir. S.J.H. Rikkert,	TU Delft
	Dr. Ir. M. van Damme,	TU Delft
	Dr. Ir. J.J. Warmink	University of Twente
	Ing. W. Zomer MSc,	BZ Ingenieurs & Managers

Student number: 4396189

An electronic version of this thesis is available at <http://repository.tudelft.nl/>.



## Preface

In front of you is my thesis on grass erosion due to wave overtopping on levees with grass cover. In my curriculum of the master Hydraulic Engineering, this subject was only briefly covered in the course Flood Defences, but it stuck with me. When the opportunity arose to dive further into this as a thesis topic, I had to take it. This thesis is all about wave overtopping experiments and the use of several models to reconstruct what happened during the experiments, leading to a method to predict when and where erosion -due to wave overtopping- causes failure of the grass cover.

This thesis is the final chord of my student career, a career that started at Saxion Hogeschool Enschede with the bachelors of applied sciences in Civil Engineering and Business Administration. Next, I started at the TU Delft with a pre-master, where after I moved on to the Civil Engineering Master Hydraulic Engineering. I value the mix of applied and academic studies because it makes me sensitive for practical and theoretical considerations. During this thesis work, it was a constant struggle to balance between theoretical research aspects and the practical diversity of the wave overtopping experiments. This struggle and balance made it challenging as well as interesting.

I would like to thank the members of my committee for their drive and guidance during my project. Especially Stephan, for the numerous sessions where he heard me out and helped to make sense out of the progress I made between the sessions. I am also thankful for the contact I had with persons in the field during this thesis; Roy Mom from Infram for welcoming me during the wave overtopping experiment at the Vechtdijk and supplying experiment data; Jentsje van der Meer for welcoming me in his office and supplying simulator data; Vera van Bergeijk from UTwente and Luc Ponsioen from Aveco de Bondt for sparring about grass erosion and support on their models; David Tax from TUDelft for discussing data-driven applications; Frans van den Berg from Deltares for discussing animal activity in levees; fellow levee-enthusiast and friend André Koelewijn for discussing numerous things, including grass erosion. I also want to thank Elma Hogeboom from Green Thesis for her cover design.

Friends and family supported me during my study-career, I am very grateful for all these persons in my life and the opportunities I was able to exploit. Finally, special thanks goes out to my wife Ingrid.

I hope you enjoy reading this thesis.

P.M. (Peter) van Dijk  
ORCID iD 0000-0002-8920-6659

31 August 2021, Arnhem

Cover design and printing by GreenThesis ([www.greenthesis.nl](http://www.greenthesis.nl))





## Abstract

Large areas of the world are protected by flood defence systems. A common part of flood defence systems is a levee with grass cover, with the primary function to protect hinterland against floods. Wave-overtopping might lead to erosion of the grass cover, followed by erosion of the inner slope and potentially levee breaching. The wave overtopping simulator (WOS) was developed for full-scale and in-situ testing of the erosional resistance of levees against wave overtopping. The first experiment with this simulator was carried out in 2007 and more followed. However, the data gathered during these overtopping experiments has always been considered on individual experiment scale or in small subsets, exception being the Cumulative Overload method. The experiments proved to be difficult to reproduce, seemingly identical experiments gave different results. The objective of this thesis is to combine WOS data and multiple grass erosion models to make a prediction for the failure of the grass cover. Key features that determine the prediction of failure are the location and moment of failure. Therefore, these are included in the main research question, which is identified as: *How can grass erosion models and WOS experiment data be combined in a new method to generate a prediction of the moment and location of the grass cover failure due to wave overtopping?*

A literature study on grass erosion and grass erosion provides the basis for modelling grass erosion, a review of combination techniques gives insight in combining results for a prediction. A selection of models is discussed and used for setting up a prediction method. These include three flow-based models which are semi-realistic simplified representations and time-independent over a single overtopping event: Cumulative Overload Method, Analytical Grass Erosion Model and Dean Stream Power. These models are, where required, adjusted to model grass cover failure and to comply with identical hydrodynamic input. A fourth model, the Wave Impact Approach, is an impact-based approach. Each model is calibrated on each WOS experiment, creating a set of calibrated models, which function as the set of predictors. The number of predictors equals the number of models times the number of experiments. During calibration, the moment of failure has been traced back using the control list of the WOS, and vice-versa, resulting in a moment during the experiment at which the grass cover failed. Detailed review of all factual reports on WOS experiments and the nature of the grass erosion models highlighted the need for a location-dependent resistance parameter to determine the location of failure. Therefore, calibration was based on a location-dependent resistance parameter; critical flow velocity for the flow-based models and critical pressure for the impact based model. This set of predictors has been used to create a set of predictions for each of the five validation experiments, input being the geometry, loading and initial condition of the slope. The initial condition given by a registration of anomalies to the average grass cover. Failure is determined by vote and averaging.

After validation, none of the final predictions proved to be fully correct. Meaning that none of the final predictions correctly indicated the location and moment of the first grass cover failure. Despite this, in four of the five validations at least one correct failure location was indicated when considering the specific anomalies. The main shortcoming is concluded to be the prediction of number of waves until grass cover failure.

Based on this research and given a certain average grass cover quality, it is concluded that the resistance against grass erosion by wave overtopping is described by resistance against erosion of anomalies. For at least 22 of 28 sections in the dataset, grass cover failure occurred at an anomaly of the average grass cover. No grass cover failures occurred related to the average grass quality. Especially mole activity showed a significant 46% decrease in the averaged calibrated critical flow velocity with relative to that for the average grass cover. This leads to the conclusion that design and safety assessments should include conditions other than the average grass quality. For future research a method is recommended that divides mole activity into classes, based on certain characteristics. Each class distinguishable by unique combination of properties and assigned a resistance against erosion. For design, the probability of occurrence of each class must be determined and combined with the corresponding influence on the resistance against erosion. For assessment, an inventory or representative sample of animal activity must be available to assess if the occurrences of animal activity are within the design requirements.



# Table of contents

Preface .....	v
Abstract .....	vii
1 Introduction .....	1
1.1 Problem .....	2
1.2 Objective.....	3
1.3 Research method.....	4
1.4 Data.....	5
2 Literature & background information .....	7
2.1 Grass erosion by wave overtopping.....	7
2.2 Grass erosion model overview .....	9
2.3 Model comparison .....	13
3 Prediction method.....	16
3.1 Outline.....	16
3.2 Set up of the prediction method .....	18
3.3 Application of the prediction method .....	25
4 Results.....	27
4.1 Calibration results.....	27
4.2 Validation results .....	31
5 Discussion.....	41
6 Conclusion and Recommendations .....	43
6.1 Conclusions .....	43
6.2 Recommendations .....	45
References.....	47
Appendix A – Overview of WOS experiments .....	49
Appendix B – Grass erosion model decompositions .....	54
Appendix C – Technical method diagram .....	59
Appendix D – Influence of wide crests and validity of the friction factor.....	61
Appendix E – WIA realizations .....	63
Appendix F – COM, AGEM & DSP calibrations.....	68
Appendix G – Technical memo of validation predictions .....	95
Appendix H – Critical velocity registration .....	107

# 1 Introduction

Large areas of the world are protected by flood defence systems. Flood safety standards are often assigned to flood defences by a government to keep flood risk within acceptable levels. Accurate assessments of levees are crucial to determine if these flood safety standards are met. Inaccurate assessments could lead to either over-engineering with high costs or worse: unexpected and premature failure of levees with potentially catastrophic damage. For levees with grass cover, one of the failure mechanisms is external erosion at the crest and landside slope (CIRIA, 2013; van der Meer et al., 2012). The aftermath of Hurricane Katrina in USA has shown the vulnerability of levee landside slopes to external erosion (US Army Corps of Engineers, 2006), Figure 1 is an example of a levee that nearly breached.



*Figure 1 Example of the vulnerability of levee landside slopes to external erosion, from the New Orleans East Basin (USACE, 2006).*

Over the years, external erosion of grass cover has been subject of research and experiments (Hoffmans, 2014; Hoven et al., 2009). The Polder2C's project is the latest to include full-scale destructive levee-tests, amongst which are grass erosion tests by wave overtopping. In the context of the wave overtopping experiments, several existing grass erosion models will be used to predict grass erosion due to overtopping. Experiment results will be used for validation of these predictions (Rikkert et al., 2020). For the full scope of the Polder2C's project, visit [www.polder2cs.eu](http://www.polder2cs.eu).

Another example of a previous large scale levee-test is the IJkdijk project, from 2006 till 2016. During one of the IJkdijk tests, the focus was emphatically on full service levee monitoring systems, not explicitly on several failure mechanisms (de Vries et al., 2013). The IJkdijk project comprised several failure mechanisms, but not erosion at the landside slope by wave overtopping. Despite this, inspirational findings emerged. After the tests, a promising result was obtained by a visualisation system based on data-driven models, which was suggested by Siemens for this project. This visualisation system combined several data-driven models and evaluated these real time, adjusting when necessary. This inspired to link grass erosion models to a wide scope of wave overtopping experiments.

Now focusing on grass erosion, experiments are relevant in understanding the failure mechanism and predicting the strength of a grass cover on a levee. For example, during experiments in the Wijmeers-II polder the observation was that the overtopping waves did initiate damage but overflow did not, indicating a difference in these processes (Van Damme et al., 2016). Grass erosion tests are carried out at different scales: on small scale laboratory tests in flumes or in small jet-erosion set-ups, to experimental set-ups in larger wave flumes or full-scale in-situ tests on real levees. All these experiments contribute in setting up models and validating these models. Some use a maximum overtopping volume (van der Meer et al., 2018) and others take the contributions of every overtopping wave in consideration, examples are: Cumulative Overload Method (COM) (van der Meer et al., 2012), Analytical Grass Erosion Model (AGEM) (van Bergeijk, et al., 2019) and Wave Impact Approach (WIA) (Ponsioen, 2016). Each model has its strengths, for example some are easily applicable and others give more information about the damage. Each model differs in how grass erosion is modelled.

Erosion in general is difficult to model: in certain applications it can be modelled quite well using mass-balance type of equations (Exner-equation), but the exact process is difficult to recreate (Bomers et al.,

2018). Factors contributing to this difficulty are turbulent flow, complicated interaction between flow and particles, small inhomogeneities that trigger large effects, measurement errors and changing geometry during erosion. For modelling erosion on levees, a general mass-balance model-type lacks precision. Precision that is less required for bed material in rivers for example; in rivers, it is about a large order of magnitude, on levees, only a few cubic decimetres are the difference between failure and success. Therefore, it is important to distinguish the onset of damage and the growth of damage when describing erosion of levees. Also, there is a difference between non-coherent soil and coherent soil (clay), with or without a root structure (grass sods) and the type of core material.

In order to understand the erosional process better, there is ongoing research on the hydrodynamics of flow by overtopping waves (Bomers et al., 2018; van Bergeijk, Warmink, van Gent, et al., 2019). Recent progress has been made in modelling the wave overtopping flow by van Bergeijk et al. (2020). With a numerical model in OpenFOAM, the velocities and stresses on the cover can be modelled for every overtopping wave. These velocities and stresses are considered to be the main loading parameters that cause grass erosion. Even though this is a sophisticated and elegant model, it is not perfect. The model is validated on measurements from experiments, but measuring overtopping flow is highly sensitive to errors. And the model demands a lot computing power, the computational time for a single wave calculation on a modern computer (i7-9700 CPU) takes 5 to 20 minutes. For a storm of 400 waves, it takes 1.5 to 5.5 days to compute flow and stress simulations. This is even not yet a grass erosion model, but a hydrodynamic model on which a grass erosion model can be applied. Bomers et al. (2018) encountered this same problem and worked around this by discretizing the volume distribution into five representative overtopping volumes to simulate the erosion during a storm.

In a recent article of Warmink et al. (2020), a by-product was the finding that the critical flow velocities of two models are different for the same circumstances. In this instance Warmink et al. (2020) referred to the Cumulative Overtopping Method and the Analytical Grass Erosion Model. Both models have a certain parameter that represented the critical flow velocity, but since both are different, this suggests that this is a model parameter and not a physical property of the grass cover.

### 1.1 Problem

Because of the tricky nature of the erosional process, several methods have been developed to model grass erosion. Models can have different starting points and have often only been validated on few experiments. In recent years, many wave overtopping experiments have taken place and over time models have been developed, but not all of them have been updated with new experimental data. A problem, or knowledge gap, that can be identified is the lack of linking models to experiments, with the aim to extract more knowledge from these experiments, see Figure 2. To the best of the authors knowledge, these models and experiments have not been combined to improve predictions on the timing and location of damage initiation during a sequence of wave overtopping events.

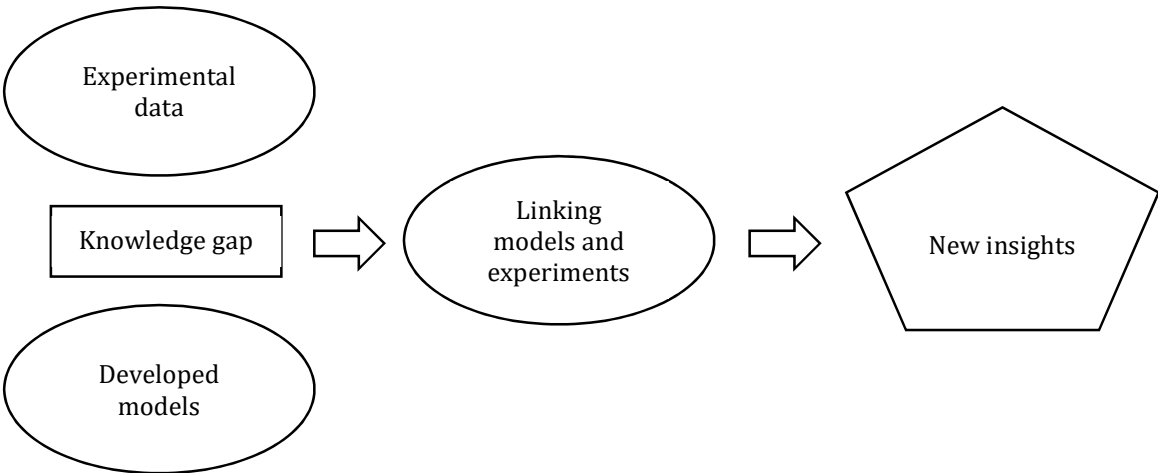


Figure 2 The knowledge gap is identified as the lack of linking models to all available experimental data.

## 1.2 Objective

The main objective of this thesis is to combine wave overtopping simulator (WOS) data and multiple grass erosion models to make a prediction of the failure of the grass cover, induced by WOS induced wave overtopping on a levee slope. (Figure 3) Instead of thoroughly modelling the computational extensive hydrodynamics, the goal is to work computationally light and give a quick prediction of the moment and location of the failure of the grass cover. Damage growth and changing geometry falls outside the scope of this research. The intention is to apply multiple grass erosion models to WOS experiments in such a way that diverse and calibrated models form a set of predictors. In the process, an imported by-catch are lessons learned from linking WOS data to several grass erosion models and comparing results.

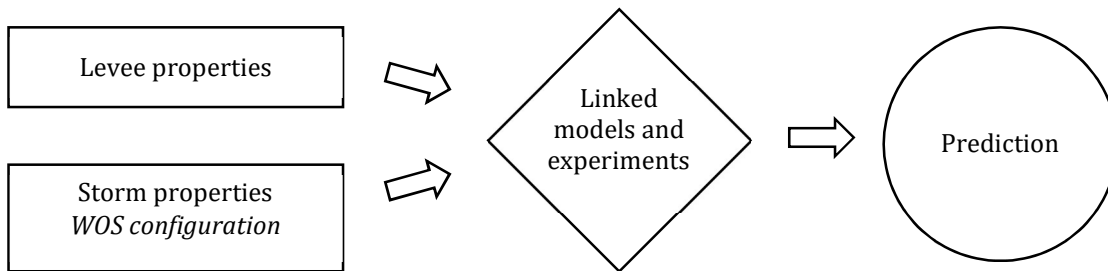


Figure 3 Diagram of the objective. With levee- and storm input from the slope being predicted for, apply linked models and experiments to obtain a prediction for the failure of the grass cover.

To reach this objective, the main research question to be answered is defined as follows:

*“How can grass erosion models and WOS experiment data be combined in a prediction method to generate a prediction of the moment and location of the grass cover failure due to wave overtopping?”*

The main research question is split into several sub questions, these need to be answered in the process towards answering the main research question.

- i) *“Which grass erosion models can be of value in the prediction method?”*
- ii) *“Which WOS experiment data can be used for calibrating and validating?”*
- iii) *“What ways are available to combine predictions of single models?”*
- iv) *“How does the prediction method perform in a prediction case?”*

### 1.3 Research method

Figure 4 represents the main aspects and phases of this thesis, as described in this section. In the following, the aspects a. until k. in Figure 4 will be mentioned and referred to.

The first part of the thesis consists of literature study on a) grass erosion models and on b) grass erosion.

Next is the preparation phase, in which all preparatory work has been identified, work needed to construct the code for the calibrations. c) The grass erosion models that need to be implemented in the new method, have been prepared and integrated in Python code. e) The outputs of these grass erosion models have been constructed in a format such that these are uniform (comparable), and contain both information of the location and the moment of grass cover failure, provided failure occurred. For calibrating and testing purposes, WOS simulator data has been d) gathered and f) prepared. The prepared WOS data consists of the input parameters of the grass erosion models and the registration of anomalies with respect to the average grass cover. The following preparations were needed; format the input parameters, shape the damage registrations in a comparable format with respect to the model output format and formulate damage threshold criterions. Next, h) the models were calibrated on the gathered data. The calibrations were completed with an analyses of the performances of the calibrated models. The final aspect of the preparation phase was g) to set up a combination method for implementation in the prediction method to combine single model predictions to make a final prediction.

Next is the development phase, i) constructing code for the prediction method and also j) testing different combination methods.

The last part is k) to validate the prediction method on un-used experiment data and analyse the results.

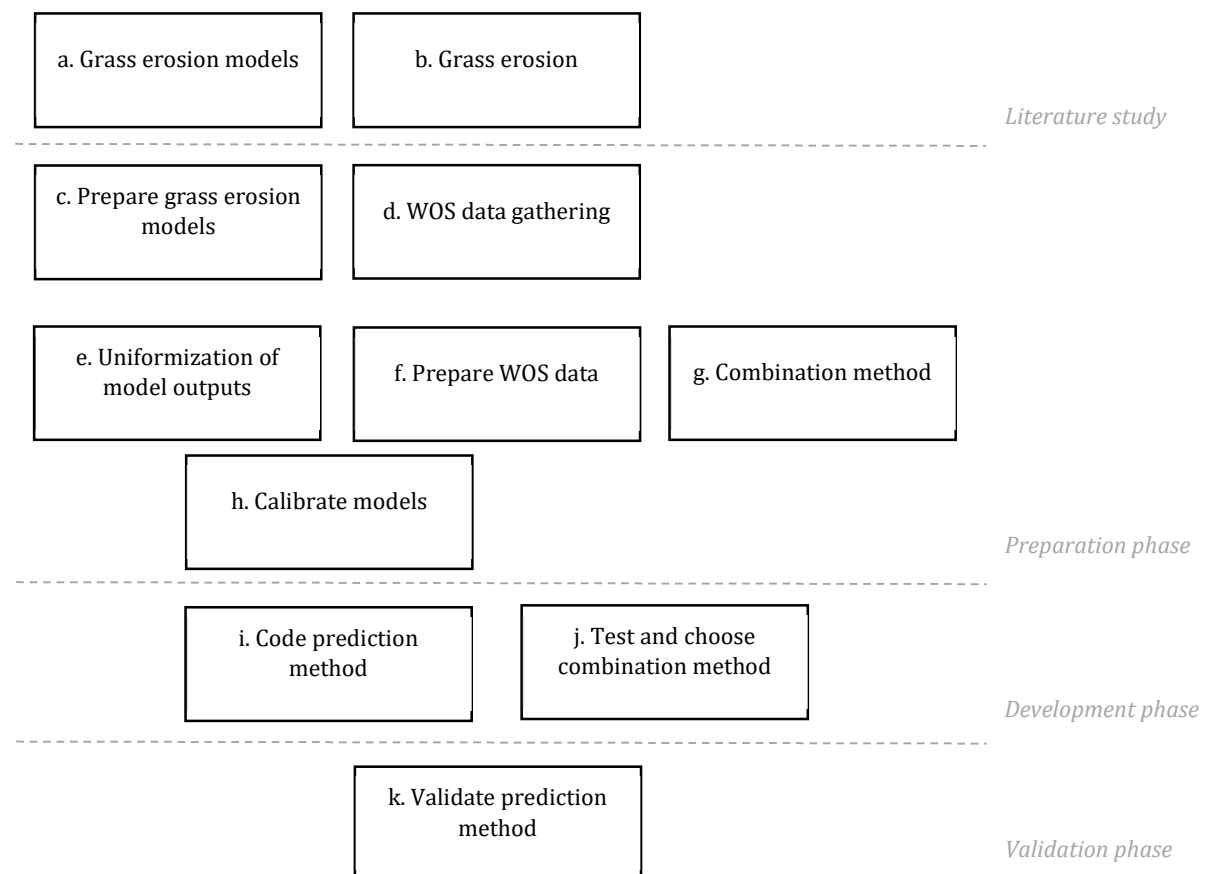


Figure 4 Thesis phases

## 1.4 Data

Data was required for designing, calibration, testing and validation of the prediction method. The data was retrieved from experiments with a wave overtopping simulator which were similar and comparable in configuration. In contrast: outcomes of flume tests or small scale tests would require more extensive manipulation to become similar since these tests only partly model a levee and can include scaling effects. This choice for wave overtopping simulator experiments was made because this is “a device to perform destructive tests on inner slopes of real dikes in order to establish the erosion resistance against overtopping waves from severe storms” (van der Meer, Schrijver, et al., 2010). The principle and configuration of this device is discussed in the first part of this section. After this, an overview of the relevant experiments is given. Next, the preparation of the data is discussed.

### 1.4.1 Wave overtopping simulator

The principle of the wave overtopping simulator is to reproduce the sequence of overtopping waves during an entire storm event for a test section. This can be done because the process of wave overtopping is known (van der Meer et al., 2018) and the wave overtopping simulator is designed to simulate this process without the need of wave generation and wave attack on the levee. During experiments the velocity- and flow depth profile of individual waves are replicated, see Figure 5.

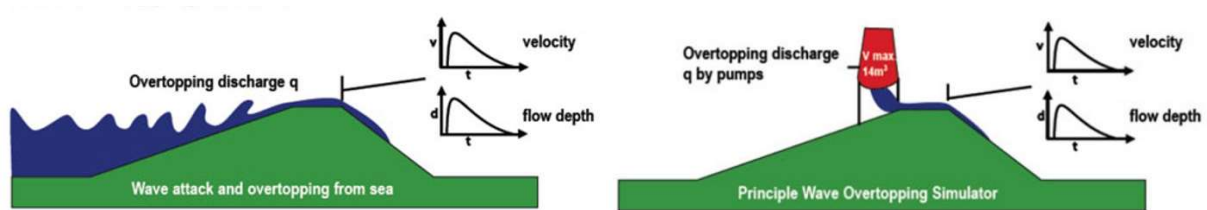


Figure 5 Principle of the wave overtopping simulator, [www.vandermeerconsulting.nl](http://www.vandermeerconsulting.nl) (2020)

The configuration of wave overtopping during experiments has been similar over the years, Figure 6. A four-meter-wide section of levee inner slope is selected, from crest to toe with constant width in the direction of the dike. The simulator is located on the crest, the distance of the outflow to the outer crest line may differ from site to site. The pump(s) provide water, via pipes, to the high level mobile box. Over the years a preference has been developed for a certain type of pump, which can be regulated from the control unit. Clear differences are notable in the placement and type of observation and control unit. Also the type and extent of measurement and monitoring equipment may differ per experiment location; constant factor over the years are photographic inspections.



Figure 6 Wave Overtopping Simulator in deployment during a field visit in January 2021 on the Vechtdijk, Zwolle (NL)

## 1.4.2 Experiments

This section gives a listing of all known wave overtopping experiments to date. An overview with general properties is attached in Appendix A – Overview of WOS experiments. All locations are listed in Table 1 in the first column. For each location one or more section(s) are tested using the WOS. These sections have been assigned identifiers and listed in the second column. Two-letter combinations identify the location. The digit identifies the section at the location. The third column lists all relevant references to reports/publications concerning the experiments.

<b>Locations</b>	<b>Section ID's</b>	<b>Reference</b>
Delfzijl, Groningen, 2007	De1, De2, De3	(van Hoven et al., 2007)
Boonweg, Friesland, 2008	Bo1, Bo2, Bo3, Bo4	(Bakker et al., 2008a)
St Philipsland, Zeeland, 2008	Sp1	(Bakker et al., 2008b)
Kattendijke, Zeeland, 2008	Ka1, Ka2	(Bakker et al., 2008b)
Afsluitdijk, 2009	Af1, Af2, Af3	(Bakker et al., 2009)
Vechtdijk, Overijssel 2010	Ve1, Ve2, Ve3, Ve4	(Bakker et al., 2010)
Tielrode/Antwerp, 2010	Ti1, Ti2, Ti3, Ti4	(Peeters et al., 2012; Steendam, 2011)
Vietnam, 2010	n/a *	(van der Meer, Bernardini, et al., 2010)
Tholen, Zeeland, 2011	Th1, Th2, Th3, Th4	(Bakker et al., 2011)
Nijmegen, Gelderland, 2013	Ni1, Ni2, Ni3	(Bakker et al., 2013)
Millingen, Gelderland, 2013	Mi1, Mi2	(Bakker et al., 2013)
Wijmeers-II, 2015	Wi1, Wi2	(Bakker & Mom, 2015; Ponsioen & Damme, 2016)
Singapore, 2020	n/a *	(van der Meer et al., 2020)
Vechtdijk, 2021	n/a *	n/a **

*Table 1 Overview of wave overtopping simulator experiments \*)These sections are not included in this thesis \*\*)In progress at the time of writing*

In the context of this thesis all experiments in the Netherlands and Belgium up to and including the year 2015 are considered. The experiments in Vietnam and Singapore are excluded since these vary significantly from those in the Netherlands and Belgium, for example in vegetation type. The time line of the experiments on the Vechtdijk in 2021 coincided with the time line of this thesis research, therefore these experiments could not be included.

The prediction method requires test data and validation data, this is implied in Figure 4. In the early stages of the research, a selection of experiments is ignored, these experiments are used for the validation of the prediction method. The remainder is available for the design, calibration and testing of the new method. After the prediction method has been validated, the method can be completed to include the entire set of experiments. The placement of experiments in the test or validation set is done such that the author's prejudice is not significantly influenced. This is achieved by refraining from (detailed) review of the experiments in the validation set.

The five validation sections are:

- Bo3 Boonweg 2008 section 3
- Af2 Afsluitdijk 2009 section 2
- Ve4 Vechtdijk 2010 section 4
- Ti1 Tielrode 2010 section 1
- Th4 Tholen 2011 section 4

## 1.4.3 Data preparation

The data is collected in the form of factual reports of the experiments and control lists of the WOS. The factual reports give information on the experiment, e.g.: geometry, initial conditions and photographic records of experiments. The control lists of the WOS give an exact description of the overtopping volumes that loaded the levee during the experiments (van Dijk, 2021). Additional information has been retrieved from contacts at Infram, van der Meer consulting and HIC Vlaanderen. This mainly concerns missing appendices from factual reports.

The data is preparation by extracting relevant levee properties, load properties, the course of the experiment and deviations from the intended control lists.

## 2 Literature & background information

This chapter covers grass erosion by wave overtopping. The first section covers the role of grass erosion by overtopping waves in the breaching process of levees, where the second section shows ways to model this type of grass erosion.

The role of wave overtopping in flood safety engineering is not limited to levees, all parts of a flood defence system may be prone to wave overtopping loads. This thesis focusses on the interaction of the overtopping wave with the grass cover on the landward slope of a levee, not on other structures nor how waves cause wave overtopping. More background information with respect to wave overtopping can be found in the EurOtop manual on wave overtopping (van der Meer et al., 2018).

### 2.1 Grass erosion by wave overtopping

Several failure mechanisms for levees can be distinguished. The International Levee Handbook (ILH) (CIRIA, 2013) names external erosion, internal erosion and instability. Jonkman et al. (2018) are more elaborate in differentiating failure mechanisms, see Figure 7. In both examples wave overtopping is included, explicitly by Jonkman et al. (2018) and implicitly in the ILH where wave overtopping is included as part of the external erosion.

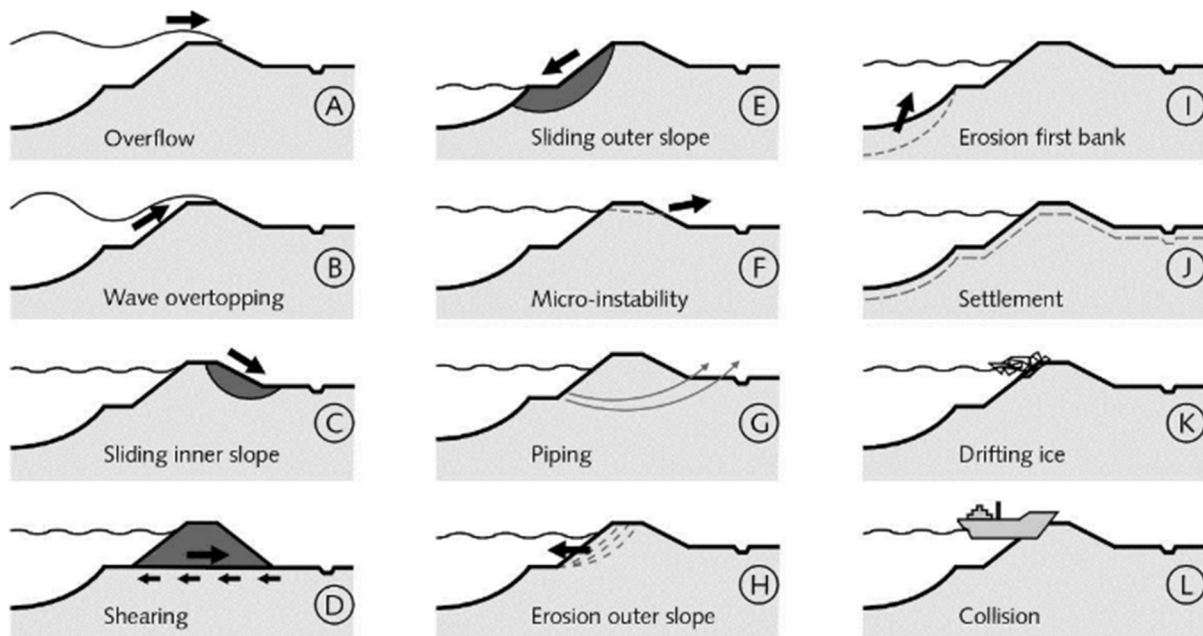


Figure 7 Schematic overview of the most relevant failure mechanisms of flood defences. (source: Flood Defence Lecture notes (Jonkman et al., 2018))

In the process of levee failure, i.e. breach, some failure criterion has to be reached to speak of a breach: one overtopping wave or a small instable section doesn't automatically result in levee failure. Before a levee breach causes a flood a certain criterion has to be reached. In the Netherlands this criterion is defined as the situation where a same-digit zip code has an average water depth of 0.2 meter. In the process of breaching of a levee by wave overtopping, D'Eliso (2007) defined six phases. Grass erosion by wave overtopping is the first phase, as long as the grass cover holds, the process will not continue to the next phase and the levee will not fail due to wave overtopping. Exceptions may be that the wave overtopping facilitates macro instability or other mechanisms. If the grass cover fails, the remaining phases lead from clay (cover) erosion to a fully formed breach in equilibrium-state. The phases described by D'Eliso are tailored to a sand core levee, this is important to consider since clay core dikes will react different in certain phases. Mainly, clay core levees are likely to have more residual strength against erosion when the cover has eroded, whereas sand core dikes are highly erodible after the cover has failed since sand is not cohesive. However, a highly erosion resistant layer has been detected during WOS experiments on sand levees with grass cover. A soil specialist was consulted; this layer is likely to be

'interne slemp' but this is to be further investigated. This phenomenon occurs when small (silt) particles in a certain highly saturated sand layer are suspended and create a layer of low permeability on which flowing water has a low erosional grip, see Figure 8. Consequently, this phenomena increases the resistance against erosion significantly.



Figure 8 "Interne slemp" at the Vechtdijk, 2021. Left: Location of erosion resistant layer. Right: Material in this layer.

Study of the factual reports, references in Table 1, show that erosion of the grass cover occurs in different ways. It is common for the first (small) waves to wash away loose material and debris. Next to this, the grass leaves are folded over, this flattens the surface and the grass leaves act as a blanket, covering small bare spots. The material close to the initial surface is eroded away relatively easy, the material inside the root structure gives more erosional resistance. From here on, two failure-tracks are identified.

- The first is the track where the grass cover is homogeneous (or constant) to some extent, the particles inside the root structure are continuously washed away, until grass sods are washed away because of the lack of anchoring by the root in the eroded soil layer. Then the grass cover is likely to be rolled up.
- The second track are the cases where the grass cover is compromised in some way and to some extent. When this is the case, the grass sods are locally poorly anchored in the soil and can be washed away with less load than the uncompromised grass cover. Examples are pavers at small depth (10cm) of the initial surface, extensive mole activity or some kind of breach of the clay layer exposing the sand cover. The latter example does not directly influence the anchoring of the grass sod roots, but this undermines the stability of the clay layer and implicitly the anchoring of the grass cover.

To illustrate the anchoring of grass sods, Figure 9 shows the extent of influence (a) the root structure of a grass clump (b) has on the exposed root system when pulling in the direction of the flow, order of magnitude of the radius is 20 centimetres. This example is purely illustrative and found on the Vechtdijk which is a sand levee with grass cover.

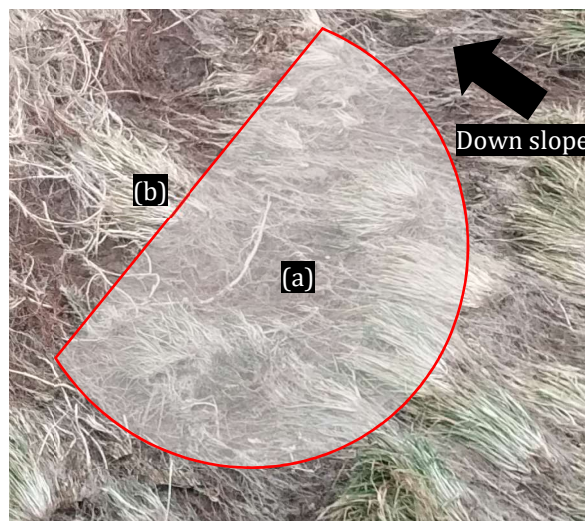


Figure 9 Area of influence of root structure, Vechtdijk, 2021. Order of magnitude of the radius is 20 centimetres.

In this thesis the emphasis is on the failure of the grass cover, the first phase defined by D'Eliso (2007). This is chosen because the grass cover is the first line of defence against levee failure by external erosion due to wave overtopping, and geometric changes are limited in the phase to the thickness of the grass cover layer. For clarity, grass cover failure is not similar to losing the water retaining function of a levee. To qualify the extent of damage to the grass cover some damage criterions have been defined.

- No damage: no significant changes, other than washing of debris and leaves folding.
- Development: ongoing development of damage.
- Failure: the grass cover is eroded or core material is exposed.

### 2.1.1 Contributing factors

The contributing factors found in the study of the factual reports are divided by the property that they either influence the strength or the load. This division can be ambiguous, e.g. does an irregularity that influences the flow reduce the strength or increase the load? In the division below, the choice is made to consider additions to- or irregularities on the slope as factors that influence the strength.

#### Strength factors

- Grass cover - Root structure (grass tensile tests, predictions by Andre van Hoven)
- Grass cover - leaves
- Soil material and accompanying properties, mainly cohesion.
- Structural elements; e.g. roads, (semi-) pavement, walls, stairs.
- Anomalies to the cover; e.g. animal activity and local irregularities
- Internal slump and similar (possibly unknown) phenomena
- Outliers, e.g. former post-hole filled with different material

#### Load factors

During a storm (simulation) the slope surface is loaded by a certain quantity of overtopping waves in an irregular sequence. The loading mechanism is driven by a certain overtopping wave, where the volume is the main factor of interest but also overtopping period and flow depth. Several factors originating from this can be distinguished. Some variant of velocity of the water interacting with the surface is a prime loading factor, frequently used in models (e.g.: COM, AGEM, DSP). Ways of quantifying the velocity are wave front velocity, depth-dependent velocity, depth-averaged velocity and terminal velocity. Other factors that determine the extent of loading are water depth, turbulence, bed roughness/friction and geometric changes. Another contributing factor that has been distinguished is the wave impact at reattachment point. Then flow reattaches when a wave volume, passes over the crest and does not follow the transition to the slope, instead the flow detaches and starts accelerating in the downward vertical direction until the flow reattaches with the slope, causing an impact on the slope. Most load factors are linked to large extent to the geometry of the levee, incorporating the crest, slope, roughness and transitions.

## 2.2 Grass erosion model overview

The first effort to model grass erosion by wave overtopping used mean overtopping discharges. These originated from the awareness of the risks caused by wave overtopping but a lack of knowledge of this phenomena at the time. Mean overtopping discharges give little information about the loading and appear to be quite conservative (van der Meer, Bernardini, et al., 2010). Over the years, research has enlarged the knowledge on the phenomena significantly. Laboratory and in-situ experiments have boosted understanding and resulted in a variety of models. The models can be divided into three types: i) simple, mean discharge and cover class; ii) semi-realistic, simplified representation of the hydraulic load on a cover with a certain strength/resistance; iii) advanced, erosion model coupled to an extensive CFD model.

For this thesis, models from the second class have been reviewed. This choice was made because these models are computationally light compared to class three and more detailed than class one. A large short coming of class two models is the fact that changing geometry in time is difficult to capture within the hydraulic representation; in some cases, the geometry should be updated after every wave (Bomers et al.,

2018). By choosing to predict the failure of the grass cover the changes in geometry are significantly reduced: these changes are limited to the thickness of the grass cover layer. The models under consideration has been divided into two types, flow- and impact-based models. The first represents the load as an exchange of momentum (velocity squared), or an exchange of energy (velocity cubes). How and on which location this velocity is defined may vary. The second type represents the loading by the wave impact of an overtopping wave, the wave impact loads the cover with normal stresses.

### 2.2.1 Cumulative Overload Method (COM)

The Cumulative Overload Method (COM) follows from (Dean et al., 2010), and states that the cumulative effect of overtopping waves causes failure of the grass cover. Over the past years the COM is extended further and applied parallel to the WOS experiments. This method is displayed in the Dutch ‘Sterkte & Belastingen Waterkeringen (SBW)’-program context and intended for design and assessment purposes (van der Meer et al., 2012).

Van der Meer et al. (2012) states that failure is induced by the cumulative load in excess of a certain critical shear stress. Not the duration of this overloading, but the extent of the overloading shear stress overload is key. This is different from the findings in Dean et al. (2010), but the cumulative effect is preserved. This leads to a basic definition of the cumulative overload:

$$D = \sum (u^2 - u_c^2) \text{ [m}^2/\text{s}^2], \text{ for } u > u_c \text{ (eq. 2.1)}$$

Where  $u^2$  [m<sup>2</sup>/s<sup>2</sup>] is a measure for the shear stress load, caused by the overtopping wave. And  $u_c^2$  [m<sup>2</sup>/s<sup>2</sup>] is a measure of the critical shear stress, i.e. the strength of the cover. The summation of all overtopping events yields the damage factor D [m<sup>2</sup>/s<sup>2</sup>], from analysis of wave overtopping experiments came several damage criterions. Please note, the following criterions are in the context of van der Meer (2012). D=500 [m<sup>2</sup>/s<sup>2</sup>] indicates the initiation of damage, D=1000 [m<sup>2</sup>/s<sup>2</sup>] indicates several bare spots and D=3500 [m<sup>2</sup>/s<sup>2</sup>] indicates the failure of the top layer (grass cover). The first two criterions are prone to large scatter.

In 2017, the Dutch flood safety standards changed and new legal assessment instruments came available, WBI2017. One of the underlying aspects included in the WBI2017 is an extended COM formula (Steendam, 2017). The extension, with respect to eq. 2.1, is in the addition of three dimensionless factors.

$$D = \sum (\alpha_M(\alpha_a u)^2 - \alpha_S u_c^2) \text{ [m}^2/\text{s}^2], \text{ for } (\alpha_M(\alpha_a u)^2 - \alpha_S u_c^2) > 0 \text{ (eq. 2.2)}$$

Where,  $\alpha_M$  is the load influence factor,  $\alpha_S$  is the strength influence factor,  $\alpha_a$  location depended acceleration factor of the wave front velocity,  $u$  [m/s] is the wave front velocity on the crest and  $u_c$  [m/s] the critical velocity parameter. An important change is the failure criterion to  $D > 7000$  [m<sup>2</sup>/s<sup>2</sup>] for grass cover failure.

### 2.2.2 Analytical Grass Erosion Model (AGEM)

The Analytical Grass Erosion Model (AGEM) of van Bergeijk, Warmink, Frankena, et al. (2019) is a coupling of an analytical flow model of flow velocities by van Bergeijk, Warmink, van Gent, et al. (2019) and an adaption of the erosion model of Hoffmans.

The analytical flow model consists of two coupled equations, one for describing the flow on a horizontal surface (i.e. a levee crest or berm) and one for describing the flow on a slope. Coupling of these two equations to levee geometry and boundary conditions yields a depth-averaged velocity profile for a certain overtopping wave volume.

$$U_{horizontal}(x) = \left( \frac{f x}{2 Q} + \frac{1}{U_{horizontal}(x=0)} \right)^{-1} \text{ [m/s]} \text{ (eq. 2.3)}$$

$$U_{slope}(x) = \frac{\alpha}{\beta} + \mu \exp(-3\alpha\beta^2 x) \text{ [m/s]} \text{ (eq. 2.4)}$$

Where:  $x$  is the distance to the outflow [m],  $f$  is the bottom coefficient [-],  $Q$  the discharge at  $x=0$  [m<sup>3</sup>/s],  $\varphi$  is the slope angle [rad]. And the parameter  $\mu$ ,  $\alpha$  and  $\beta$  are given by:

$$\mu = U_{slope,0} - \frac{\alpha}{\beta}, \quad \alpha = \sqrt[3]{g \sin \varphi}, \quad \beta = \sqrt[2]{\frac{f}{2Q}} \quad (\text{eq. 2.4, 2.5, 2.6})$$

The boundary conditions depend on the overtopping volumes and are determined using the empirical formulas of van der Meer, Hardeman, et al. (2010).

$$U_{Horizontal,0} = 4.5 V^{0.3}, \quad h_0 = 0.133 V^{0.5}, \quad Q = U_{Horizontal,0} h_0 \quad (\text{eq. 2.7, 2.8, 2.9})$$

For modelling the erosion, the erosion model of Hoffmans is adapted to include variations in hydraulic load and cover strength along the levee profile. The inclusion of varying load is reached by the location-dependent turbulence intensity and location-dependent strength is included by providing  $U_c$  as function of  $x$ . The erosion depth  $d$  for an overtopping event is calculated as follows

$$d(x) = (\omega(x)^2 U(x)^2 - U_c(x)^2) T_0 C_E, \quad \text{for } \omega(x) U(x) \geq U_c(x) \quad (\text{eq. 2.10})$$

Where:  $U$  is the flow velocity [m/s],  $U_c$  is the critical flow velocity parameter [m/s],  $T_0$  is the overtopping period [s],  $C_E$  is the strength parameter [s/m] and  $\omega$  is the turbulence parameter [-].  $T_0$  is calculated using the empirical relation by Hughes et al. (2012).  $\omega$  is a function of the turbulence intensity  $r_0$ .  $T_0$  and  $\omega$  can be obtained as follows

$$\omega(x) = 1.5 + 5r_0(x), \quad T_0 = 3.9 V^{0.46} \quad (\text{eq. 2.11, 2.12})$$

In the context of modelling transitions van Bergeijk, Warmink, Frankena, et al. (2019) displayed three formulations of  $r_0$  for a case study, these are: as a constant, formulation by Hoffmans and turbulence input from mixing.

Please note, Warmink et al. (2020) showed that the critical velocity parameters for the COM and AGEM were not interchangeable in the context of the study concerned.

### 2.2.3 Dean Stream Power (DSP)

The Dean Stream Power (DSP) model resulted from the 'Erosional equivalences, erosional indices' approach from Dean et al. (2010) and the relationship between the concepts of 'flow work' and 'stream power' shown by Hughes (2011). In the context of the research by Dean et al. (2010) the work-based erosion index showed to be most appropriate for erosion considerations, since this index has the lowest error. Figure 10 gives a comparison for the velocity, shear stress and work based erosional indices. This shows that the work-based index outperforms the other two indices mainly in loading events of less than 4 hours with relatively high velocities (> 4 m/s).

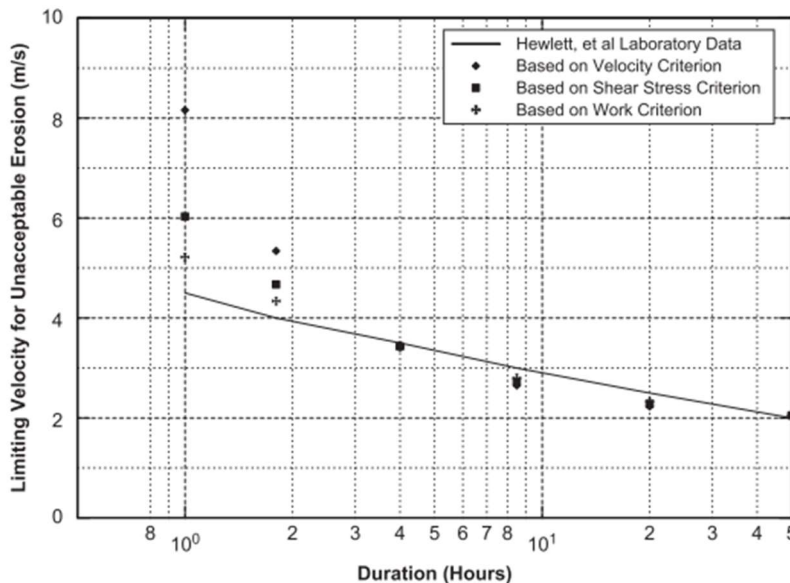


Figure 10 Comparison of fits of three erosion indices results to Hewlett's measurements for "Plain Grass - good cover" (Dean et al., 2010).

From Dean et al. (2010), Equation 2.13 is used to implement the erosional equivalences approach as Dean Stream Power (DSP).

$$EWU = \sum_{n=1}^N (u_n^3 - u_c^3)T_0 \text{ [m}^3/\text{s}^2], \quad \text{for } u > u_c \text{ (eq. 2.13)}$$

Where EWU [m<sup>3</sup>/s<sup>2</sup>] represents the erosional work units, u<sub>n</sub> is the velocity representation related to overtopping event n [m/s], T<sub>0</sub> is the duration that u > u<sub>c</sub> during overtopping event n [s] and u<sub>c</sub> is the threshold velocity [m/s]. Failure is reached when a certain erosion limit is reached, see equation 2.14.

$$EWU \leq \frac{E}{K\beta} \text{ [m}^3/\text{s}^2] \text{ (eq. 2.14)}$$

Where E represents the erosion, K a work erosional coefficient and β a grouping of terms, including mass density of water and a shear stress coefficient. Without further derivation, Dean et al. (2010) identifies erosion limits for three plain grass cover conditions: good, average and poor, with the respective limits of 4.92\*10<sup>5</sup>, 2.29\*10<sup>5</sup> and 1.03\*10<sup>5</sup> m<sup>3</sup>/s<sup>2</sup>.

In the case of overtopping events, Dean et al. (2010) uses a terminal velocity formulation as representation of the flow velocity on the landside slope. These are argued to be a good representation in the context; concerning a 1:6 slope and overtopping discharges in the order of 50 to 200 l/s per meter leading to 2 to 3.2 m/s terminal velocities. Further in this context, critical velocities for the cover conditions are composed as 1.80, 1.30 and 0.76 m/s for respective good, average and poor cover conditions.

2.2.4 Wave Impact Approach (WIA)

The Wave Impact Approach (WIA) is fundamentally different from the previous models. Where the previous models use some velocity-linked representation to model the load, the WIA models the load as the impact perpendicular to the slope of each wave when reattaching to the slope after detachment at the crest, see Figure 11. For each wave where the load exceeds the strength, the total excess momentum transferred increases and the failure mechanism advances. This model is covered in Ponsioen (2016) and Ponsioen et al. (2019).

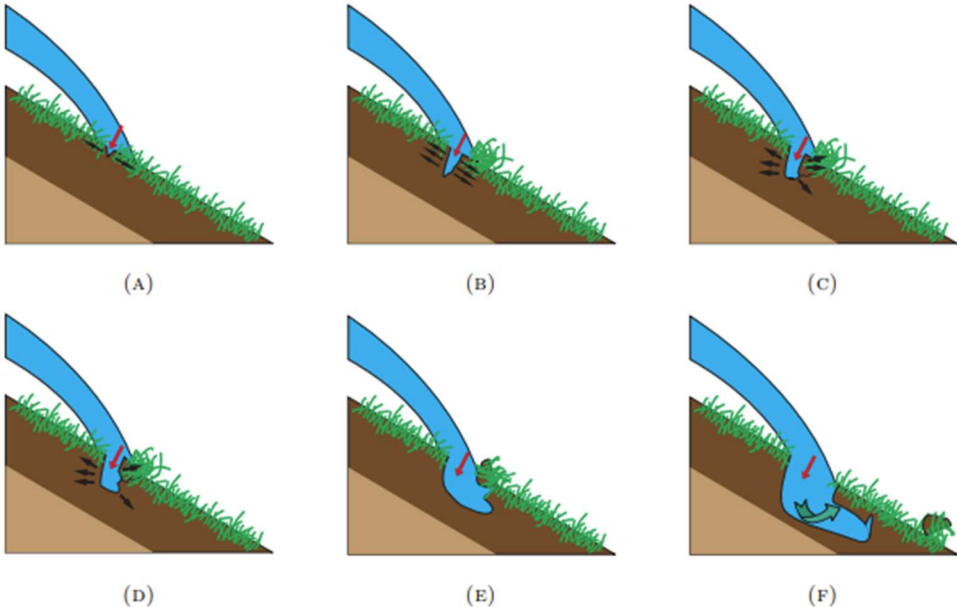


Figure 11 Loading by wave impact, clarified in six steps. (Ponsioen, 2016)  
 A) Small crack in the cover B) Impact pressure pushes the walls further aside and deepens the crack C) Widening of the hole below the grass cover D) Tunnelling under the grass cover E) The flow over the grass cover and overpressure in the tunnel separates the grass sods from the clay layer, causing washing of grass sods. F) Repetition of the D and E causing more washing of grass sods.

The total excess momentum transferred,  $J_E$  in  $\text{kN s} / \text{m}^2$ , is given in equation 2.15.

$$J_E = \sum_{n=1}^N \int_t^T (\sigma_n(X, t) - P_c) dt \left[ \frac{\text{kN s}}{\text{m}^2} \right], \quad \text{for } \sigma_n(X, t) > P_c \text{ (eq. 2.15)}$$

Where,  $\sigma$  is the impact stress component perpendicular to the slope [ $\text{kN}/\text{m}^2$ ] and  $P_c$  the critical pressure [ $\text{kN}/\text{m}^2$ ]. For each overtopping event,  $n$ , the excess load of the impact,  $\sigma(X, t) - P_c$  is integrated over the impact duration. Summation of all  $N$  contributions gives  $J_E$ , since  $\sigma$  is location-dependent,  $J_E$  is also location dependent. This model also has the function to include the effect of the changing impact location during a single overtopping event, this function will be included in all calculations in the context of this research.

Grass cover failure is reached if  $J_E$  exceeds a certain critical threshold, this threshold is not yet identified. Also the critical pressure,  $P_c$ , is not identified, but a range is given where  $P_c$  is expected to be found. This range is a function of the undrained cohesion,  $c'$ , and is given as:  $2c' \leq P_c \leq 5c'$ .

### 2.3 Model comparison

This section shows a comparison of the four introduced models. The comparison is presented in Table 2 and Table 3, whereas Figure 12 displays plots of comparable model outputs. Decompositions of the formulae are given in Appendix B.

The models are compared in nine areas to give an overview of how these models operate with respect to the others, see Table 2.

	<b>Cumulative overload method (COM)</b>	<b>Analytical grass erosion model (AGEM)</b>	<b>Dean, Stream Power (DSP)</b>	<b>Wave impact approach (WIA)</b>
<b>Distinctive characteristic</b>	Use in Dutch guidelines	Analytical flow velocity model	Third power velocity	Impact based
<b>Typical limitation</b>	Empirical, spread in damage factor $D$	Validated on one experiment	Conceptually proven by Dean	Validated on two experiments
<b>Hydraulic model</b>	Flow velocity on the crest as constant along slope or increasing using acceleration factor	Analytical flow velocity model	Terminal velocity or measured velocities	Wave impact at reattachment point
<b>Hydraulic boundary condition(s)</b>	Overtopping wave volume per wave	Overtopping volume per wave	Overtopping discharge	Overtopping volume per wave
<b>Initial condition</b>	Geometry and cover strength	Geometry and cover strength	Geometry and cover strength	Geometry and cohesion of cover material
<b>Strength parameter</b>	Critical flow velocity parameter	Critical flow velocity parameter and strength parameter $C_E$	Critical flow velocity parameter	Critical pressure parameter
<b>Calibration parameter(s)</b>	Critical flow velocity parameter, influence factors	Critical flow velocity parameter, strength parameter $C_E$ , turbulence intensity	Critical flow velocity parameter	Critical pressure parameter
<b>Output shape</b>	Damage factor $D$ for the entire slope or $D(x)$ as function of the location on the slope	Erosion depth as function of the location on the slope	Cumulative erosional work units, can be function of $x$	Total excess of momentum as function of the location on the slope
<b>Failure criterion</b>	Exceedance of $D_{\text{critical}}$	Certain erosion depth	Exceedance of erosion limit for the respective cover	Exceedance of certain unknown critical load indicator

Table 2 Gras erosion model overview.

Table 3 gives a comparison of the models on a parametric level without geometric properties and thresholds, this shows that none of the parameters emerges in the same form in all four models. Close comparisons can be found by interpreting the flow velocities as a reworked form of the overtopping wave volume. This way the wave overtopping volume emerges as a common parameter.

	<b>COM</b>	<b>AGEM</b>	<b>DSP</b>	<b>WIA</b>
<b>COM</b>	$\alpha_M, \alpha_a, \alpha_S$ $u^2, u^2_{\text{critical COM}}$	$u^2$	-	-
<b>AGEM</b>	$u^2$	$C_E, T_0, \omega$ $u^2, u^2_{\text{critical AGEM}}$	$T_0$	$T_0$
<b>DSP</b>	-	$T_0$	$T_0$ $u^3, u^3_{\text{critical DSP}}$	$T_0$
<b>WIA</b>	-	$T_0$	$T_0$	$T_0, P_{\text{critical}}$ $V$

Table 3 Common parameters of the models, other than geometric properties and threshold values. Interpreting the flow velocities as a reworked representation of the wave volume, the wave volume is the only common parameter.

For illustrative purposes, all models have been computed using an arbitrary levee configuration and an arbitrary wave sequence, the main settings are given in Figure 12(a). The computations are executed for varying strength parameters. All other non-wave related parameters in Table 3 are kept constant. For the wave volumes, the control list is used for the second experiment location at Millingen a/d Rijn (Mi2). In Figure 12(b) a selection of velocity profiles is plotted, the profiles are computed with the analytical flow velocity model, Equations 2.3 and 2.4. The three velocity-based erosion models are computed with the analytical flow velocity model as hydrodynamic input: Cumulative Overload Method in Figure 12(c), Analytical Grass Erosion Model in Figure 12(d) and Dean Stream Power in Figure 12(e). The Wave Impact Approach (WIA) is plotted in Figure 12(f). Comparing these plots, it is evident that the COM, AGEM and DSP indicate the main extent of erosion at the lower part of the slope with this default configuration but with varying strength parameter. For the WIA, the centre of the erosion shifts down the slope and decreases in size when the strength parameter increases.

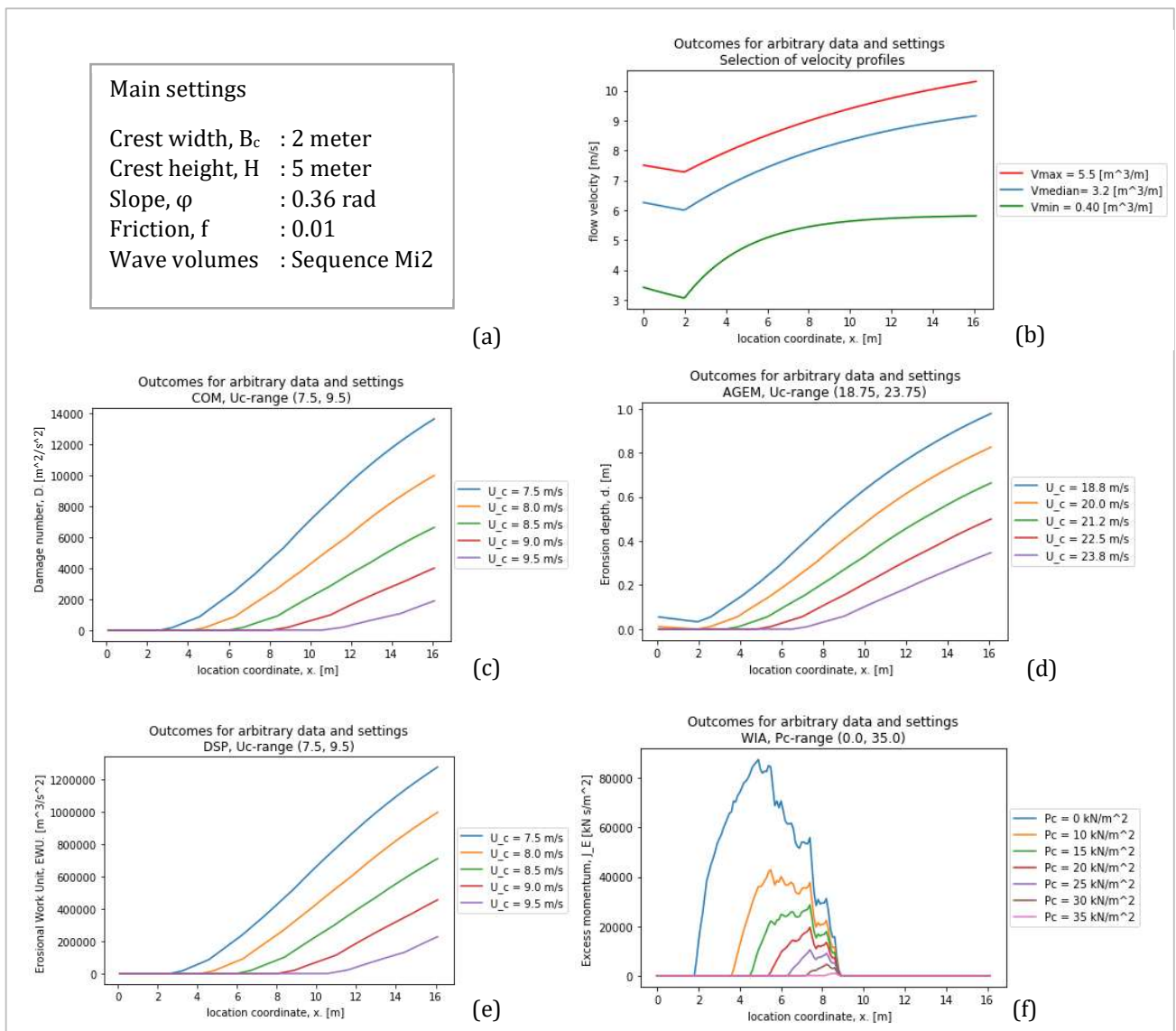


Figure 12 Model outcome comparison for arbitrary data

### 3 Prediction method

This chapter introduces the new prediction method. First, the outline of the new method is presented. The process of setting up the method is described in the Section two, including design choices. Application of the method is specified in Section three.

#### 3.1 Outline

The prediction method is a tool to combine experimental data from WOS experiments with grass erosion models to come to a prediction for a WOS experiment. The core of the prediction method is the creation of a set of predictions, combination of these predictions leads to the final prediction. The set of predictions is created by the set of predictors; each predictor provides one prediction. The predictors are configured by fitting grass erosion models to known WOS experiments leading to calibrated models that form the set of predictors; each combination of experiment and grass erosion model yields one predictor.

The input for the method consists of geometric-properties, anomalies (of the grass cover) and load properties. All input is related to the experiment that is subject of prediction, all predictors are computed using this input. All output of the predictors is combined into a final prediction. Figure 13 shows a conceptual representation of the outline, an technical diagram is provided in Appendix C.

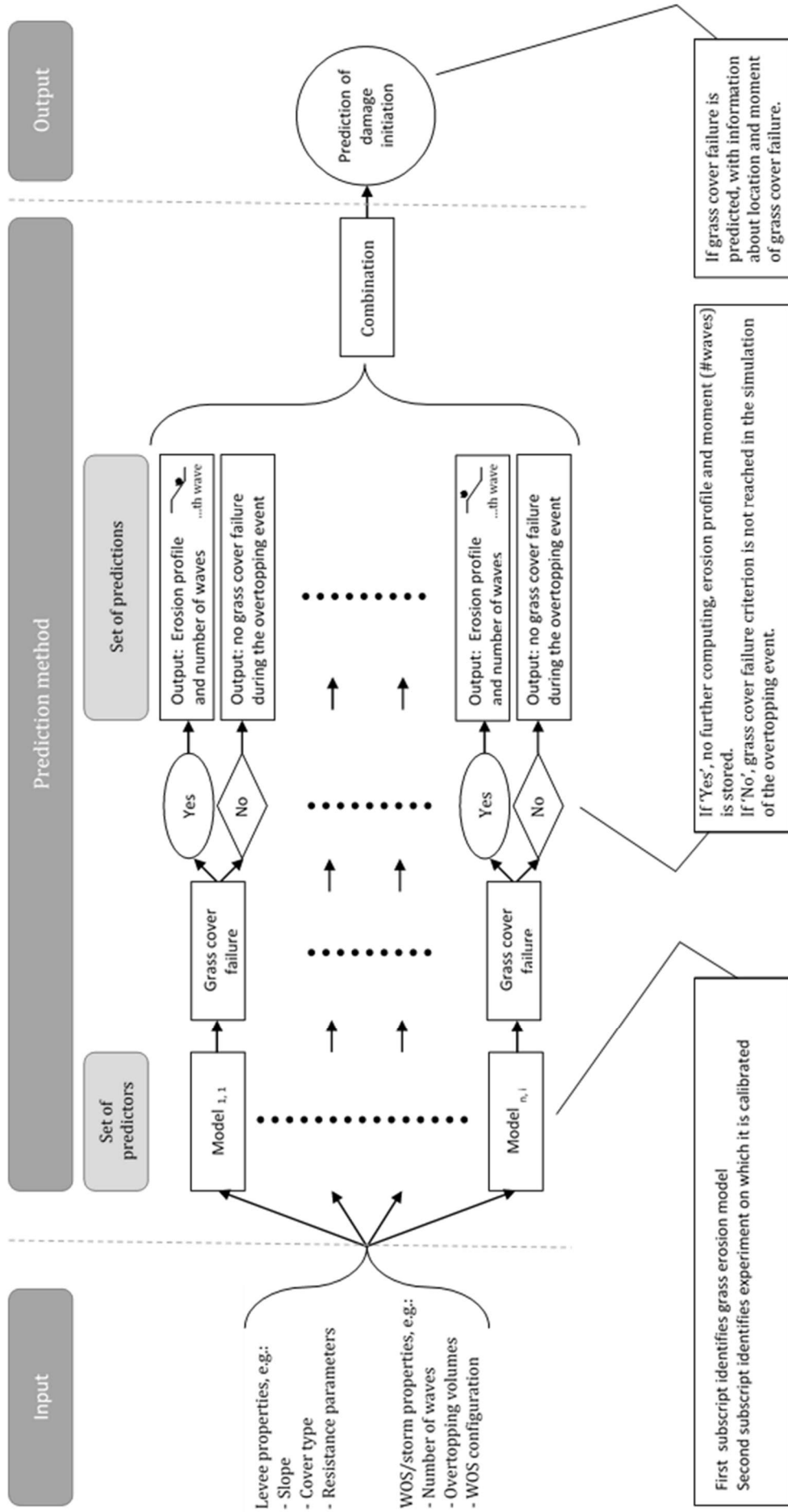


Figure 13 Prediction method. The core of the prediction method is the creation of a set of predictions, combination of these predictions leads to the final prediction.

## 3.2 Set up of the prediction method

This section describes how the prediction method is set-up, which steps have been followed and the design choices that have been made.

### 3.2.1 Geometry

The geometries incorporated in the method are defined by three parameters: crest width  $B_c$ , crest height  $H$  and slope angle  $\varphi$ . Definition of these geometric parameters is given in Figure 14 for the case of Figure 12 in the previous chapter. All slopes-shapes are modelled as a straight slope.

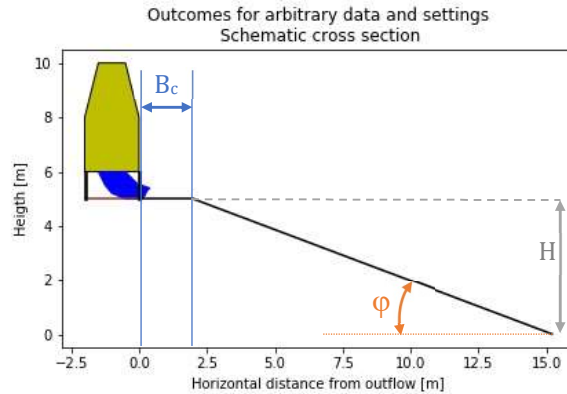


Figure 14 Definition of geometric input

### 3.2.2 Hydraulic input

The hydraulic input is the form of a wave volume sequence released by the wave overtopping simulator. This sequence can either be obtained from control lists files or specific control lists can be generated on request by using the wave overtopping volume theory. A control list is a list of the wave volumes that are to be deployed by the WOS, simulating wave overtopping during a storm event. In the context of this thesis, control lists of the experiments have been retrieved and where applicable these have been adjusted to comply with the descriptions in the corresponding factual reports for each experiment. In specific cases the deployed sequences deviated from the intended sequences. Examples of these specific cases are; added wave volumes for demonstration to visitors, changes in the order in a sequence and termination of the experiment before end of the intended sequence. Van Dijk (2021) contains the intended and adjusted sequences for each experiment, where the adjusted sequences mimic the deployed sequences. The choice for these adjusted control lists is made to reduce the noise in the simulation when calibrating on experiment-outcomes. Consequently, all assumptions made to come to the control lists are included in the factual reports. Some of these are given in Appendix A being the significant wave height, overtopping discharges and intended duration per discharge session are given.

### 3.2.3 Hydraulic modelling

The hydraulic modelling consists of two parts; an empirical part and an analytical part. The empirical part provides for each wave volume realizations of the flow velocity at the outflow  $u_0$ , flow depth at the outflow  $h_0$ , the discharge at the outflow  $Q_0$ , all by van der Meer, Hardeman, et al. (2010), and the overtopping period  $T_0$  by Hughes et al. (2012). These are all empirical relations of the overtopping volume are introduced in section 2.2, and are defined as:

$$u_0 = 4.5 V^{0.3}, \quad h_0 = 0.133 V^{0.5}, \quad Q = u_0 h_0, \quad T_0 = 3.9 V^{0.46} \text{ (eq. 3.1 – 3.4)}$$

The analytical part is computed using the coupled equations of van Bergeijk, et al. (2019), using  $u_0$  and  $Q_0$  from the empirical hydraulic modelling as boundary conditions. Input parameters are: the wave volume sequence, bed friction coefficient  $f$ , slope angle  $\varphi$ , crest height  $H$ , crest width  $B_c$  and grid points along the levee surface. The wave volume sequence and levee-geometry ( $\varphi$ ,  $H$ ,  $B_c$ ) are provided as input of the prediction method. The bed friction coefficient  $f$  is fixed at 0.01. Elaboration on the bed friction coefficient is provided in Appendix D – Influence of wide crests and validity of the friction factor  $f$ . The grid points along the levee surface are set up using a step size of 0.1 meter. The coupled equations are introduced in Section 2.2, and are defined as:

$$U_{horizontal}(x) = \left( \frac{f x}{2 Q} + \frac{1}{u_0} \right)^{-1} \quad [m/s] \quad (\text{eq. 3.5})$$

$$U_{slope}(x) = \frac{\alpha}{\beta} + \mu \exp(-3\alpha\beta^2 x) \quad [m/s] \quad (\text{eq. 3.6})$$

### 3.2.4 Erosion modelling

The next step is to model the erosion.

#### *Erosion models*

The Cumulative Overload Method (COM) is applied in the form as introduced in 2.2.1, but with the following changes. The analytical flow velocity model is used for the hydrodynamic input and all alpha-factors values ( $\alpha_M, \alpha_a, \alpha_S$ ) are equal to 1. In the process, results are compared with the results of the conventional velocity parameter with acceleration factor  $\alpha_a$ , and this shows that the analytical flow velocity model accounts for the acceleration factor  $\alpha_a$  influence. This yields:

$$D = \sum (\alpha_M (\alpha_a u)^2 - \alpha_S u_c^2) \quad [m^2/s^2], \quad \text{for } (\alpha_M (\alpha_a u)^2 - \alpha_S u_c^2) > 0 \quad (\text{eq. 3.7})$$

The Analytical Grass Erosion Model (AGEM) is applied in the form as introduced in 2.2.2. The hydrodynamic input comes from the analytical model, the overtopping period  $T_0$  follows from the empirical relation, further: the erosion strength parameter  $C_E$  is fixed at  $1e-6[s/m]$  (Frankena, 2019) and the turbulence intensity  $r_0$  is fixed at  $0.25[-]$  which represents mild slopes in the context of Frankena (2019).

$$d(x) = (2.75^2 * U(x)^2 - U_c(x)^2) T_0 * 10^{-6}, \quad \text{for } \omega(x)U(x) \geq U_c(x) \quad (\text{eq. 3.8})$$

Since the Dean Stream Power (DSP) has not been used before as such, the model is applied in the form as introduced in Section 2.2.3.. With the analytical flow velocity model as hydrodynamic input for  $u_n$  and the empirical relation by Hughes et al. (2012) for the overtopping period  $T_0$ .

$$EWU = \sum_{n=1}^N (u_n^3 - u_c^3) T_{0,n} \quad [m^3/s^2], \quad \text{for } u > u_c \quad (\text{eq. 3.9})$$

The Wave Impact Approach (WIA) is applied as introduced in Section 2.2.4. The hydrodynamic input is the wave volume sequence.

$$J_E = \sum_{n=1}^N \int_t^T (\sigma_n(X, t) - P_c) dt, \quad \text{for } \sigma_n(X, t) > P_c \quad (\text{eq. 3.10})$$

#### *Erosion thresholds*

Each of the erosion models use a damage criterion, this criterion acts as a threshold. If this threshold is exceeded, the output indicates failure. The failure definitions introduced in this thesis for the COM and AGEM differ from definitions in other applications. This is substantiated as follows: The definitions in Table 4 are established and used on all sections in the test data set, therefor setting a new standard which is correct in the context of this thesis. Doing this allows for combining the grass erosion models for the prediction method. Next to the critical damage criterions which indicate failure of the grass cover, two other criterions are defined per model, but these are less accurate, see Table 4. The damage criterions are:

- No damage      no significant changes, other than washing of debris and leaves folding
- Development    ongoing development of damage
- Failure          the grass cover is eroded or core material is exposed.

Table 4 also contains a column with standardized damage criterions, these criterions are used for comparing extent of computed erosion by the different models later on. Equivalence amongst the models was achieved during the iterative process of defining thresholds and calibrating models on experiment outcomes. A standardized criterion is introduced due to the different scales and units in which the erosion

models produce the output. Determining criterions for the WIA does not appear to be possible on the basis of the available data, this is clarified in section on calibration of the WIA.

	<b>COM</b>	<b>AGEM</b>	<b>DSP</b>	<b>Standardized</b>
No damage	< 1500 m <sup>2</sup> /s <sup>2</sup>	< 0.04 m	< 1 *10 <sup>5</sup> m <sup>3</sup> /s <sup>2</sup>	0.1-0.2
Development	~3500 m <sup>2</sup> /s <sup>2</sup>	~0.10 m	~2.5 *10 <sup>5</sup> m <sup>3</sup> /s <sup>2</sup>	0.5-0.75
Failure	> 7000 m <sup>2</sup> /s <sup>2</sup>	> 0.20 m	> 4.92 *10 <sup>5</sup> m <sup>3</sup> /s <sup>2</sup>	1.0

*Table 4 Damage criterions*

Because the factual reports do not include detailed (continuous) measurements of erosion depth, the erosion depth 'd' for the AGEM is estimated using the damage criterions instead of the actual physical erosion depth. When the reports indicate failure of the grass cover, it is assumed in this thesis that the erosion depth exceeds 0.20m for the AGEM.

### 3.2.5 Calibration

An important step in setting up the new method is the calibration of the grass erosion models to create the set of predictors. The set of predictors consists of calibrated grass erosion models on WOS experiments; one predictor for each combination of grass erosion model and experiment. The following covers selection of a common calibration parameter, the calibration approach and the used performance metric.

#### *Calibration parameter*

As described in Section 2.1, two tracks are identified for the failure path of the grass cover by wave overtopping. The first track, regarding an even and uncompromised grass cover, is likely to initiate failure on locations where the load is high. The second track, regarding a compromised grass cover, can lead to failure either on a location with relatively low loads or after a loading sequence that regions with uncompromised cover were easily able to resist. The second track can lead to the failure early on in the loading sequence, without clear signs of an increase of load it is likely that the strength is compromised. Important side note: often a local increase in load and a decrease in strength go hand in hand; an irregularity may expose a spot that is more vulnerable to erosion and doing so, influence geometry and therefore the flow of water creating a local peak in the load. Due to the nature of all considered cases in the research, the choice is made that the most appropriate way of including this phenomenon, and to be able to predict failure on locations where the load is not at or near maximum, is by modelling this as a local decrease of erosional resistance (= strength). This requires spatial variability of the strength.

Established that a spatial variation of the strength needs to be included, an approach to include this aspect is to be chosen. During certain experiments a substantial development of erosion-patches occur during a load which is well below the average threshold load, indicating that this cannot be modelled by a parameter outside the threshold condition. Additionally, a common parameter is preferred to avoid cluttering of parameters in the models. As shown in the model comparison, Section 2.3, there is no common strength parameter. Regarding the flow-based models, (COM, AGEM, DSP), the critical flow velocity parameter influences the threshold criterion, and despite not being interchangeable, all three are critical flow velocity parameters. Therefore, spatial variation of the strength is modelled using a location-dependent critical flow velocity parameter. For the impact-based model (WIA) a location-dependent critical pressure is used.

Consequence of this strength-based calibration parameter is the conditionally location dependency of the critical flow velocities. The initial condition (anomalies) of the slope has to be known in order to determine the local decrease of erosional resistance; if the condition of the slope is not known or unknown conditions occur, the performance of the method will be affected.

### *Calibration approach*

This section describes the calibration approach for each predictor. A predictor is one of the grass erosion models calibrated on a single WOS experiment, with the strength parameter as calibration parameter. The goal is that each of the four grass erosion models is calibrated on each WOS experiment in the test dataset.

Each calibration consists of the follow steps:

1. **Geometry**  
Retrieve from the relevant factual report approximations for the crest width, crest height and slope angle, also see Appendix A – Overview of WOS experiments. The crest width depends on the placement of the simulator and the crest-line definition, account for deviations from definitions in the factual reports due to protective measures at the outflow. The crest height can usually be determined from measurements. For the slope angle a representative value needs to be chosen; all slopes are modelled as a straight slope, convex and concave shapes are not included.
2. **Anomalies**  
Inventory the initial condition of the slope using the factual report, yielding a registration of anomalies on the slope. Anomalies such as animal activity and tracks, indications of a compromised grass cover, need to be registered.
3. **Erosion analysis**  
Detailed review of the reported and photographed erosion development during each loading step. Link erosional development to anomalies if the locations match. Appendix A includes a table with summarized remarks on the developed damages and failure.
4. **Loading sequence**  
Using the factual reports, reconstruct the control list used for deployment of waves on the slope during each loading step. See van Dijk (2021) for sequences until 2015.
5. **Computations**
  - a. **Sequences – hydraulic input**  
Join loading sequences in correct order to simulate the entire experiment.
  - b. **Geometry**  
Use geometry parameters to make a model of the crest and slope.
  - c. **Hydrodynamics**  
Compute the hydrodynamics.
  - d. **Erosion**  
Compute the erosion for a range of calibration parameter value's.
6. **Calibration**
  - a. **Baseline calibration** - Calibrate for the uncompromised grass cover.
  - b. **Anomaly calibration** – When applicable, calibrate for each anomaly if damage development occurs. Taking into account the location and the moment that the damage criterion is reached.

Figure 15 and Figure 16 complement the calibration of flow velocity model, specifically the COM on the St. Philipsland experiment. Figure 15 shows a range of critical velocities, with each critical velocity constant over the profile.

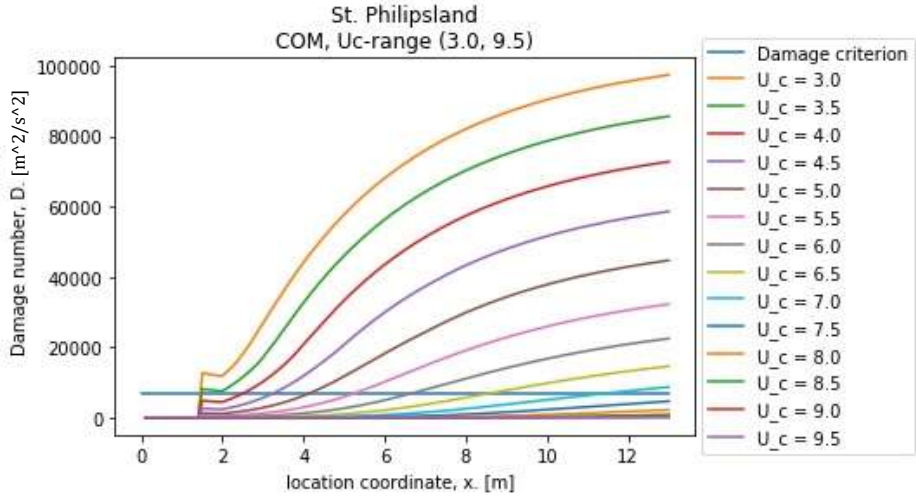


Figure 15 Calibration-range of critical velocities, St. Philipsland

From the factual report and using the definitions from table 4 please note that at 10 meters from the outflow of the simulator failure occurred located at an anomaly (track) indicating  $D > 7000$ , at 5.5 meters from the outflow damage was developing at a different anomaly (mole activity) indicating  $D \sim 3500$ . The uncompromised grass cover showed no signs of erosion, indicating  $D < 1500$ .

Figure 15 indicates the order of magnitude of the critical velocities, computations show that at  $x=10$  the critical velocity is close to 6.75 m/s, at  $x=5.5$  the critical velocity is 6.5 m/s. Figure 16 shows the model with the calibrated critical flow velocities and the track and mole activity and a smaller range for the baseline determination. The peaks in figure 16 come from the calibrated critical flow velocities for the respective locations. The baseline is in the order of 8.5 m/s, based on the region near the end of the slope in figure 16. Alongside these visual aids, the output of the computations is used for more accurate approximations.

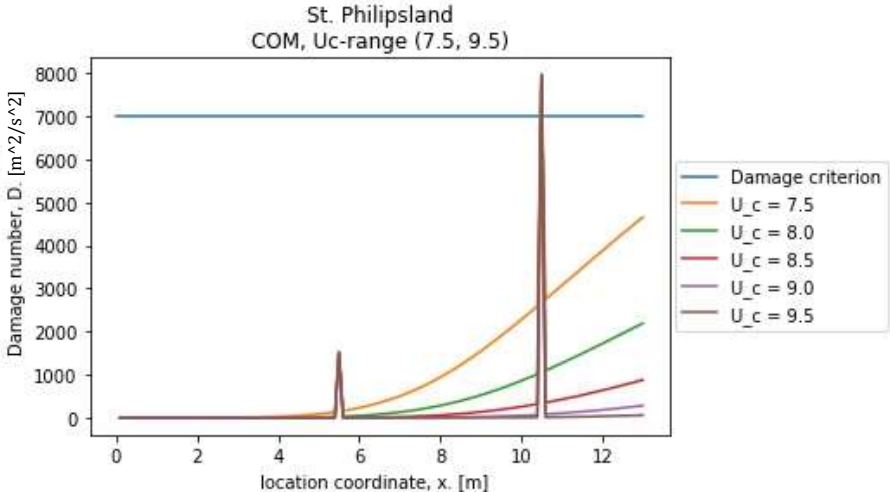


Figure 16. Realization of the calibrated model, with a range for the baseline critical velocity from which  $u_c$  8.5 m/s is chosen, St. Philipsland

In some cases, calibration was not possible due to specific circumstances, examples are; course of experiment; up-slope failure; mitigation measures; missing initial condition registration.

The calibration for the impact-based model(WIA) is similar to that of the flow-based models (COM, AGEM, DSP). The first effort was to find a baseline critical pressure for each section. Because no indication of damage criterions for the total excess transferred momentum,  $J_{cr}$ , has previously been found,

determination of the critical pressure and damage criteria is a parallel process. Figure 17 shows the realization of the Wave Impact Approach (WIA) for the case of the sections at Delfzijl, with varying critical pressures. Appendix G contains WIA realizations with varying critical pressure for each section. In these plots, the domain of influence of this model is represented as areas with an excess of transferred momentum, for increasing critical pressure this domain shrinks. As only increasingly larger waves cause loads that can exceed the increasing critical pressure, this is assumed to be physically correct.

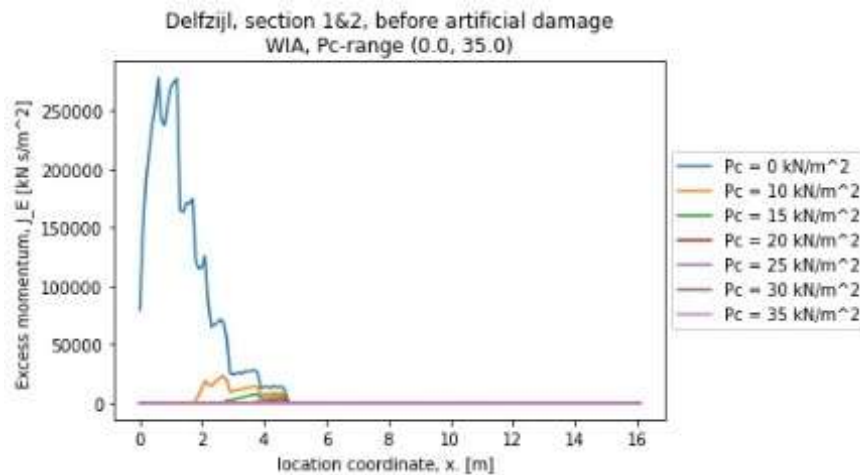


Figure 17 WIA realization at Delfzijl

Analysing WIA realizations of all test sections and the locations where erosion is noted, only six sections show erosion inside the WIA domain of influence. Of these six sections, four sections show that the location of erosion coincided with initial damages. Of the remaining two sections, one section is loaded with small waves and shows very low values for the excess transferred momentum. The last remaining section is section 1 at the Wijmeers-II experiment, from where the WIA originated. This analysis shows that the influence of impact based loading is limited and if it occurs it is likely to be at a location with initial damage. It is concluded that the impact-based approach does not have a substantial influence and more importantly, the critical pressure and failure criterion cannot be unambiguously determined. Despite the expected range of  $2c' \leq P_c \leq 5c'$  (Ponsioen et al., 2019). Therefore, the WIA will not be included in the prediction method. Appendix E contains all WIA realisations.

#### Calibration performance

This section provides insight in the performance of each predictor on the experiment it is calibrated upon. In order to compare performances, standardization is introduced. Standardization is required because the order of magnitude of waves changes per experiment and the erosion is expressed in different units per model. The standardization is represented by the ratio between the model output and the experiment output. With a ratio of 1, the model exactly mimics the experiment outcome, a ratio larger than one indicates an over-estimation and a ratio smaller than one indicates under-estimation.

The performance is represented using two ratios, wave-ratio and the erosion-ratio. The ratios are between the model output and the experiment output. With a ratio of 1, the model exactly mimics the experiment outcome, a ratio larger than one indicates over-estimation and a ratio smaller than one indicates under-estimation. The wave-ratio is the ratio between the computed number of waves (model output) and the actual number of waves (experiment output). The erosion-ratio is the ratio between the computed erosion (model output) and the observed erosion in the factual reports (experiment output). The erosion is expressed in the definitions in Table 4. Ratio-scores  $1 \pm 0.40$  are considered acceptable within the context of this thesis. The calibration of the predictor is aimed to fall inside the  $1 \pm 0.40$  interval.

The principle of the performance metric is illustrated in Figure 18.

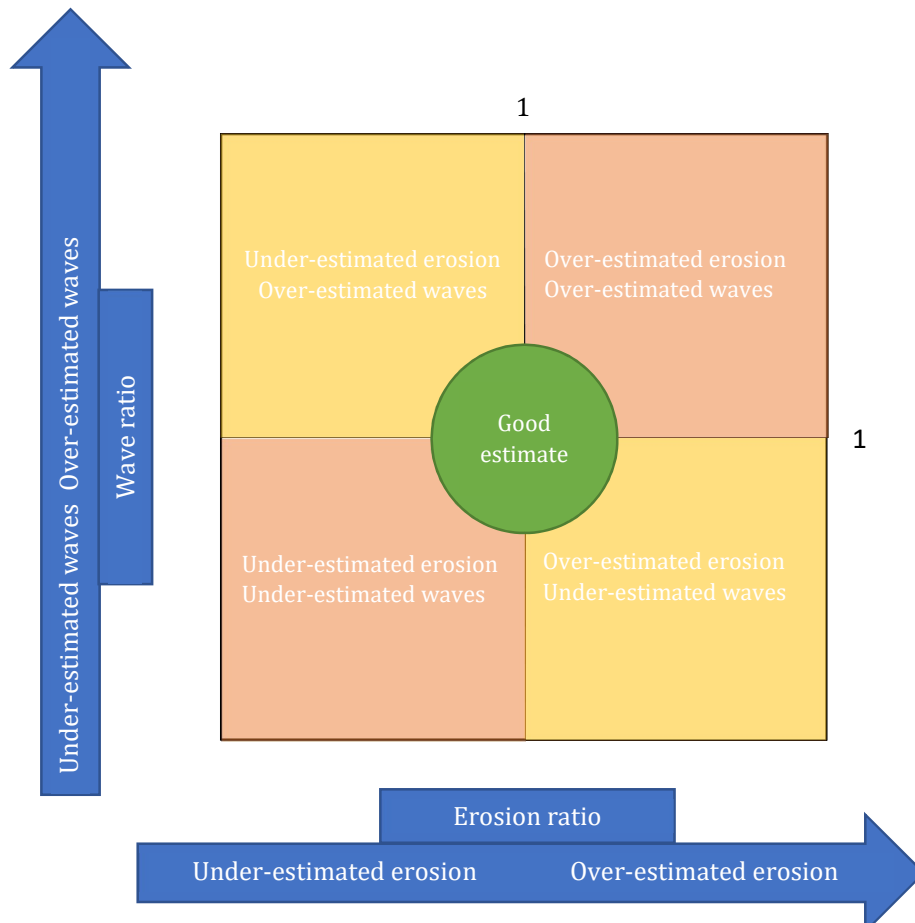


Figure 18 Performance metric for calibration performance

### 3.2.6 Combination method

The combination of experiment data and grass erosion models in this thesis is achieved by combining multiple predictions, each prediction based on a specific experiment and specific grass erosion model.

At first, a data-driven algorithm was aspired. Due to small set of available learning data, it is highly unlikely that a machine learning algorithm can add value at this stage. The learning dataset may have an order size of 10 to 100, machine learning algorithms require an order size of ten thousand or more. (Interview D.M.J. Tax; EWI TUDelft, Meer et al., 2018). The key-feature of a such an algorithm is that it can reproduce probability density functions(pdf's) for all kind of circumstances, for instance taking different varying parameters into account for different scenario's. Figure 19 shows how some pdf composed using a five samples can deviate significantly from some random pdf where the samples are taken from. The sample-pdf renders the levee stronger in that specific scenario then is the case in reality, vice versa is possible for a different sample set. This touches the core problem when trying to use machine learning techniques in this application: a machine learning algorithm will not be able to accurately reproduce valid pdf's for all scenario's. For example, the different scenarios of a mole hill on the slope: is it situated in clay or sand, does in reach into the core, is it washed shut, etc. There are too many unknowns and variables for the small number of data points.

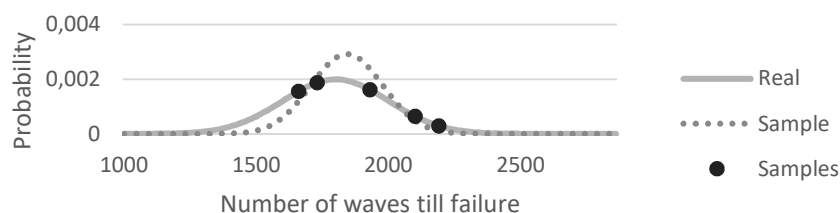


Figure 19 Reproducing probability density function from a sample

Due to the relatively small dataset the choice is made to use a low tech combination method, which consists of three steps. The first two steps must be applied to baseline-predictions and to applicable anomaly-predictions. The first step is to cope with predictions that predict that the grass cover will not fail during the experiment. This is done by a vote amongst the predictors; if the majority predicts “no-failure” this represents the prediction and step two is omitted, if the majority predicts “failure” step two follows. Step two consists of taking the average of the number of waves until grass cover failure of the predictors that predict failure.

The first two steps lead to a baseline prediction and respective predictions linked to anomalies and their locations. The final step is to select the final prediction, this is the prediction that indicates grass cover failure after the least number of waves, this is the final prediction including the location and number of waves till grass cover failure. If none predict failure, the final prediction is that the grass cover will not fail during the experiment.

### 3.3 Application of the prediction method

This section describes the steps to apply the prediction method. The method uses geometry, anomalies and the loading sequence of the section subject of the prediction. In the method, this input is used to compute predictions by predictors that contain experience gained from previous experiments. All these predictions are combined to give a prediction if grass cover failure will occur, and if so, at which location and after how many waves.

Application of the new method requires certain properties of the experiment to be predicted. Hereby, no calibration is required; the method gives a prediction for an experiment based on the configuration and (inter-dependent) calibration of elements in the method. If any of the underlying parameters in the hydraulic- or erosional modelling in the prediction method are changed or calibrated, the entire configuration and calibration of the prediction method is in need of reviewing. Application of the new prediction method consists of steps that cover preparation, computation and evaluation. These steps are described in this section.

#### 1. Preparation

The first step is to prepare the input for the computations. The input includes the geometry, anomalies and loading sequences.

##### a. Geometry

Geometric parameters are the crest width, crest height and slope angle. The crest width depends on the placement of the simulator and the crest-line definition. The crest height follows from measurements. For the slope angle, a representative value needs to be chosen; determine a straight slope that best fits the actual slope-shape.

##### b. Anomalies

In this thesis, the method has been configured for only three anomalies: mole activity, tracks and non-homogeneous toe conditions. Registration of the presence and the location of anomalies is required, in line with registrations in preceding factual reports.

##### c. Loading sequence

During preparations of an experiment, the load has been specified by the applicable hydraulic conditions, outer-slope of the levee and the overtopping discharge. The best results are expected when using identical wave sequences to those that controlled the simulator, see van Dijk (2021) for sequences until 2015. If sequences are unavailable, the loading sequences can be reconstructed by making use of the relevant theory. The latter approach is not included in this thesis.

## 2. Computation

After preparation all input for the computations is available, the principle of the computations is given below. For writing a script, deviations are possible for efficiency.

- a. Geometry  
Use the geometry parameters to set-up a computational grid, as model for the crest and slope surface. If anomalies are present, the location and type are coupled and located on the grid.
- b. Loading sequences  
Depending on the datatype and -shape of the available wave sequences, computations are required to obtain a single sequence that contains all wave volumes in the correct order.
- c. Hydrodynamics  
Use the hydrodynamic models, geometry parameters, wave sequences and the computational grid to compute the hydrodynamics. This yields the velocity profile per wave and the overtopping period per wave. The depth-averaged velocity is computed on each grid point for each overtopping event, resulting in a 2D-matrix with the size of the number of overtopping events by the number of grid points.
- d. Critical velocity  
A critical velocity profile is constructed for each predictor; this yields 63 critical velocity profiles. Combine the critical velocity information on the baseline and anomalies of each predictor with the geometry and anomalies of the section subject of prediction.
- e. Erosion  
For each predictor, combine the hydrodynamics and critical velocity profile to compute the erosional contribution per overtopping event. Take the cumulative sum to yield the development of erosion during the simulation. The output is in the form of combinations of 'locations' and 'number of waves': locations where the failure-damage criterion is reached and if this criterion is reached, the number of waves after this occurred first on that location. Each location where the computed erosion exceeds the failure-damage criterion has to be either linked to the anomaly on that location or to the baseline-prediction if no anomaly is present. Extract the number of waves -after which the failure-damage criterion is reached- from the erosional contributions and linked to the location.
- f. Combination  
Combine all predictions per type: baseline and each anomaly. First determine if failure occurs for the type by voting, if failure occurs determine the number of waves until failure. The prediction with the earliest failure represents the final prediction, if failure is predicted, otherwise the prediction is that no failure occurs.

## 3. Evaluation

When the experiment outcome is known, the performance is to be mapped using the performance metric introduced in Section 3.2.5. Wave-ratio can be swapped for number of waves.

## 4 Results

This chapter consists of the most important results of the calibrations performed for the prediction method and the results of the predictions that act as validation of the new method.

### 4.1 Calibration results

This section states the values of the calibrated critical flow velocities and the performance of the calibrated models. Following the method in Chapter 3, the grass erosion models are fitted to each of the 23 sections in the test data set. 21 sections in the test-dataset showed useful results, 2 sections are ignored because of insufficient information about the initial conditions of the slope and damage development. The result of calibration consists of critical flow velocities on the baseline strength and 3 anomalies: mole activity, track and non-homogeneous toe conditions. Anomalies that occurred only once during the calibrations efforts are not included. 19 experiments proved useful for baseline calibrations, 14 instances of mole activity on a total of 11 experiments, 5 instances of tracks on a total of 3 experiments and 9 instances of toe conditions on a total of 11 experiments. The calibration results and performance are given in the following sections per type.

Appendix F – COM, AGEM & DSP calibrations shows tables with full overview of calibrated critical flow velocities and calibration plots per section per model.

#### 4.1.1 Baseline

The baseline calibrated critical flow velocities are shown in Figure 20. The average baseline critical flow velocity for respectively the COM, AGEM and DSP is: 7.8 m/s, 22.4 m/s and 7.8 m/s.

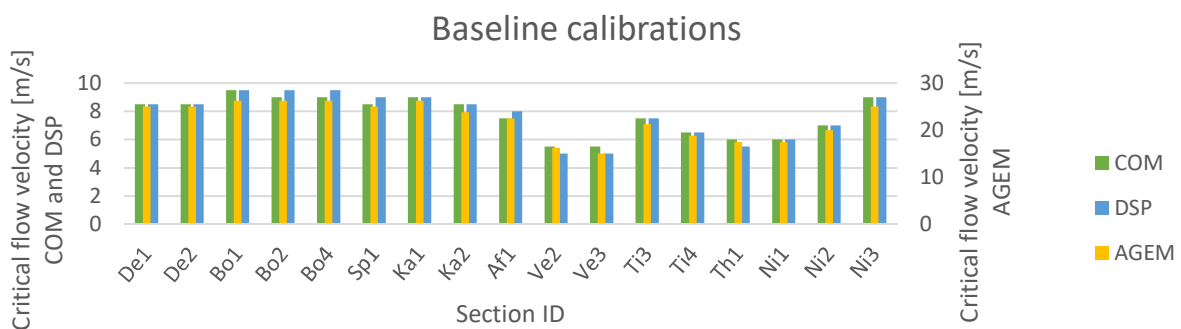


Figure 20 Baseline calibrated critical flow velocities

49 of the 57 calibrations perform within the 0.40- interval, 25 lay inside the 0.20-interval, see Figure 21. The spread in the performance can be clarified because in none of the cases the failure criterion is reached and the large influence of small steps in the calibration parameter. First, when the failure criterion is not reached, calibration is performed on a criterion with a lower threshold, which increases the sensitivity of the erosion ratio. (smaller denominator in case of a lower threshold) See Section 3.2.5 for explanation on the erosion ratio. Second, for some cases the sensitivity of the calibration parameter is such that step means the erosion ratio jumps from 0.50 to 2.00, with step size 0.5 m/s for COM and DSP and for AGEM 1.25 m/s.

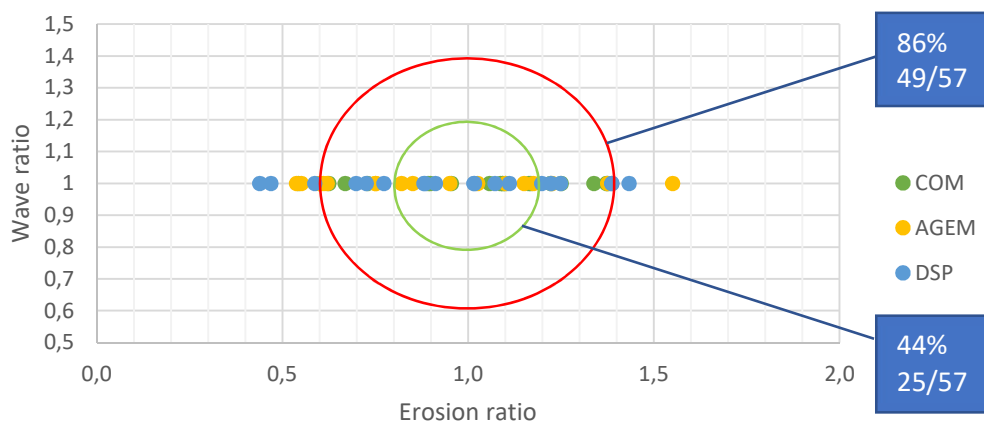


Figure 21 Performance baseline calibrations

The 8 points that fall outside the 0.40-interval are further elaborated in Table 5. This table contains erosion ratios linked to points outside the 0.40 interval in Figure 21, for each point the corresponding section, model, threshold and realisation is given. The sensitivity is illustrated by the realisations for the case of plus and minus a stepwise of 0.5 m/s of the critical flow velocity. The threshold-column gives the threshold that indicates an erosion ratio of 1. The realisation-column gives the erosion computed after calibration of the critical flow velocity. The -/+ step-column give the erosion computed for respectively minus and plus 0.5 m/s with respect to the calibrated critical flow velocity ( $u_c$ ), see Figure 20 and Appendix F – COM, AGEM & DSP calibrations for the calibrated critical flow velocities.

Erosion ratio	Section	Model	Threshold	Realisation with chosen $u_c$	$u_c - 0.5$ m/s	$u_c + 0.5$ m/s	Unit
0.54	Mi1	COM	700	380	1800	40	$m^2/s^2$
0.54	Mi2	AGEM	0.04	0.0215	0.091	0	m
0.55	Ka1	AGEM	0.02	0.011	0.032	>0.001	m
1.55	Mi1	AGEM	0.02	0.031	0.1	0.006	m
0.44	Mi2	DSP	0.9e5	0.43e5	1.97e5	0	$m^3/s^2$
0.47	Mi1	DSP	0.5e5	0.23e5	0.95e5	0.03e5	$m^3/s^2$
0.59	Sp1	DSP	0.5e5	0.29e5	0.80e5	0.07e5	$m^3/s^2$
1.43	Ka1	DSP	0.5e5	0.71e5	1.65e5	0.24e5	$m^3/s^2$

Table 5 Sensitivity of baseline calibration outliers to the critical flow velocity.

Calibration of baseline critical flow velocities are calibrations where the grass cover failure criterion is not reached, an unambiguous target in the form of grass cover failure is missing. The calibrated critical flow velocities act as a lower limit for the baseline resistance against erosion; the calibrated critical flow velocities are not substantiated with failure of the grass cover.

#### 4.1.2 Mole

The calibrated critical flow velocities on mole activity are shown in Figure 22. The average critical flow velocity for respectively the COM, AGEM and DSP is: 4.5 m/s, 12.7 m/s and 3.8 m/s.

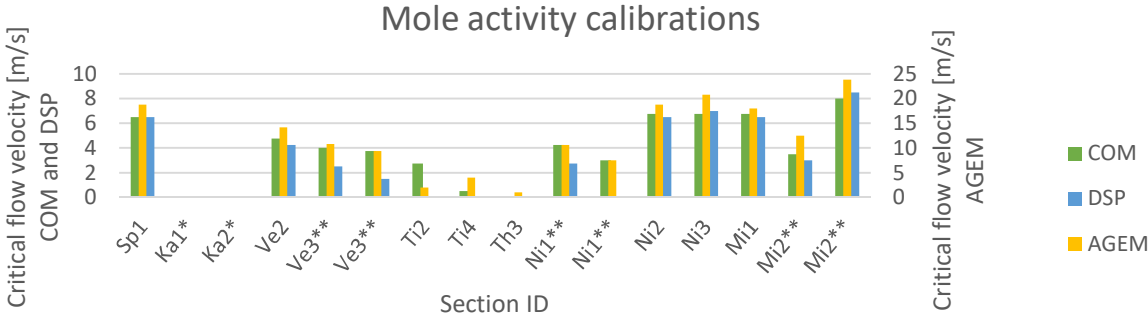


Figure 22 Mole activity calibrated critical flow velocities \*) Mole activity, but this had no influence on the course of the experiment \*\*) In some cases several locations with mole activity could be calibrated to retrieve a calibrated critical flow

37 of the 42 calibrations perform within the 0.40-interval, 31 lay within the 0.20 interval, see Figure 23. The failure criterion is often reached at mole-activity, having this high threshold (failure) leads to a better performance.

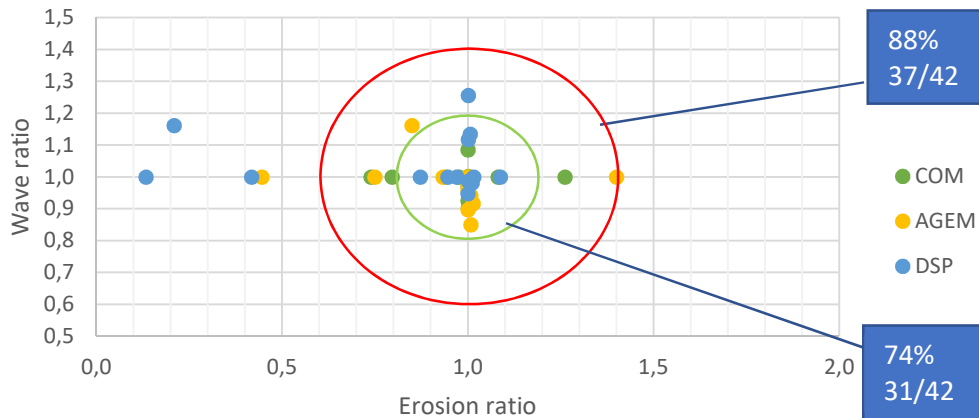


Figure 23 Performance mole activity calibration

The five cases that lay outside the 0.40-interval are the AGEM and DSP calibration on Th3, and the DSP calibrations on Ti2, Ti4. In these cases, the failure criterion was not reached even with extremely low critical velocities.

#### 4.1.3 Track

The calibrated critical flow velocities on tracks are shown in Figure 24. The average critical flow velocity for respectively the COM, AGEM and DSP is: 6.3 m/s, 18.8 m/s and 6.5 m/s.

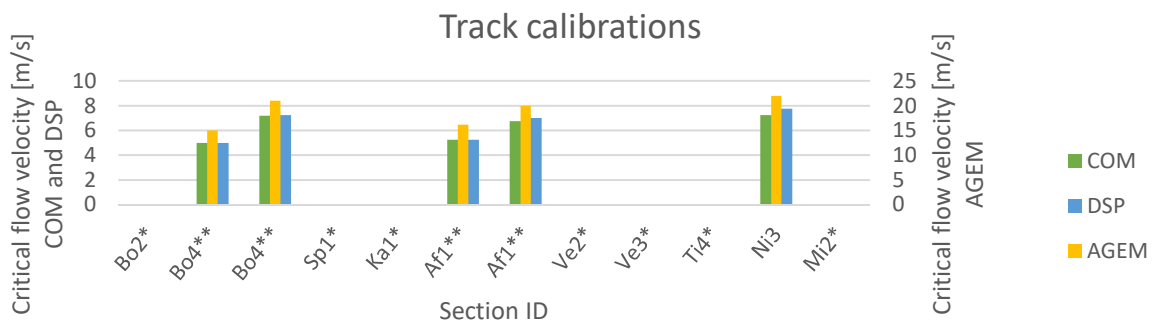


Figure 24 Track calibrated critical flow velocities \*) Track, but this had no influence on the course of the experiment  
\*\*) In some cases several locations with a track could be calibrated to retrieve a calibrated critical flow velocity parameter

Calibrated critical velocities for the track-mode show good performance: 100% lies inside the 0.40-interval and 87% lies inside the 0.20-interval. See Figure 25.

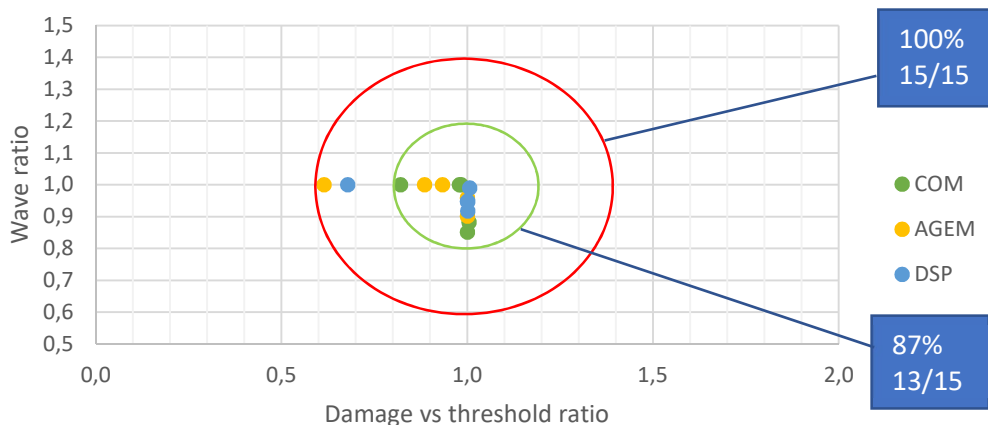


Figure 25 Performance track calibration

#### 4.1.4 Toe

The calibrated critical flow velocities for non-homogeneous toe conditions are shown in Figure 26. The average critical flow velocity for respectively the COM, AGEM and DSP is: 6.0 m/s, 16.7 m/s and 4.7 m/s.

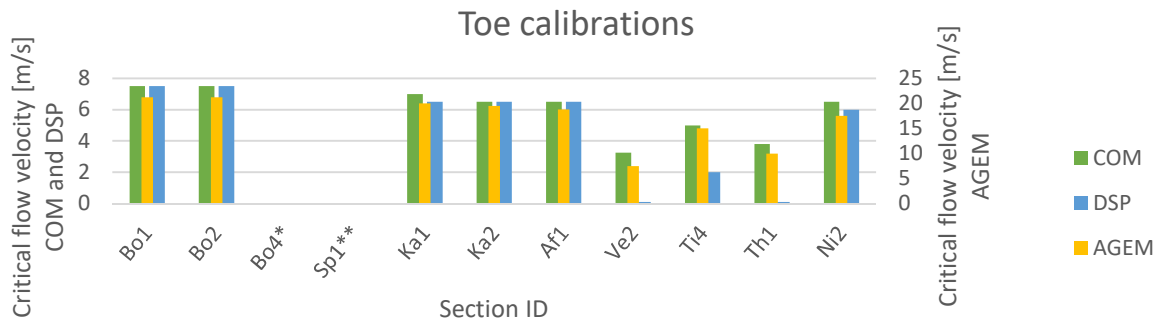


Figure 26 Non-homogeneous toe condition calibrated critical flow velocities \*) Non-homogeneous toe conditions, but this had no influence on the course of the experiment \*\*) Not suitable for calibration

Calibrated critical velocities for the toe-mode show good performance: 100% lies inside the 0.40-interval and 87% lies inside the 0.20-interval circle. See Figure 27.

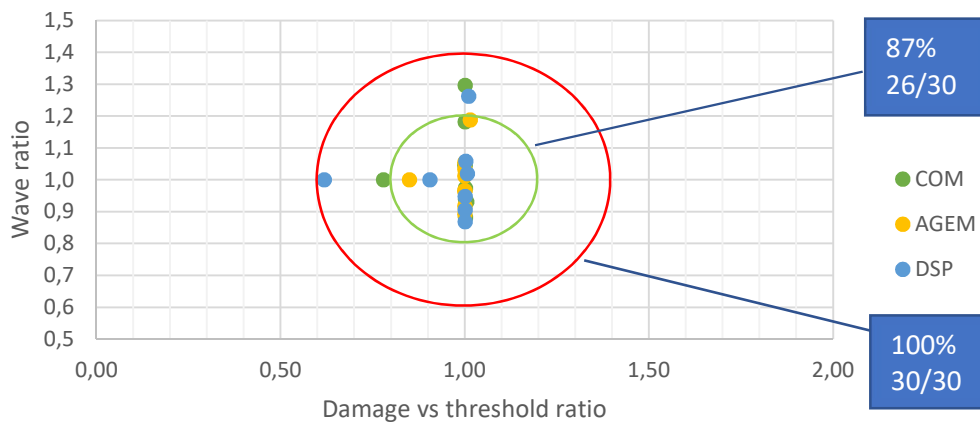


Figure 27 Performance non-homogeneous toe condition calibrations

#### 4.1.5 Concluding remarks

The calibration of the models on the baseline and the considered anomalies show a considerable lower average critical flow velocities for the cases with anomalies. For the mole activity anomalies, the critical velocity is on average decreased with 46%. For the track anomalies this is 18% and for toe anomalies 29%. Because the grass erosion models use an exponentiation of these velocities, these percentages do not represent a certain linear relationship with the permissible load.

As noted, the baseline calibrated critical velocities represent a certain lower limit of the strength. In none of the experiments used for calibration the average grass cover failed. In all cases of failure, this was initiated at the location of an anomaly. How these anomalies exactly reduce the strength is not included in the calibration method. This can be a combination of a geometrical anomaly with an anomaly in the grass cover, or either of these separate, or an opening straight to the soil layer (sand) below.

## 4.2 Validation results

At the start of this thesis five sections were put aside as validation data-set. Some basic properties were known, but the course of the experiments has been kept unknown until after the prediction method was definitive. In this chapter, the prediction-results are compared with the respective actual course of the experiment. As described in 1.4.3, the five validation sections are:

- Bo3 Boonweg 2008 section 3
- Af2 Afsluitdijk 2009 section 2
- Ve4 Vechtdijk 2010 section 4
- Ti1 Tielrode 2010 section 1
- Th4 Tholen 2011 section 4

The most important findings are summarized in the following section, Appendix G – Technical memo of validation predictions contains a more elaborate memo.

### 4.2.1 Boonweg section 3

The section is loaded with six incremental loading, or until failure of the slope occurs. Each of the six loading steps represents a specific storm condition that last for six hours, the significant wave height is 2 meters and all loading steps combined consist of 5369 overtopping waves. The loading steps range from 0.1 to 75 l/m/s. The test section has a crest height of 7.25 meters, a crest width of 3 meters and a slope of 0.322 radians or 18.4 degrees.

Three anomalies are identified, all three are tracks. These are located at 3, 8 and 16.5 meters from the outflow. Other occurring anomalies are not incorporated in the prediction method.

Using the above as input, this yields a predictions for the baseline and the included anomalies, see Figure 28. The final prediction is the failure that occurs first, in this case both the track at 3 and 8 meters are predicted to fail around the same moment in time near the end of the 10 l/s per meter sessions.

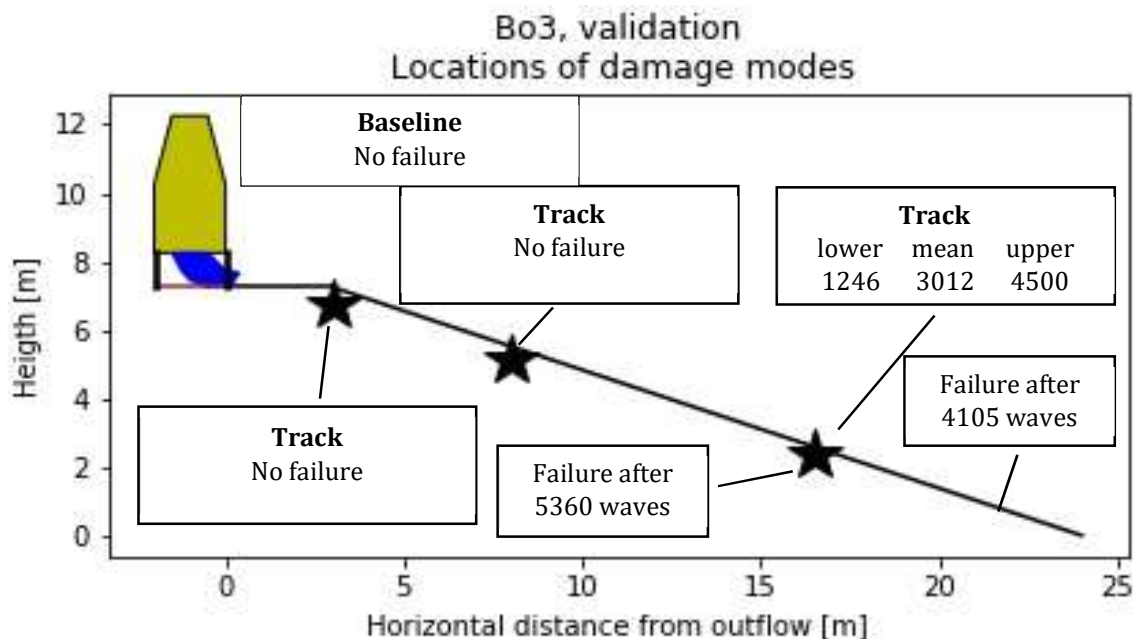


Figure 28 Prediction Boonweg section 3, Bo3. In bold, the baseline or respective anomaly. 'lower' and 'upper' refer to the lower and upper bound of the specific predictions. The boxes with "failure" indicate the failure locations during the experiment, including the number of waves until failure.

The outcome of the experiment is grass cover failure at two locations; at the location of mice activity around 22 meters from the outflow and around the track 16.5 meters from the outflow. The failure of the grass cover occurred during the 75 l/s per meter sessions. The first failure showed after 1.5hour (4105 waves) at the mice activity, see Figure 29 left. The second near the end of the experiment near the location

of the track. Both failures showed the bulging mechanism. The road after the toe is not noted in the null-inspection and no damage was noted at this road.

The prediction of the method did not include the failure at the location of mice activity, this is explained by the lack of this anomalies causing damage in the test dataset. As for the predictions made, the location of the final prediction is correct and the 'no-failure' predictions proved to be correct. The moment of grass failure was predicted earlier than the experiment showed, indicating a conservative estimation of the resistance against erosion.



Figure 29 Left: first grass cover failure after 1.5hr. Right: End result, including the 30min extension. Bo3.

The performance of the final prediction is plotted in Figure 30 for the failure of the grass cover (erosion ratio 1) at the end of the experiment (wave ratio 1). The final prediction also has an erosion ratio of 1, since the erosion prediction is identical to the experiment outcome. The wave ratio of the final prediction is  $3012 / 5360 = 0.56$ , falling outside the 0.40-interval. Consequently, the prediction of the moment of failure is considered not good.

Performance plot - track at x=16.5

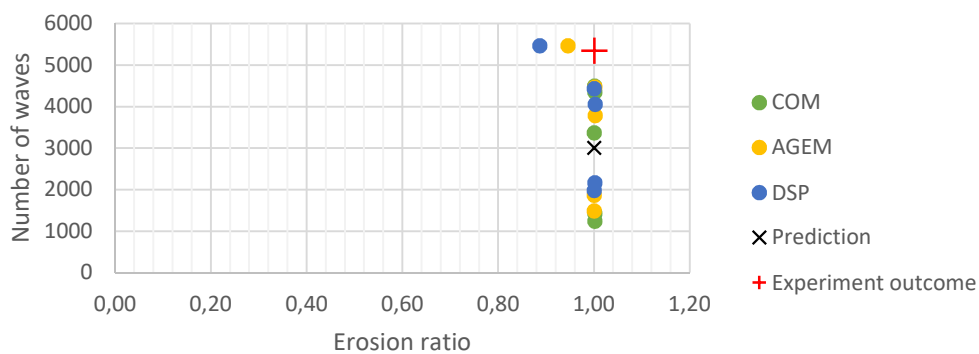


Figure 30 Performance plot final prediction, Bo3. Erosion ratio 1.0 represents failure.

#### 4.2.2 Afsluitdijk section 2

The section is loaded with incremental loading, or until failure of the slope occurs. Each of the five loading step represents a specific storm condition that last for six hours, the significant wave height is 2 meters and all loading steps combined consist of 5360 overtopping waves. The loading steps range from 1 to 75 l/m/s. The test section has a crest height of 2.9 meters, a crest width of 0.7 meters and a slope of 0.367 radians or 21 degrees.

Two anomalies are incorporated in the prediction method. A track at 4 meters from the outflow and the situation after the toe, trampled grass and pavement. Other anomalies are not incorporated in the prediction method.

Using the above as input, this yields a baseline-prediction and two anomaly-predictions, see figure 31. The final prediction is failure of after the toe, during the second 30 l/s per meter session.

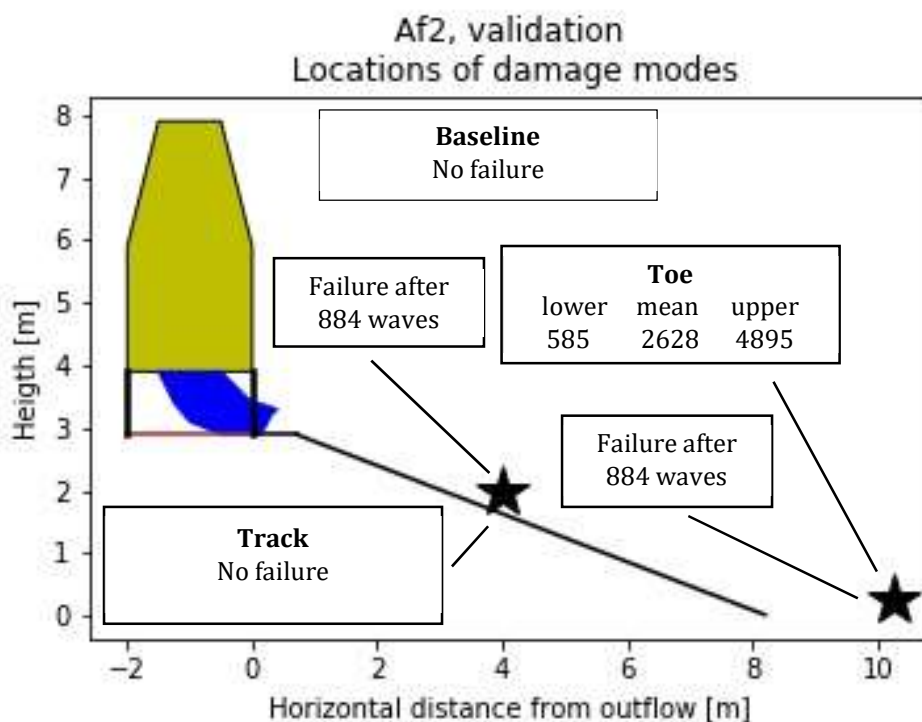


Figure 31 Test prediction, Af2. In bold, the baseline or respective mode. 'lower' and 'upper' refer to the lower and upper bound of the specific predictions. The boxes with "failure" indicate the failure locations during the experiment, including the number of waves until failure.

The outcome of the experiment was that after 75min of 10l/s per meter (282 waves), the first damage developed at the location of the heavy track, with a pit 0.13-meter-deep, and after the toe. At the end of the 10l/s per meter sessions (884 waves) the grass cover has failed. Also erosion occurred just after the toe where the fence was removed and where the grass was trampled and muddy, the grass cover was removed at certain places. After 4hours and 20min of 30 l/s per meter (1795 waves), the experiment was stopped due to excessive erosion of the pavement elements. See Figure 33.

The erosion at the heavy track developed into failure in contrast with the prediction, only at the pit of 0.13-meter-deep in this track. Failure at the toe occurred earlier than predicted.



Figure 33 Left: after 10 l/s per m sessions. Right: after experiment termination, 4hr and 20min of 30l/s per meter. Af2.

Figure 32 shows the performance plot of the prediction for the track. 6 of the 15 predictors did predict failure, these 6 predictors are calibrated on Bo4 and Af1. A combination of these six predictions would correctly predict failure at this location, being off with a wave ratio of 3.72. Indicating that the considered track varies significantly with tracks in the test dataset.

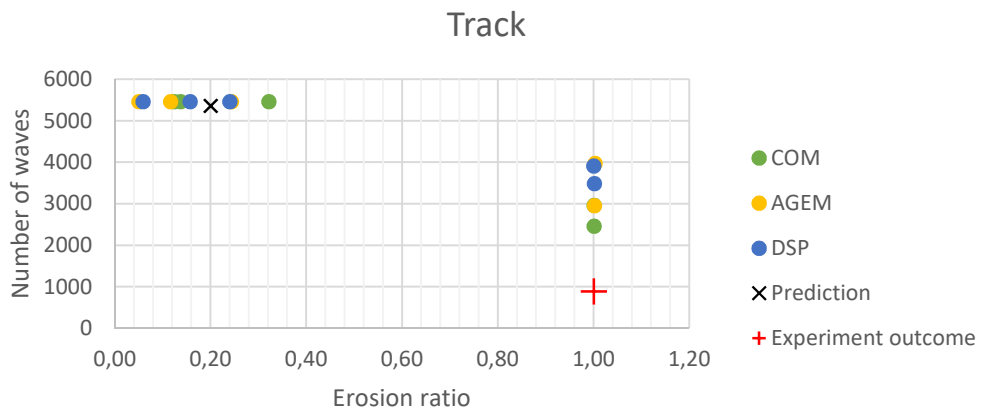


Figure 32 Performance plot track prediction, Af2. Erosion ratio 1.0 represents failure.

The performance of the toe-prediction is plotted in Figure 34. Prediction indicates failure (erosion ratio 1) before end of the experiment at the location of the toe. The wave ratio of 3 indicates that the prediction is to optimistic, the actual resistance against erosion was lower than predicted. A small cluster of predictors proved to accurate for the moment of failure.

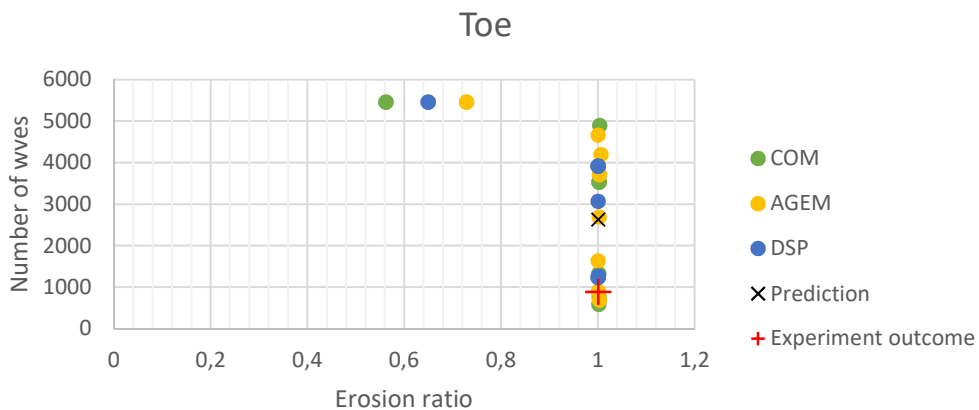


Figure 34 Performance plot toe prediction, Af2. Erosion ratio 1.0 represents failure.

#### 4.2.3 Vechtdijk section 4

The section is loaded with incremental loading, or until failure of the slope occurs. Each of the six loading step represents a specific storm condition that last for six hours, the significant wave height is 3 meters and all loading steps combined consist of 2487 overtopping waves. The loading steps range from 0.1 to 75 l/m/s. The test section has a crest height of 3.2 meters, a crest width of 2.5 meters and a slope of 0.201 radians or 12 degrees.

Three anomalies are incorporated in the prediction method. A track at 2.8 meters from the outflow and two areas with large mole activity, the first between 4 and 6 meters and the second between 12 and 13 meters from the outflow. These are represented as mole activity at 6 and 13 meters from the outflow.

Using the above as input, this yields a baseline-prediction and three anomaly predictions, see Figure 35. The final prediction is failure at 13 meters from the outflow, in the two hours of the 10 l/s per meter loading. If the experiment is continued, the grass cover will fail at 6 meters from the outflow during the first 50 l/s per meter session.

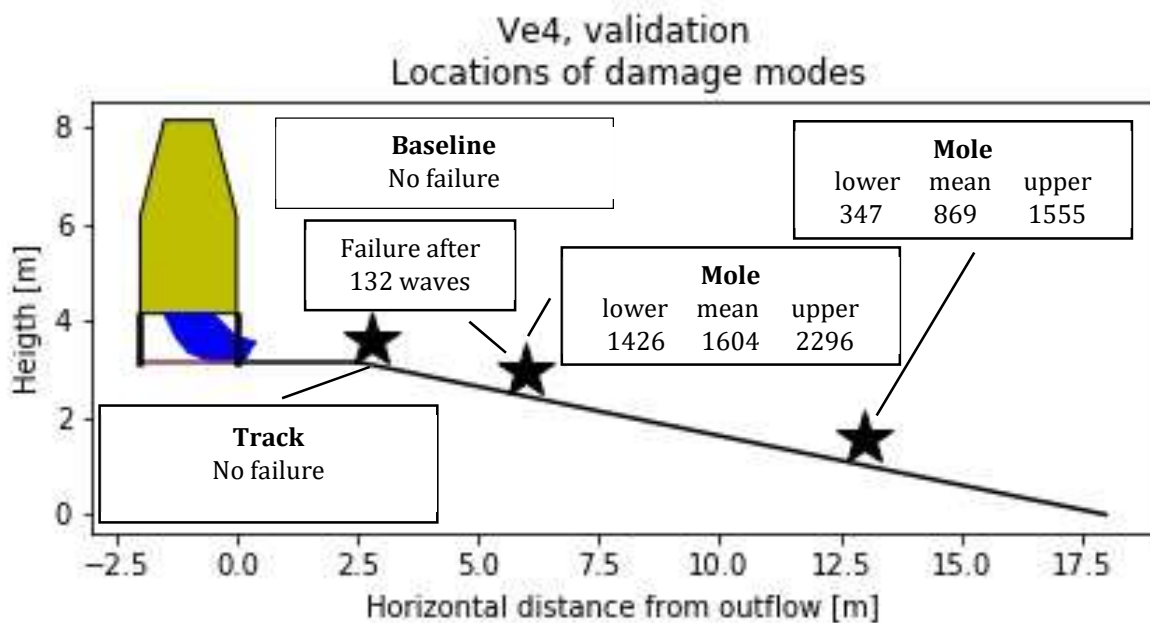


Figure 35 Test prediction, Ve4. In bold, the baseline or respective mode. 'lower' and 'upper' refer to the lower and upper bound of the specific predictions. The box with "failure" indicate the failure locations during the experiment, including the number of waves until failure.

During the first 5 l/s per meter session, the grass cover failed at two places in the upper mole activity region (53 till 132 waves). After the 5 l/s per meter sessions (290 waves), the erosion expanded downstream and only marginally in depth. See Figure 37. These kept expanding, until the experiment was stopped after 1hr of 30 l/s per meter (825 waves) due to a large hole that formed at 19 meters from the outflow, after the upstream erosion connected with the erosion at 19 meters from the outflow, see Figure 36.

The final prediction, cover failure at 13 meters from the outflow, is not correct. The grass cover failed at 6 meters from the outflow, but the prediction for this location was too optimistic, the failure occurred earlier than predicted.



Figure 37 Left: after the first 5 l/s/m session. Right: after the last 5 l/s/m session. Ve4.



Figure 36 After termination Ve4.

The experiment was stopped after 825 waves when the damage initiated at 6 meters from the outflow led to a large erosion pit downstream. Because the development of the damage, the only grass cover that is evaluated is that at the mole activity 6 meters after the outflow. Figure 38 shows the performance plot of this prediction. The cover failure is predicted correct, albeit later on in the experiment than it actually occurred. As can be seen in the performance plot, the experiment outcome falls outside the reach of the set of predictors.

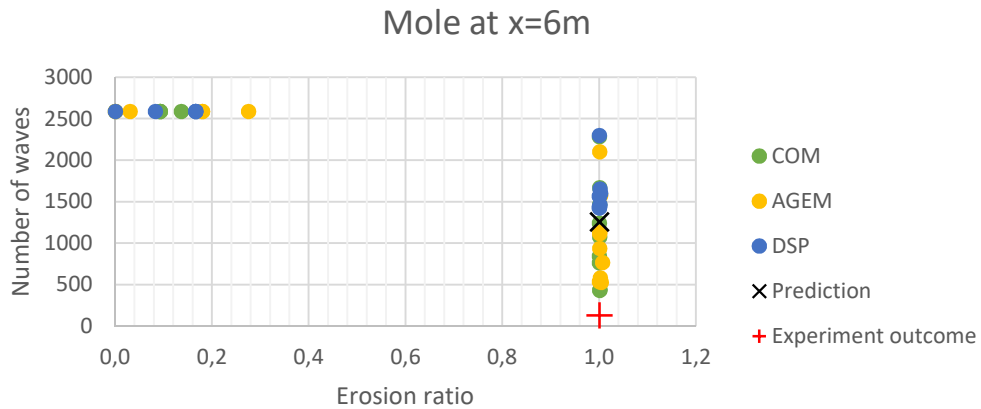


Figure 38 Performance plot mole at x=6m prediction, Ve4. Erosion ratio 1.0 represents failure.

#### 4.2.4 Tielrode section 1

The section is loaded with incremental loading, or until failure of the slope occurs. Each of the four loading steps represents a specific storm condition that last for two hours, the significant wave height is 0.75 to 1 meters and all loading steps combined consist of 2558 overtopping waves. The loading steps range from 1 to 50 l/m/s. The test section has a crest height of 5.2 meters, a crest width of 2 meters and a slope of 0.381 radians or 22 degrees.

Three anomalies are incorporated in the prediction method. A track at 1.5 meters from the outflow and the situation after the toe. An unknown anomaly, a small cliff in the slope, is included as mole-activity, too test if this would be representative since this is expected to be a weak spot.

Using the above as input, this yields a baseline-prediction and three anomaly-predictions, see Figure 39. The final prediction is no failure of the grass cover during the experiment.

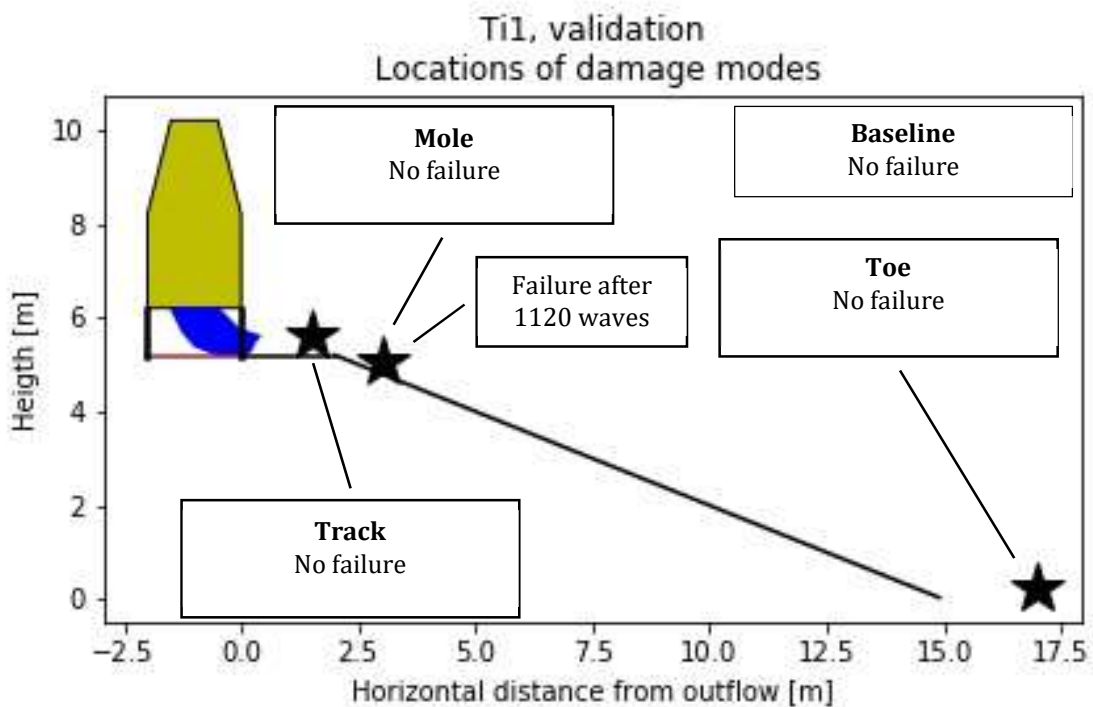


Figure 39 Test prediction, Ti1 In bold, the baseline or respective mode. 'lower' and 'upper' refer to the lower and upper bound of the specific predictions. The box with "failure" indicate the failure locations during the experiment, including the number of waves until failure.

After 36 minutes in the 30 l/s per meter session (1120 waves) the grass cover failed at the location of the cliff, modelled as mole activity, see figure 40. No damage was noted after the toe. The experiment was stopped after 40 minutes of 30 l/s per meter (1150 waves).

The final prediction was incorrect. The grass cover failed at 3 meters from the outflow, no other significant erosion development was noted.

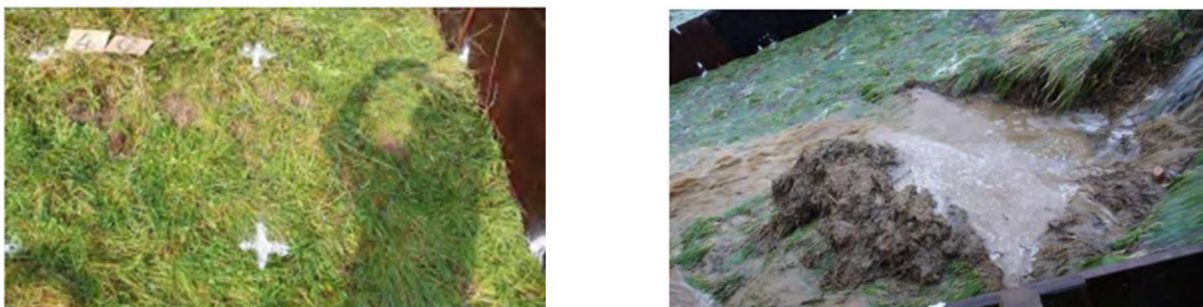


Figure 40 Small cliff, Ti1. Right: Initial condition. Left: Just before experiment termination

The location of failure was included in the prediction method as mole activity, based on experience it was expected that the cliff anomaly would have influence. Despite this, the failure was not predicted as the majority of predictors indicate no-failure, see the performance plot in Figure 41. Noted that the cliff is no mole activity, it is significant that some predictors indicated failure on the location before the end of the experiment.

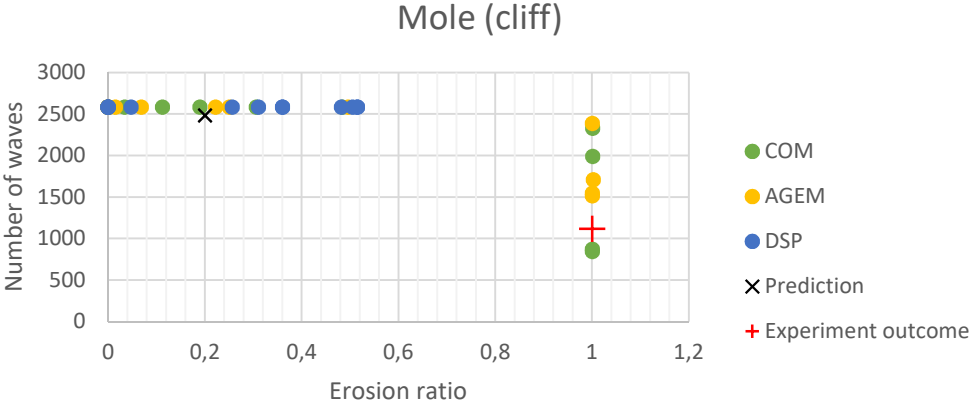


Figure 41 Performance plot mole (cliff) prediction, Ti1. Erosion ratio 1.0 represents failure.

4.2.5 Tholen section 4

The section is loaded with incremental loading, or until failure of the slope occurs. Each of the six loading steps represents a specific storm condition that last for 6 hours, the significant wave height is 2 meters and all loading steps combined consist of 5806 overtopping waves. The loading steps range from 1 to 50 l/m/s. The test section has a crest height of 5 meters, a crest width of 2 meters and a slope of 0.395 radians or 23 degrees.

Three anomalies are incorporated in the prediction method. The situation after the toe and mole-activity modelled at 5 and 11 meters from the outflow.

Using the above as input, this yields a baseline-prediction and three anomaly-predictions, see figure 42. The final prediction is failure at 5m and 11m after respectively 1562 and 1795 waves, both in the third 10 l/s per meter session. Toe failure after 2629 waves if the experiment is continued.

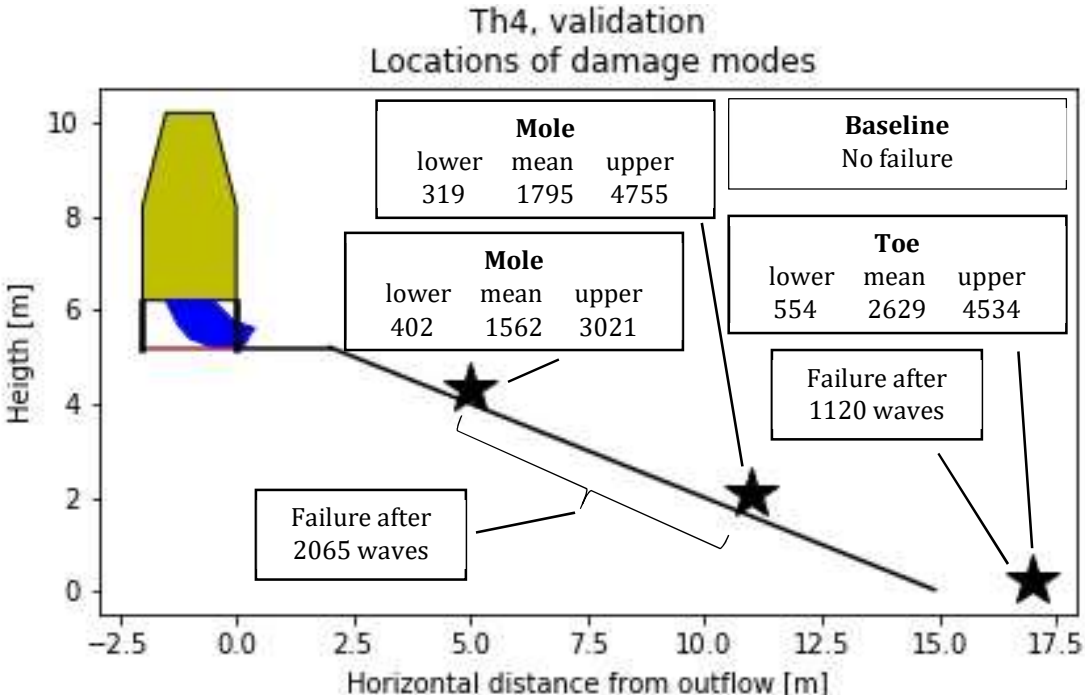


Figure 42 Test prediction, Th4. In bold, the baseline or respective mode. 'lower' and 'upper' refer to the lower and upper bound of the specific predictions. The boxes with "failure" indicate the failure locations during the experiment, including the number of waves until failure.

During the 5l/s per meter sessions erosion was developing just after the toe where a track and mole activity was present. At the end of the last session (1321 waves) the grass cover failed at the toe. After four hours in of 10 l/s per meter almost the entire toe has failed. After 4hr and 45min the session was paused. The damage was mitigated and 10 l/s per meter session finished. While the first 30 l/s per meter session did not change much, one and a half hour into the second session (2065 waves), the experiment was terminated due to large amounts of expelled sand. The origin of the sand moments later, when a large section subsided between 5 and 11 meters from the outflow.

Failure due to the mole activity did not emerge after 1562 or 1795 waves, but after 2065 waves when the surrounding slope subsided. But arguably the failure criterion was reached earlier, in the form of expelled sand. Detection of the expelled sand is not noted, as a result of mitigation measures for the toe. The toe-strength is predicted too optimistic, since it failed earlier than predicted. In both instances, the method was correct as for locating the failures. See Figure 43 for the end result, with the mitigation measures removed.



Figure 43 End result Th4

In Figure 44 and Figure 46 the performance plots are given of the predictions regarding the mole activity, using 2065 waves as moment of failure. In both cases the prediction is considered good, since both falls inside the 0.40-interval. Both predict failure (erosion ratio = 1), additionally, the prediction for x=5 has a wave ratio of 0.76 and for x=11 0.87.

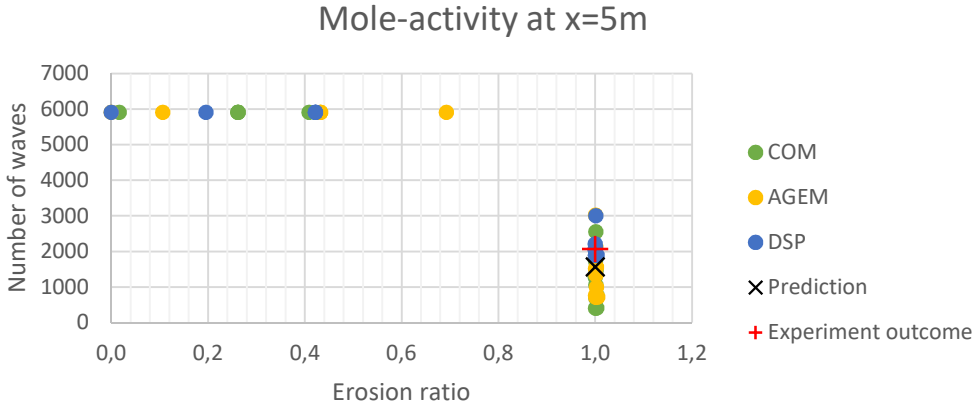


Figure 44 Performance plot mole-activity at x=5m prediction, Th4. Erosion ratio 1.0 represents failure.

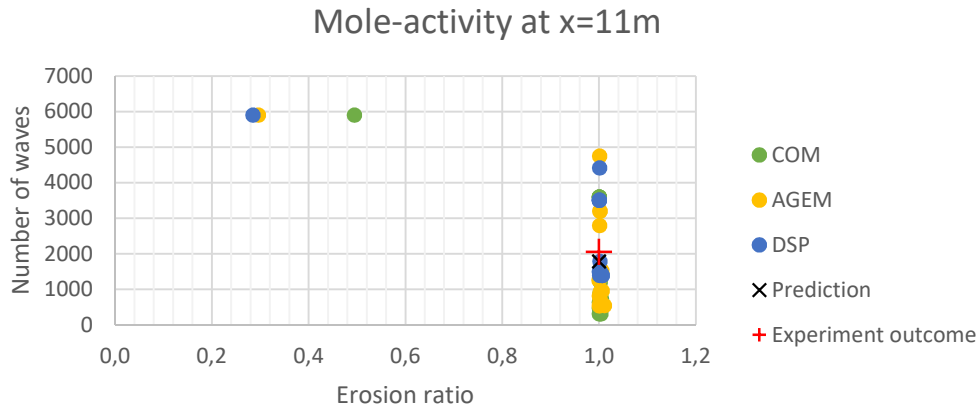


Figure 46 Performance plot mole-activity at x=11m prediction, Th4. Erosion ratio 1.0 represents failure.

Figure 45 shows the performance of the toe-prediction. The prediction that the grass cover would fail is correct, but the prediction is off by a factor 2 in the number of waves.

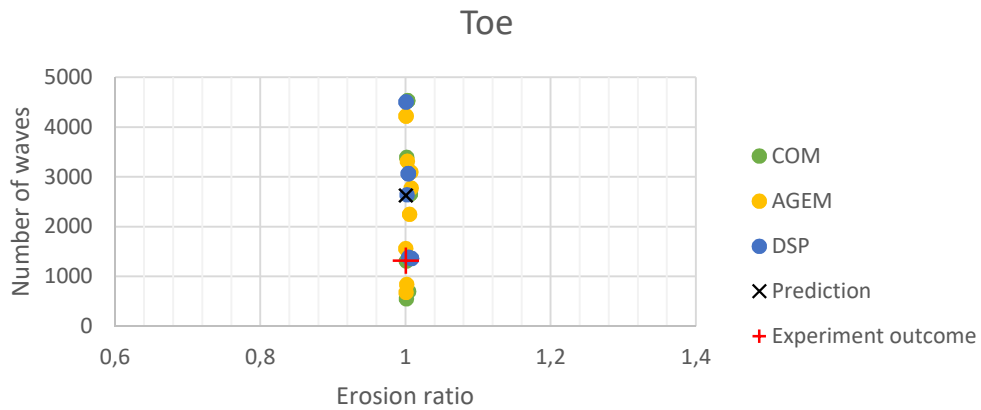


Figure 45 Performance plot toe prediction, Th4. Erosion ratio 1.0 represents failure.

#### 4.2.6 Validation summary

All grass cover failures in the validation set occurred on locations of anomalies, indicating the relevance of anomalies in predicting the course of an WOS experiment. The prediction method was able to indicate a failure location in four of the five validations, but in only one case the prediction method was able to predict the moment of failure within the 0.40-interval. Generally, the method is likely to overestimate the resistance against erosion in the validation. Either the grass cover fails before the predicted number of waves, or the grass cover fails when no failure was predicted.

## 5 Discussion

### **Animal activity**

In the evaluated set of experiments multiple incidents of animal activity are reported. This activity mainly consists of tunnelling of mice and moles. Whereas mice activity shown influence once, mole activity has frequently shown influence. The largest influence of animal activity emerged at incidents were washing of core material(sand) started early on, yielding very low calibrated critical velocities. This suggests that sand-core dikes are extra sensitive to this kind of conditions. The at Wijmeers-II suspected rabbit hole can be grouped under the previous case. In other cases of mole activity, the erosional resistance seems to be maintained, however only incidentally to the same extent as a grass cover without mole activity. This causes a spread in the calibrated critical flow velocities for locations with animal activity, these calibrated critical flow velocities represent the erosional resistance.

### **Relevance of grass cover quality**

Of all 23 experiments, 21 experiments showed damage development or failure at recorded anomalies on the slope before the overall erosion of the grass cover. Of the remaining two sections the anomalies were not recorded, as this was not part of the protocol in the beginning of WOS experimenting. This suggests that, when anomalies such as mole activity and tyre tracks compromise the overall grass cover, the grass cover quality is not the deciding factor. When a certain threshold grass quality is maintained, the erosional resistance is likely to depend on strength-aspects other than the grass cover quality. However, it is not necessarily the least erosional resistant area that is the weakest link, it is a coupling of resistance and loading that cause the extent of erosion that causes failure of the grass cover.

### **Strength vs. load based**

The prediction method includes a strength-based approach to link the underlying grass erosion models to the WOS experiments. When opting for a load based approach, a recording of anomalies in the grass cover may be avoided. Without neglecting the possible load variability, in the context of this research, an increase of load is not considered as a complete physical representation. Mathematically, it has limited meaning to choose between a load- or strength-based approach. For understanding the course of an experiment, a combination of load- and strength-based approach is expected to represent the physics better.

Despite this thesis is focussed on erosion of the crest and inner-slope, a pattern emerged outside the scope concerning the toe of the levee and beyond. Damage development in the region past the slope occurred frequently, 12 times in the test dataset and twice in the validation dataset. Bergeijk, Warmink, Frankena, et al. (2019) suggest that the damage development is due to an increase of load. Zooming into each individual damage development this study suggests that it is not only a possible increase of load that causes the damage development, but a decrease of strength may contribute significantly. Examples: gravel boxes and pavers just below the surfaces, causing a failure plane; semi-pavement; asphalt-pavement. All 10 cases of failure at the toe the test dataset showed signs of a decrease in strength.

### **Dataset size**

This research is based on full scale wave overtopping experiments using the wave overtopping simulator, this results in 32 sections that have undergone a wave overtopping experiment with a comparable test set-up. Despite the comparable test set-up, the experiment outcomes vary significantly per test section due to variations in the anomalies, which made the reproducibility of experiment outcomes very poor. Because of the limited dataset and the varying experiment outcomes, it is difficult to draw conclusions. For anomalies, especially for anomalies that show no or limited damage development, this is even more difficult. A possible conclusion is that these cases due to early termination of the experiment are not relevant, but this can be a false conclusion since experiments are often terminated early due to failure on a different location.

### **Sample quality**

If the set of experiments were to represent a sample of all existing levees, it is questionable how (un)biased this sample is. Often, the selection of test-sections is done to be representative for the relative levee-trajectory, or sometimes a section is chosen to include a certain element. During a field visit at the Vechtdijk 2021 it became apparent that it is common practice that an experienced worker sets out the test sections, with the aim to set representative sections with respect to the surrounding levee conditions. This

implies that the test sections are not a result of random sampling, but are biased to represent the expected average. Without (dis)approval of this method to set the sections, it is important to keep this in mind when extrapolating to the bigger picture. Since the resistance against erosion of the inner-slope appears to be too large extent dependent on the locations where the grass cover is distorted, instead of overall grass cover quality. This suggests that the majority of experiments are not part of a representative sampling, since non-representative conditions of surrounding levee conditions are excluded. This means that the weakest links are possibly excluded from the sample.

### **Initial damage registration**

Factual reports include initial registrations that are an important source of information (“nul opnames” in Dutch). These initial registrations are records of a close inspection of each individual test section before the start of the experiment on that section, the initial condition of the slope in the test section. The registrations have to be interpreted with care, since the method, assessment of the circumstances and wording for these registrations can be ambiguous. Despite this, these registrations give a rendering of the overall state to help understand the influence of anomalies and interpret experiment outcomes.

### **Failure criterion Dean Stream Power**

Dean et al. (2010) suggested different failure criteria for poor, moderate and good grass covers. In this research the threshold for good grass covers is chosen at  $4.92 \cdot 10^5 \text{ m}^3/\text{s}^2$ . However, even with extremely low values for the critical flow velocity the failure criterion could not be met for three cases of mole activity. This suggests that the cover-dependent failure criterion of Dean et al. (2010) may be included in certain circumstances, at cases of extremely low erosional resistance.

### **Wave Impact Approach**

The Wave Impact Approach looked promising because of the distinct modelling of the load. The load is modelled as transferred moment perpendicular to the slope-surface caused by the re-attachment of the overtopping wave. The failure process is using the exchange of momentum, initiated by the impact of the flow when reattaching to the surface. This is fundamentally different from the flow-based models. The flow-based models describe the failure process as an exchange of momentum (velocity squared) or as an exchange of energy (velocity cubed) with the surface when the overtopping water flows over the surface.

When comparing the WIA- realization per section with the experiment outcome of the respective section, six sections show an overlap in WIA-influence and damage development. Unfortunately, the sections with overlap provided too little information to calibrate the WIA for use in the prediction method.

### **Performance metric**

The performance metric used in this thesis is capable to present in one figure for one location i) if grass cover failure is predicted correct and ii) if this is predicted after the correct number of waves. With a performance metric for the baseline and one per anomaly. The erosion ratio is introduced to compare outputs of different models, with respect to the outcome of the experiment. This is applicable for performance of the calibrations and for the performance of the validation predictions. The wave ratio is introduced to compare experiments with different number of waves before failure of the grass cover. This applicable for the calibration performance, for prediction performance the number of waves is used.

The dots in the performance metric are prone to lie close to either the line of erosion ratio = 1 or wave ratio = 1. This occurs during calibration due to a certain combination of erosion and number of waves acting as a target for the calibration. Fitting the model to the combination frequently caused one of the ratio's to be a near perfect match, with a deviation for the other. In other cases, a small deviation of both ratios was most approvable. For the performance metric of predictions, the dots on a vertical line indicate the same erosion prediction, this has to be taken relative to the experiment outcome.

The performance metric lacks the capability to include multiple locations, since a separate metric is constructed for each location of interest (baseline and anomalies). Also, at this stage no differentiation has been made in the predictors to group predictions based on specific properties. In the research for this thesis no ground for differentiation has been identified, considering general levee properties. Future research may lead to a performance metric to include location and give proof that certain properties can be used for differentiation. Suggestion for differentiation is the depth of anomalies or other properties of anomalies.

## 6 Conclusion and Recommendations

This thesis provides a method to produce predictions of wave overtopping experiments and a large scale comparison of models and experiments. The prediction method is a tool to combine experimental data from WOS experiments with grass erosion models to come to a prediction for a WOS experiment. The core of the prediction method is the creation of a set of predictions, combination of these predictions leads to the final prediction. The set of predictions is created by the set of predictors; each predictor provides a prediction. The predictors are configured by fitting grass erosion models to known WOS experiments leading to calibrated models that form the set of predictors; each combination of experiment and grass erosion model yields one predictor. The validations show that the method is able to indicate failure on non-maximum load locations but indication of the moment of failure is less successful.

### 6.1 Conclusions

#### **Which models can be of value in the prediction method?**

Four models are used in this thesis, as these are expected to be of value in the new method because of their variety in approach. The Cumulative Overload Method (COM) is in use since the start of the WOS experiments and is a model that gives the extent of erosion in the form of damage number  $D$ , as a measure of the overloading of the critical shear stress. The shear stress is represented by the flow velocity squared as a loading parameter, and as a critical flow velocity as a strength parameter. The Analytical Grass Erosion Model (AGEM) is a more physical model, as it gives the extent of erosion as erosion depth. The erosional modelling is covered by an adapted version of the model of Hoffmans, which is, like the COM, shear stress based but computed using flow velocity squared. The Dean Stream Power model (DSP) is introduced in this thesis and gives the extent of erosion in a physical but abstract unit, erosion work units. In contrast to the first two, the DSP uses velocity cubed in the computations. The fourth model that can be of value to the new method is the Wave Impact Approach (WIA), this model is fundamentally different from the previous three in the way the load and strength is modelled. During the course of the research it appeared that the COM, AGEM and DSP methods were valuable as part of the new method developed in this thesis. Unfortunately, it is concluded that the WIA does not have a substantial overlap with the grass cover erosion during the experiments and more importantly, the strength parameter and failure criterion could not be unambiguously determined.

#### **Which WOS experiment data can be used for calibrating/validating?**

The majority of the available data obtained from the factual reports, with accompanying reports and appendices. The control lists of the WOS were available in different formats over the years, these have been prepared for use in calibration of the new method without changing the loading sequences. Data from experiments outside of the Netherlands are available, but these are intentionally not included in this research because of very different circumstances. In total 32 sections were available, of which 23 sections were used in development, calibration and testing of the new method, five sections were used to validate the new model, four sections were omitted since non-grass elements dominated the tests.

#### **What ways are available to combine predictions of single models?**

Due to the limited dataset and variability in the dataset, it is concluded that averaging is the only applicable way in the context of this thesis. To combine failure- and no-failure predictions a voting-step is incorporated in the combination method of the prediction method. The conditions of the experiments vary to a large extent with respect to initial and loading conditions, geometry and outcomes. In addition, experiments seem to be very hard to reproduce as they yield very different outcomes on test sections only a few meters apart. Some trend may be seen when considering sand and clay levees, but all experiments on sand levee sections come from the Vechtdijk 2010 experiments.

#### **How does the prediction method perform in a prediction case?**

The validation set consists of five experiments that are put aside at the start of the research. For two anomalies the method was unable to predict failure, because no such failure occurred in the test dataset. All grass cover failures in the validation set occurred on locations of anomalies, indicating the relevance of anomalies in predicting the course of a WOS experiment. The prediction method was able to indicate at least one correct failure location in four of the five validations, but in only at Tholen section 4 the prediction method was able to predict the moment of failure within the 0.40-interval. Unfortunately, grass cover failure occurred on another location before this. Generally, the method is likely to overestimate the resistance against erosion. This means either the grass cover fails before the predicted number of waves, or the grass cover fails when no failure was predicted.

### **How can grass erosion models and WOS experiment data be combined in a prediction method to generate predictions of the moment and location of the damage initiation by grass erosion due to wave overtopping?**

In order to model the location of damage initiation in the method presented in this thesis, the load has been made location dependent for all models. For the COM, AGEM and DSP this is achieved by using the analytical flow velocity model as load input. This load input has the additional advantage that this creates a level playing field for these three velocity-based models, preventing that different ways of hydrodynamic modelling can add noise in the erosion predictions. In addition, the analytical flow velocity model computes the load per overtopping event, yielding the opportunity to compute the moment of grass cover failure. For the AGEM, this is acceptable since this model is originally based on this hydrodynamic model. For the COM it has shown to be acceptable to use the analytical flow velocity model as input because of the similar results of the COM with the analytical hydrodynamic model and the COM with the acceleration factor. The work-based approach by Dean et al. (2010) is coupled with the stream power derivation by Hughes (2011) to create the DSP model. The input for the DSP from the analytical hydrodynamic model provides a more realistic description of the flow velocity than the terminal velocity approach as used by Dean et al. (2010).

Simulations showed that a baseline strength with location dependent flow velocity input could not include damage initiation predictions higher up the slope. In order to implement this in the models, either the load or the strength has to be influenced locally and be spatially limited. Study of the factual reports on WOS experiments suggested that a strength-based influence is physically the most applicable, this gave rise to a location dependent and damage scenario dependent strength parameter for all velocity-based models.

During validation, none of the final predictions were fully correct. Meaning that none of the final predictions correctly indicated the location and moment of the first grass cover failure. Despite this, in four of the five validations at least one correct failure location was indicated when considering the specific anomalies. The main shortcoming is concluded to be the prediction of number of waves until grass cover failure.

#### **Animal activity**

At 13, of the 23 test-data sections, mole activity on the slope was recorded as initial condition. Of these 13 sections, mole activity had a negative outcome at 11 sections. These are used to calibrate the resistance against erosion in case of mole activity (critical velocities). The average resistance of the mole activity of these 11 sections decreased with 46% relative to the average of all sections with a calibrated critical velocity for the undistorted grass cover. Respectively for the COM, AGEM and DSP in m/s: 4.5 vs. 7.8, 12.7 vs. 22.4 and 3.8 vs. 7.8. This shows a significant likelihood of decrease of the resistance against erosion when mole activity is present at the slope. Next to mole activity, at one section rabbit-activity was suspected, this activity had destructive consequences similar to the more destructive cases of mole activity. On several sections mice-activity was recorded, but this only led to failure at one section in the validation set. Activity from other animals is not recorded in the studied experiments.

#### **Grass cover quality**

Of the 28 sections in the data set, at least 22 times the failure condition was reached due to something else than erosion of the average grass cover. This suggests that an approach where the average grass cover is normative will overestimate the erosional resistance, because anomalies are excluded from this type of average.

For design this means that also conditions, other than the average grass quality, should be considered. For instance, the probability of the occurrence of animal activity or tyre tracks, with a corresponding erosional resistance.

For safety assessments this means that the erosional resistance is not strictly dependent on the average grass cover, it is more likely that this is dependent on locations with the low erosional resistance. This suggests that a complete and detailed inventory of the levee slope surface is needed, which may not be feasible. Other approaches to include locations with low erosional resistance should include considerations to include possible extreme values.

## **Relevance**

This is not a finished method to implement for levee design. This method is a suggestion to use experimental data to understand and model the process of grass cover erosion, to help the understanding of relevant conditions and parameters, to guide future research. This model can be used to predict future experiments and help understanding the course of these experiments.

## **6.2 Recommendations**

Based on the findings, recommendations have been drawn up.

### **Contributing factors**

It has been shown that failure is often initiated on locations where the initial condition differs from the uncompromised grass cover and often at locations where the load is not maximum. Focus on initial conditions (anomalies) other than average grass quality and maximum load locations can be of value in understanding the resistance against erosion of a levee inner-slope. Monitoring and registration of these can be a challenge because these can vary and can be difficult to identify. Innovative monitoring systems may offer a solution to better map the condition of the grass cover of levees. This way, potential weak spots can be detected and monitored in an early stage. Measures can be taken if necessary.

### **Hydraulic calibration**

In this thesis, a single calibration of the hydrodynamic model is applied in the form of the friction parameter  $f$  equal to 0.01. Application of this model with constant  $f$  yielded sensible results and for the large wave volumes the influence of  $f$  is proven to be limited (Appendix E), therefore this is considered sufficiently accurate in this context knowing that the large wave volumes are usually normative. In order to conclude if the assumption is truly valid, a future research question may be: Does extensive calibration of the hydrodynamic model on each individual experiment result in an increased accuracy of predictions?

### **Data-set size**

Ongoing Wave Overtopping Simulator testing will increase the dataset. Including the new data in the prediction method will likely improve predictions and may result in identifying causality between experiments. In addition, future research may also lead to some way of including initially ignored experiment data, for example, if it is proven to be correct to mix experimental data from different areas in the world.

Next to increasing the size of the data-set, it could be beneficial to apply more detailed models to get more insight into the erosional processes when zooming in into a specific circumstance. For instance, why a certain case of mole activity or tyre track showed less erosional resistance to a comparable case. Unfortunately, data availability may prove to be problematic. The accuracy of registrations of the dimensions of the specific circumstances can be insufficient and hydraulic measurements are not a common part of the experiments.

### **Combination**

To improve predictions, an improved way of handling the “no-failure” predictions is recommended. In the current form the majority vote is necessary to cope with the combination of numerical values and Boolean values (failure=1, non-failure=0) in the ensemble, this can create a distorted image if the ensemble majority predicts “failure”. This distortion finds its origin in the fact that optimistic “non-failure” predictions are excluded from the average, because “non-failure” are not included in the average and only “Failure” is included. Including “non-failure” as a numerical value is non-trivial, because which numerical value is representative in each specific case? A suggestion is to weigh the average accordingly with some representation the number of “no-failure” predictions.

Next to this, the combination technique may be further developed by specific study on combinations, for instance conditionality. In the context of this thesis it is concluded not to be appropriate to differentiate based on the present knowledge, progressive insights may prove to suggest a correct and optimized combination technique.

### **Length-effects**

Anomalies in the grass cover can lead to a decrease in erosional resistance of the levee slope against wave overtopping. For WOS experiment test sections, anomalies are registered before the start of the

experiment. These registrations include anomalies that had no influence on the course of the experiment, and anomalies where grass cover failure occurred. Extrapolating this to a levee trajectory, the length-effect principle indicates that more extreme anomalies cannot be excluded. Therefore, it is recommended to not only investigate influence of anomalies at the level of a test section, but also investigate the spatial distribution of anomalies at the level of levee trajectories.

### **Animal activity**

This research indicates a decrease of strength at anomalies, especially at places with animal(mole) activity. Therefore, it is recommended to focus on understanding how animal activity affects the erosional resistance of the grass cover. And next how, despite this influence, a certain strength-level still can be guaranteed, keeping in mind the large spread observed in the experiment outcomes.

In The Netherlands, the levee manager has the duty of care (*Zorgplicht*) and has to assess regularly if the levee is in accordance with the (design)requirements(*Helpdesk Water, 2021*). How to tread animal activity during an assessment is not stated, and if the design did not account for animal activity no guidelines are given. Because of the significant influence of animal activity on the resistance against grass erosion due to wave overtopping, it is recommended to develop a protocol to include this in the guidelines for the duty of care.

Accounting for animal activity in design and/or assessment can be done by assuming a certain critical flow velocity that represents the resistance against erosion, since it is highly likely that a levee will be subjected to animal activity during its lifetime. A first suggestion could be assuming 46% of the critical flow velocity for the expected average grass cover, implying a dependency between these two aspects. However, based on the study of the factual reports, this dependency may not be accurate. It is more likely that the influence of the animal activity depends on properties of the anomaly, for instance if this anomaly reaches the sand core of a levee.

A definitive approach to incorporate animal activity (or other anomalies) in either design or assessment practices is not to be concluded based on this thesis. For future research, the following approach is suggested. Divide the cases of mole activity into classes, based on for example either certain characteristics or a certain damage development. Each class is assigned a certain resistance against erosion and provide for each class certain unique characteristics to distinguish between classes. For design, based on the specific attributes of the design, the probability of occurrence of each class must be determined and combined with the corresponding influence on the resistance against erosion. For assessment, an inventory or representative sample of animal activity must be available to asses if the occurrences of animal activity are within the design requirements.

## References

- Bakker, J. J., Galema, A. A., Mom, R. J. C., & Steendam, G. J. (2010). *Factual Report / Overslagproef Vechtdijk*.
- Bakker, J. J., Melis, R., & Mom, R. J. C. (2013). *Factual Report: Overslagproeven Rivierenland*. 105.
- Bakker, J. J., & Mom, R. J. C. (2015). *Factual report / overslagproef Wijmeers 2*.
- Bakker, J. J., Mom, R. J. C., & Steendam, G. J. (2008a). *Factual Report / Golfoverslagproeven Friese Waddenzeedijk* (Issue Imc).
- Bakker, J. J., Mom, R. J. C., & Steendam, G. J. (2008b). *Factual Report / Golfoverslagproeven Zeeuwse zeedijken*.
- Bakker, J. J., Mom, R. J. C., & Steendam, G. J. (2009). *Factual Report / Overslagproeven en afschuifproef Afsluitdijk*.
- Bakker, J. J., Mom, R. J. C., Steendam, G. J., & Meer, J. W. van der. (2011). *Factual Report / Overslagproeven en oploopproof Tholen* (Issue Imc).
- Bomers, A., Aguilar Lopez, J. P., Warmink, J. J., & Hulscher, S. J. M. H. (2018). Modelling effects of an asphalt road at a dike crest on dike cover erosion onset during wave overtopping. *Natural Hazards*, 93(1). <https://doi.org/10.1007/s11069-018-3287-y>
- CIRIA. (2013). The International Levee Handbook. In *Ciria C731*. §
- D'Eliso, C. (2007). *Breaching of sea dikes initiated by wave overtopping: A tiered and modular modelling approach* (Issue May).
- de Vries, G., ter Brake, C. K. E., de Bruijn, H., Koelewijn, A. R., van Lottum, H., Langius, E. A. F., & Zomer, W. S. (2013). *Dijkmonitoring: beoordeling van meettechnieken en visualisatiesystemen Eindrapport*. 108.
- Dean, R. G., Rosati, J. D., Walton, T. L., & Edge, B. L. (2010). Erosional equivalences of levees: Steady and intermittent wave overtopping. *Ocean Engineering*, 37(1), 104–113. <https://doi.org/10.1016/j.oceaneng.2009.07.016>
- Frankena, M. (2019). Modelling the influence of transitions in dikes on grass cover erosion by wave overtopping. *Master Thesis, University of Twente, Water Engineering and Management, July*. [https://essay.utwente.nl/79017/1/Frankena%2C M. 1570234 \\_openbaar.pdf](https://essay.utwente.nl/79017/1/Frankena%2C%20M.1570234_openbaar.pdf)
- Helpdesk Water*. (2021). <https://www.helpdeskwater.nl/onderwerpen/waterveiligheid/primaire/zorgplicht/>
- Hoffmans, G. (2014). *Erosiebestendigheid overgangen*.
- Hughes, S. A. (2011). Adaptation of the levee erosional equivalence method for the hurricane storm damage risk reduction system (HSDRRS). *Erdc\Chl Tr-11-3, May*, 1–142.
- Hughes, S., Thornton, C., Meer, J. W. van der, & Scholl, B. (2012). Improvements in describing wave overtopping processes. *Proceedings of the Coastal Engineering Conference*, 1–15. <https://doi.org/10.9753/icce.v33.waves.35>
- Jonkman, S. N., Jorissen, R. E., & Schweckendiek, T. (2018). *Flood defences / Lecture notes CIE5314 3rd edition 2018*.
- Peeters, P., Vos, L. de, Vandevoorde, B., Taverniers, E., & Mostaert, F. (2012). *Stabiliteit van de grasmat bij golfoverslag / Golfoverslagproeven Tielrodebroek (versie 2.0)*.
- Ponsioen, L. A. (2016). *Overflow and wave overtopping induced failure processes on the land-side slope of a dike*. TU Delft.
- Ponsioen, L. A., & Damme, M. Van. (2016). *Breach experiment Wijmeers II / Breach initiation due to overflow and overtopping*.
- Ponsioen, L. A., Van Damme, M., Hofland, B., & Peeters, P. (2019). *Relating grass failure on the landside slope to wave overtopping induced excess normal stresses*. 8.

<https://doi.org/10.1016/j.coastaleng.2018.12.009>

- Rikkert, S. J. H., Koelewijn, A. R., Depreiter, D., Peeters, P., Verelst, K., & Vercruyssen, J. (2020). *Model validation plan\_v2*.
- Steendam, G. J. (2011). *VERSLAG GOLFOVERSLAGPROEVEN TIELRODE*.
- Steendam, G. J. (2017). *Eisen grasbekledingen*.
- US Army Corps of Engineers. (2006). *Performance Evaluation of the New Orleans and Southeast Louisiana Hurricane Protection System: Final Report of the Interagency Performance Evaluation Task Force: Vol. V* (Issue June). <https://ipet.wes.army.mil/>
- van Bergeijk, V. M., Warmink, J. J., Frankena, M., & Hulscher, S. J. M. H. (2019). Modelling Dike Cover Erosion by Overtopping Waves: The Effects of Transitions. *Hydraulic Engineering Repository*, 1097–1106. <https://doi.org/10.18451/978-3-939230-64-9>
- van Bergeijk, V. M., Warmink, J. J., & Hulscher, S. J. M. H. (2020). Modelling the wave overtopping flow over the crest and the landward slope of grass-covered flood defences. *Journal of Marine Science and Engineering*, 8(7), 1–30. <https://doi.org/10.3390/JMSE8070489>
- van Bergeijk, V. M., Warmink, J. J., van Gent, M. R. A., & Hulscher, S. J. M. H. (2019). An analytical model of wave overtopping flow velocities on dike crests and landward slopes. *Coastal Engineering*, 149(October 2018), 28–38. <https://doi.org/10.1016/j.coastaleng.2019.03.001>
- Van Damme, M., Ponsioen, L., Herrero, M., & Peeters, P. (2016). Comparing overflow and wave-overtopping induced breach initiation mechanisms in an embankment breach experiment. *E3S Web of Conferences*, 7(June). <https://doi.org/10.1051/e3sconf/20160703004>
- van der Meer, J. W., Allsop, N. W. H., Bruce, T., De Rouck, J., Kortenhaus, A., Pullen, T., Schüttrumpf, H., Troch, P., & Zanuttigh, B. (2018). *Manual on wave overtopping of sea defences and related structures / An overtopping manual largely based on European research, but for worldwide application*. 320.
- van der Meer, J. W., Bernardini, P., Steendam, G. J., Akkerman, G. J., & Hoffmans, G. (2010). *Wave Overtopping Simulator tests in Viet Nam*. 645–656. [https://doi.org/10.1142/9789814282024\\_0057](https://doi.org/10.1142/9789814282024_0057)
- van der Meer, J. W., Hardeman, B., Steendam, G. J., Schüttrumpf, H., & Verheij, H. (2010). FLOW DEPTHS AND VELOCITIES AT CREST AND LANDWARD SLOPE OF A DIKE, IN THEORY AND WITH THE WAVE OVERTOPPING SIMULATOR. *Coastal Engineering*, 2007.
- van der Meer, J. W., Hoven, A. van, Paulissen, M., Steendam, G. J., Verheij, H., Hoffmans, G., & Kruse, G. (2012). *Handreiking Toetsen Grasbekledingen op Dijken t.b.v. het opstellen van het beheersoordeel (BO) in de verlengde derde toetsronde*. 196.
- van der Meer, J. W., Schrijver, R., Hardeman, B., Van Hoven, A., Verheij, H., & Steendam, G. J. (2010). Guidance on erosion resistance of inner slopes of dikes from three years of testing with the Wave Overtopping Simulator. *Coasts, Marine Structures and Breakwaters: Adapting to Change - Proceedings of the 9th International Conference*, 2(1994), 460–473. <https://doi.org/10.1680/cmsb.41318.0044>
- van der Meer, J. W., Steendam, G. J., Mosca, C. A., Bolatti Guzzo, L., Takata, K., Cheong, N. S., Eng, C. K., Lj, L. A., Ling, G. P., Wee, C., Seng, C. W., Karthikeyan, M., Yap SC, F., & Govindasamy, V. (2020). *WAVE OVERTOPPING TESTS TO DETERMINE TROPICAL GRASS SPECIES AND TOPSOILS FOR POLDER DIKES IN A TROPICAL COUNTRY*. 1–15.
- van Dijk, P. M. (2021). *Wave Overtopping Simulator Control List Files*. <https://doi.org/10.4121/15173100>
- van Hoven, A., Groot, M. B. de, van der Meer, J. W., Akkerman, G. J., Verheij, H. J., Frissel, J. Y., & Steendam, G. J. (2007). *Golfoverslag en Sterkte Grasbekleding / Fase 1D Evaluatie Delfzijl* (Issue December).
- van Hoven, A., Verheij, H. J., & van der Meer, J. W. (2009). *SBW Golfoverslag Grasbekleding en Sterkte*.
- Warmink, J. J., van Bergeijk, V. M., Frankena, M., van Steeg, P., & Hulscher, S. J. M. H. (2020). MODELLING TRANSITIONS IN GRASS COVERS TO QUANTIFY WAVE OVERTOPPING a b. *ICCE*, 1–8. <https://doi.org/https://doi.org/10.9753/icce.v36.papers.53>

## Appendix A – Overview of WOS experiments

Part of the research was an extensive study of the factual reports regarding the wave overtopping experiments. References to the factual reports can be found in the table below. The study of these factual reports is partially summarized in the “Properties” table and “Remarks” table of this Appendix. The “Properties” table covers the test datasets and contains the geometry properties of the sections, basic soil parameters, basic loading parameters and the occurrence of animal activity. The “Remarks” table contains remarks concerning erosion development and failure modes.

<b>Locations</b>	<b>Section ID's</b>	<b>Reference</b>
Delfzijl, Groningen, 2007	De1, De2, De3	van Hoven, A., Groot, M. B. de, van der Meer, J. W., Akkerman, G. J., Verheij, H. J., Frissel, J. Y., & Steendam, G. J. (2007). <i>Golfoverslag en Sterkte Grasbekleding / Fase 1D Evaluatie Delfzijl</i> (Issue December).
Boonweg, Friesland, 2008	Bo1, Bo2, Bo3, Bo4	Bakker, J. J., Mom, R. J. C., & Steendam, G. J. (2008a). <i>Factual Report / Golfoverslagproeven Friese Waddenzeedijk</i> (Issue Imc).
St Philipsland, Zeeland, 2008	Sp1	Bakker, J. J., Mom, R. J. C., & Steendam, G. J. (2008b). <i>Factual Report / Golfoverslagproeven Zeeuwse zeedijken</i> .
Kattendijke, Zeeland, 2008	Ka1, Ka2	Bakker, J. J., Mom, R. J. C., & Steendam, G. J. (2008b). <i>Factual Report / Golfoverslagproeven Zeeuwse zeedijken</i> .
Afsluitdijk, 2009	Af1, Af2, Af3	Bakker, J. J., Mom, R. J. C., & Steendam, G. J. (2009). <i>Factual Report / Overslagproeven en afschuifproef Afsluitdijk</i> .
Vechtdijk, Overijssel 2010	Ve1, Ve2, Ve3, Ve4	Bakker, J. J., Galema, A. A., Mom, R. J. C., & Steendam, G. J. (2010). <i>Factual Report / Overslagproef Vechtdijk</i> .
Tielrode/Antwerp, 2010	Ti1, Ti2, Ti3, Ti4	Peeters, P., Vos, L. de, Vandevoorde, B., Taverniers, E., & Mostaert, F. (2012). <i>Stabiliteit van de grasmat bij golfoverslag /Golfoverslagproeven Tielrodebroek (versie 2.0)</i> . Steendam, G. J. (2011). <i>VERSLAG GOLFOVERSLAGPROEVEN TIELRODE</i> .
Tholen, Zeeland, 2011	Th1, Th2, Th3, Th4	Bakker, J. J., Mom, R. J. C., Steendam, G. J., & Meer, J. W. van der. (2011). <i>Factual Report / Overslagproeven en oplooproef Tholen</i> (Issue Imc).
Nijmegen, Gelderland, 2013	Ni1, Ni2, Ni3	Bakker, J. J., Melis, R., & Mom, R. J. C. (2013). <i>Factual Report: Overslagproeven Rivierenland</i> . 105.
Millingen, Gelderland, 2013	Mi1, Mi2	Bakker, J. J., Melis, R., & Mom, R. J. C. (2013). <i>Factual Report: Overslagproeven Rivierenland</i> . 105.
Wijmeers-II, 2015	Wi1, Wi2	Bakker, J. J., & Mom, R. J. C. (2015). <i>Factual report / overslagproef Wijmeers 2</i> . Ponsioen, L. A., & Damme, M. Van. (2016). <i>Breach experiment Wijmeers II / Breach initiation due to overflow and overtopping</i> .

# Properties table

	Bc: distance outflow-inner crest line	H: Crest height	phi: slope angle	core material	Clay cover	specified clay layer thickness	average sand content	max sand content	Hs: significant wave height	Discharges l/s/m	Intended duration per discharge session (hr)	Mice	Mole	Rabbit	Track
De1	0.1	5.4	0.343	Clay	Yes	n/a	0.27	0.59	2	0.1; 1; 10; 20; 30 ;50	6				
De2	0.1	5.4	0.343	Clay	Yes	n/a	0.27	0.59	2	0.1; 1; 10; 20; 30 ;50	6				
Bo1	3	7.25	0.332	Sand	Yes	0.60 m	0.66	0.69	2	0.1; 1; 10; 30; 50; 75	6				
Bo2	3	7.25	0.332	Sand	Yes	0.60 m	0.66	0.69	2	0.1; 1; 10; 30; 50; 75	6	X			X
Bo4	4	7.25	0.332	Sand	Yes	0.60 m	0.66	0.69	2	0.1; 1; 10; 30; 50; 75	6	X			X
Sp1	2	4.25	0.395	Sand	Yes	0.40 m	0.51	0.52	2	0.1; 1; 10; 30; 50	6		X		X
Ka1	2	4.7	0.322	Sand	Yes	0.75 m	0.66	0.69	2	0.1; 1; 10; 30; 50; 75	6		X		X
Ka2	2.5	4.5	0.322	Sand	Yes	0.75 m	0.66	0.69	2	30; 50	6		X		X
Af1	0.1	2.9	0.367	Sand	Yes	0.40m + 1m	0.51	0.64	2	1; 10; 30; 50; 75	6				X
Ve2	3	2.7	0.201	Sand	No	n/a	Sand	0.93	2	0.1; 1; 5; 10; 30; 50	6		X		X
Ve3	3	3	0.201	Sand	No	n/a	Sand	0.93	1	0.1; 1; 5; 10; 30; 50	6		X		X
Ti2	1.5	5.2	0.381	Clay	No <sup>(1)</sup>	n/a	0.61	0.65	0.75/1	1; 10; 30	2		X		X

Ti3	2	4.8	0.278	Clay <sup>(2)</sup>	No <sup>(1)</sup>	n/a	0.44	0.51	0.75/1	1; 10; 30; 50; 1; 10; 30; 50;	2			
Ti4	1.5	5.4	0.381	Clay	No <sup>(1)</sup>	n/a	0.61	0.65	3	1; 5; 10	2		X	X
Th1	2	2.6	0.257	Clay	Yes	1 m	0.45	0.47	2	1; 10; 30	6			
Th3	2	4.6	0.367	Clay	Yes	1 m	0.4	0.47	2	1; 5; (10; 30; 50)	6		X	
Ni1	5	2.8	0.355	Sand	Yes	0.60 m <sup>(3)</sup>	0.49	0.56	1	1; 10; 50; 100	6		X	
Ni2	1	3.5	0.343	Sand	Yes	0.60 m <sup>(3)</sup>	0.49	0.56	1	1; 10; 50; 100; 200	6		X	
Ni3	1.8	3	0.322	Sand	Yes	0.60 m <sup>(3)</sup>	0.49	0.56	1	Uc test	n/a		X	
Mi1	6	5	0.303	Sand	Yes	0.60 m <sup>(3)</sup>	0.21	0.35	1	1; 10; 50; 100	6		X	
Mi2	4	5.5	0.332	Sand	Yes	0.60 m <sup>(3)</sup>	0.21	0.35	n/a	HM and Uc test	n/a		X	
Wi1	3	3.5	0.507	Sand	Yes		n/a	0.8	0.4 -> 1.3	1; 5; 10; 25; 50	2		X	X
Wi2	3	3.5	0.484	Sand	Yes		n/a	0.8	n/a; 1.2	HM; 25	2			

<sup>1)</sup> Clayey and silty fine sand

<sup>2)</sup> Dike profile adjusted with sand and a cover of clayey/silty soil

<sup>3)</sup> At least

## Remarks table

Section	ID	Usage	Remarks	Damage mode	Damage remarks
Delfzijl, section 1	De1	Ensemble		No failure	Before damage introduction only
Delfzijl, section 2	De2	Ensemble	Geogrid	No failure	Before damage introduction only
Delfzijl, section 3	De3	Omitted	Bare clay		
Boonweg, section 1	Bo1	Ensemble		Toe failure	Pavers at 10cm depth at toe
Boonweg, section 2	Bo2	Ensemble		Toe failure	Pavers at 10cm depth at toe
Boonweg, section 3	Bo3	Validation			
Boonweg, section 4	Bo4	Ensemble		Track; Heavy track	Failure after "bulge" at heavy track
St Philipsland, section 1	Sp1	Ensemble		Mole; Jump; Road after toe	Failure at jump (influence of after toe erosion); mole activity; holes at road mitigated; not calibrated on 'road after toe'
Kattendijke, section 1	Ka1	Ensemble		Road after toe; Toe gravel box	Mole activity but no influence
Kattendijke, section 2	Ka2	Ensemble		Injector cut near toe; Toe gravel box	Injector cut damage development, not failure mode; Mole activity but no influence
Afsluitdijk, section 1	Af1	Ensemble		light track; light track; Toe failure	Grass cover after toe was eroded before grass cover on slope eroded. Damage started at a weak spot
Afsluitdijk, section 2	Af2	Validation			
Afsluitdijk, section 3	Af3	Omitted	Stairs		
Vechtdijk, section 1	Ve1	Omitted	Road midway of slope		
Vechtdijk, section 2	Ve2	Ensemble	Tree just after toe line	Grass blocks; Bare spot; Mole_2; Tree after toe	First failure at tree, second at bare spot and (almost) at mole
Vechtdijk, section 3	Ve3	Ensemble	Several holes 0.1 to 0.4m depth, by moles.	Mole_1; mole_2	All holes were at the location of initial mole holes
Vechtdijk, section 4	Ve4	Validation			
Tielrode, section 1	Ti1	Validation			
Tielrode, section 2	Ti2	Ensemble		Mole_1	Early failure at mole hole

Tielrode, section 3	Ti3	Ensemble	Development of introduced damage not included	No failure; Ashpalt_transition2	Some erosion at asphalt transition on crest
Tielrode, section 4	Ti4	Ensemble		Mole_1; toe_road	Failure due to mole activity. Extensive mole activity
Tholen, section 1	Th1	Ensemble		toe_road	Termination due to failure after toe (road)
Tholen, section 2	Th2	Omitted	Stairs		
Tholen, section 3	Th3	Ensemble	Fence	mole_2	Only up until first failure at mole, extensive mitigation efforts first failure.
Tholen, section 4	Th4	Validation			
Nijmegen, section 1	Ni1	Ensemble	Concrete structure at crest. Concrete apron on sheet pile at toe	mole & structural element;mole_1;mole_2	Extensive mole activity
Nijmegen, section 2	Ni2	Ensemble	Concrete apron after toe	Mole_2; Toe_semipaved	Termination due to slow damage development, mitigation efforts and delayed time frame due to
Nijmegen, section 3	Ni3	Ensemble		Mole_2; track	
Millingen, section 1	Mi1	Ensemble		Mole_1; Road on crest_1; Road on crest_2	Erosion signs at mole activity. Road at crest cause of termination.
Millingen, section 2	Mi2	Ensemble		Mole_1 ; Mole_2	Suspected mole just below crest
Wijmeers, section 1	Wi1	Ensemble	Insufficient registration of initial condition	Rabbit	Calibration not appropriate
Wijmeers, section 2	Wi2	Ensemble	Insufficient registration of initial condition		Only till 1hr 25l/s; due to lacking initial condition registration, no mode identified. Calibration not appropriate

## Appendix B – Grass erosion model decompositions

The following diagrams contain decompositions of the grass erosion models considered for the prediction method. These models are the Cumulative Overload Method(COM), Analytical Grass Erosion Models(AGEM), Dean Stream Power(DSP) and Wave Impact Approach(WIA). For references, please refer to the main document.

Cumulative overload method, WBI2017 extension. Dissection of the formula

**Failure thresholds:**

Failure :  $D = 7000$   
 Damage spots:  $D = 4000$   
 First damage:  $D = 1000$   
 (v/d Meer)

Have been updated after new definition of  $U_0$ :  $5 \cdot V^{0.34}$  changed to  $4.5 \cdot V^{0.3}$

**$\alpha_M$  : Load factor [-]**

Can be location dependent.  
 Influence on threshold condition.

If larger than 1, increases D.  
 If smaller than 1, decreases D.

Other perspective:  
 If larger than 1, the strength of the slope decreases.

**$\alpha_S$  : Strength factor [-]**

Can be location dependent.  
 Influence on threshold condition.

If larger than 1, decreases D.  
 If smaller than 1, increases D.

Other perspective:  
 If larger than 1, the load on the slope decreases.

**Damage number [  $m^2/s^2$  ]**

Summation of overloading events on the slope. Load and strength linked to the shear stresses: velocity squared.

If entries are location dependent, D can be location depended. Originally one value for the entire slope.

The damage number can only increase. Only positive contributions are taken into account:  $\alpha_M(\alpha_a u)^2 - \alpha_S u_c^2 > 0$

$$D = \sum (\alpha_M (\alpha_a u)^2 - \alpha_S u_c^2) \text{ [ } m^2 / s^2 \text{ , for } \alpha_M (\alpha_a u)^2 - \alpha_S u_c^2 > 0$$

**Threshold condition**

If the threshold condition is not exceeded, the accompanying contribution is not taken into account.

**$\alpha_a$  : Acceleration factor [-]**

Can be location dependent.  
 Influence on threshold condition.  
 This factor is squared in the computation

If larger than 1, increases D.  
 If smaller than 1, decreases D.

Other perspective:  
 If larger than 1, the strength of the slope decreases.

**$u$  : Flow velocity**

Traditionally, the wave front velocity is used, linked to  $U_0$ .  
 One value for the entire slope.

Coupling the COM to an analytical hydrodynamic model, this  $u$  becomes location dependent,  $u(x)$ . Preliminary result show that the need for the acceleration diminishes significantly when using this hydrodynamic model as input for the flow velocity.

**$U_c$  : Critical flow velocity**

Usually determined after an experiment and not location depended. Traditionally hard to predict beforehand.

Preliminary conclusion: if the grass cover is somewhat present, the  $U_c$  for non-compromised grass covers are in the order of 8 m/s.

## Analytical grass erosion formula. Dissection of the formula

### Failure thresholds:

Usually the point where the top layer is eroded away. No fixed value.

Order of magnitude: 0.2 m

### d(x) : erosion depth [ m ]

Location dependent erosion depth, caused by a single overtopping event. Total erosion depth by summing all contributions.

Shear stress approach, velocity squared.

The erosion depth can only increase.

Only positive contributions are taken into account:  $\omega(x)U(x) \geq U_c(x)$

### T<sub>0</sub> : Overtopping period [s]

Property of a specific overtopping event.  
No influence on threshold condition.

Not location dependent.

### C<sub>E</sub> : Erosion resistance parameter [s/m]

Originally not location dependent.  
No influence on threshold condition.  
Can be modelled as some function.

If this parameter increases, the erosion depth increase **if and only if** erosion would occur in the first place.

Other perspective:

When this parameter increases, the number of overtopping events does not increase. Only the contribution of the contributing events.

$$d(x) = (\omega(x)^2 U(x)^2 - U_c(x)^2) T_0 C_E, \quad \text{when } \omega(x)U(x) \geq U_c(x)$$

### Threshold condition

If the threshold condition is not exceeded, the accompanying contribution is not taken into account.

### ω : Turbulence parameter [-]

Can be location dependent.

Influence on threshold condition.

This parameter is squared in the computation.

Function of turbulence intensity  $r_0$

$$\omega(x) = 1.5 + 5r_0(x)$$

$r_0$  typically in range ( 0.2 , 0.45), several definitions of  $r_0$  in Bergeijk 2019a.

If larger than 1, increases d(x).

If smaller than 1, decreases d(x).

Other perspective:

If larger than 1, the strength of the slope decreases.

### U(x) : Flow velocity

Typically the analytical hydrodynamic model is used.

Which models horizontal flow as:

$$U_{horizontal}(x) = \left( \frac{f x}{2 Q} + \frac{1}{U_{horizontal}(x=0)} \right)^{-1} \quad [m/s]$$

and flow on a slope as:

$$U_{slope}(x) = \frac{\alpha}{\beta} + \mu \exp\left(\frac{-3\alpha\beta^2 x}{\cos \varphi}\right) \quad [m/s]$$

$$\text{where } \mu = U_{slope,0} - \frac{\alpha}{\beta}, \quad \alpha = \sqrt[3]{g \sin \varphi}, \quad \beta = \sqrt[2]{\frac{f}{2Q}}$$

See literature for more detail.

### U<sub>c</sub>(x) : Critical flow velocity

Can be location dependent

Strength parameter

Influence on threshold condition

Only strength parameter that has influence on the threshold condition.

## Dean Stream Power: Dissection of the formula.

### Failure thresholds:

Identified by Dean (2010) as erosion limits:

Good cover :  $EWU_{critical} = 0.492 \cdot 10^5 \text{ m}^3/\text{s}^2$   
 Poor cover :  $EWU_{critical} = 0.229 \cdot 10^5 \text{ m}^3/\text{s}^2$   
 Bad cover :  $EWU_{critical} = 0.103 \cdot 10^5 \text{ m}^3/\text{s}^2$

### Dean Stream Power (DSP):

This model finds its origin in this thesis by combining findings of Dean (2010) and Hughes (2011) with the analytical flow model from Bergeijk(2019a).

No similar model has been found at the time of writing.

### $\Delta t$ : Overtopping period [s]

Property of a specific overtopping event.  
No influence on threshold condition.

Not location dependent.

$$EWU(x) = \sum (u^3 - u_c^3) \Delta t \text{ when } u > u_c$$

### EWU: Erosional Work Units

**[m<sup>3</sup>/s<sup>2</sup>]**

Summation of the erosional work units on the slope. Load and strength linked to the work: velocity cubed.

### Threshold condition

If the threshold condition is not exceeded, the accompanying contribution is not taken into account.

### u : Flow velocity

Cubed in the computation. Dean et al. (2010) used terminal velocities, in the context of this thesis the analytical flow model is used. Which models horizontal flow as:

$$U_{horizontal}(x) = \left( \frac{f x}{2 Q} + \frac{1}{U_{horizontal}(x=0)} \right) [m/s]$$

and flow on a slope as:

$$U_{slope}(x) = \frac{\alpha}{\beta} + \mu \exp\left(\frac{-3\alpha\beta^2 x}{\cos \varphi}\right) [m/s]$$

$$\text{where } \mu = U_{slope,0} - \frac{\alpha}{\beta}, \alpha = \sqrt[3]{g \sin \varphi}, \beta = \sqrt{\frac{f}{2Q}}$$

See literature for more detail

### U<sub>c</sub>: Critical flow velocity

Can be location dependent  
Strength parameter, cubed in the computation.  
Influence on threshold condition  
Only strength parameter that has influence on the threshold condition.

## Wave Impact Approach: Dissection of the formula.

### Failure thresholds:

In theory, failure occurs when a certain threshold of transferred excess momentum is reached. This threshold is not yet identified.

### dt : Impact duration [s]

Property of a specific overtopping event.  
No influence on threshold condition.

The integral integrates over the impact duration of each wave on each location where the wave reattaches with the slope. The concept of the depth-dependency, 'changing impact location during an overtopping event', is included in the computations.

### Wave Impact Approach (DSP):

This model finds its origin in the observation that the WOS sections at Wijmeers-II failed in the zone where the waves reattached.

The need for a model that incorporates the impact stress emerged, the Wave Impact Approach followed.

$$J_E = \sum_{n=1}^N \int_t^T (\sigma_n(X, t) - P_c) dt \left[ \frac{kN s}{m^2} \right], \quad \text{when: } \sigma_n(X, t) > P_c$$

### J<sub>E</sub>: Total excess momentum transferred [ kN s/m<sup>2</sup> ]

Summation of the excess momentum transferred on the slope. The surplus of impact stress (  $\sigma_n - P_c$  ) is integrated over the impact duration on each location for each overtopping event that meets the threshold condition, these N contributions are summed resulting in a total excess momentum transferred as function of X.

### $\sigma_n(X, t)$ : Impact stress

The stress exerted by the reattachment of the wave, perpendicular to the slope.

$$\sigma_n(X, t) = \rho ( u_{\text{crest}}^2(t) + 2 g X(t) \tan\theta ) \sin(\beta)$$

See literature for more detail. (Ponsoen et al, 2019)

### Threshold condition

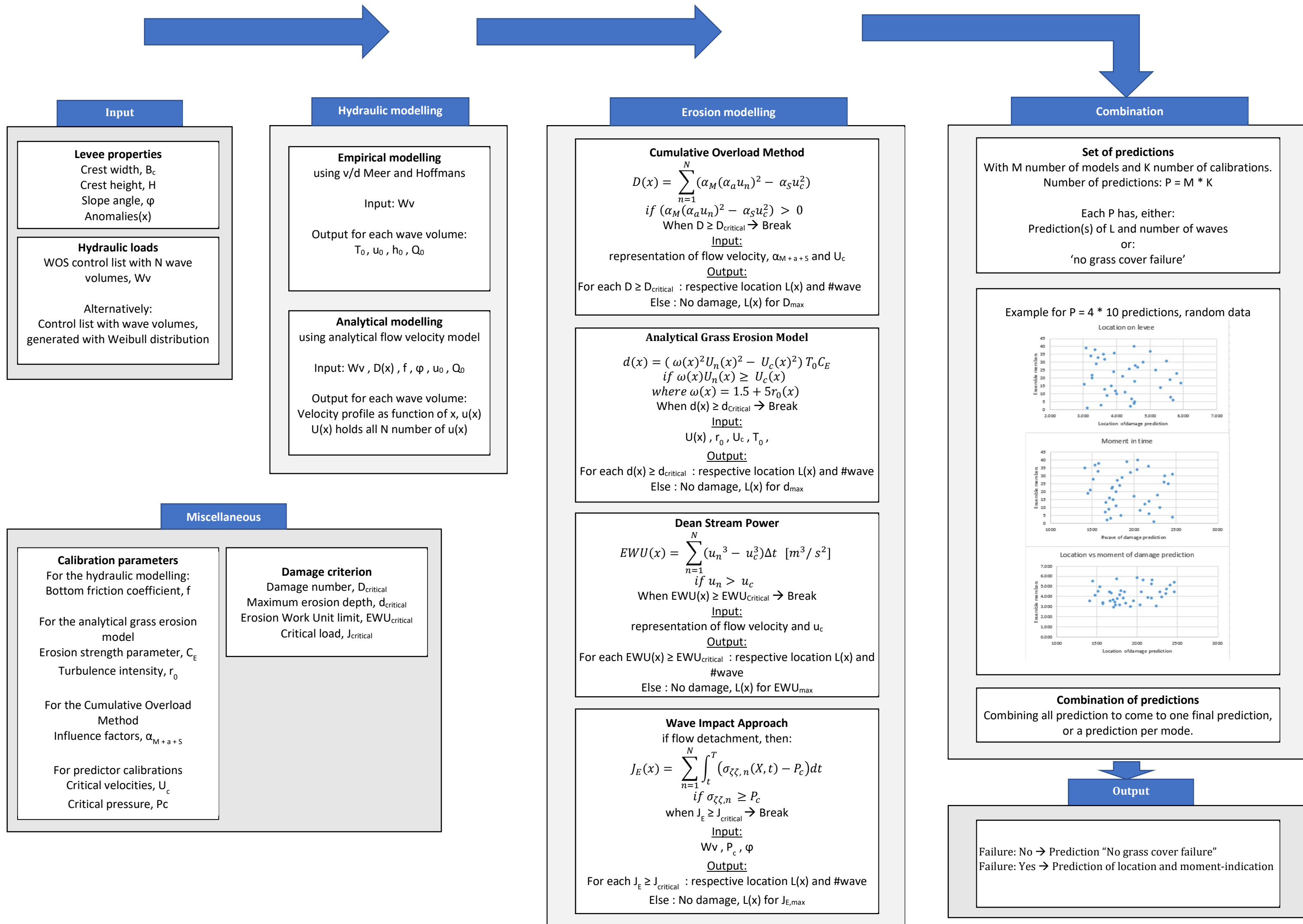
If the threshold condition is not exceeded, the accompanying contribution is not taken into account.

### P<sub>c</sub>: Critical pressure

Can be location dependent.  
Strength parameter.  
Influence on threshold condition  
Assumed to be in the order of  $2c' \leq P_c \leq 5c'$ .

## Appendix C – Technical method diagram

The Technical method diagram is an elaborated version of Figure 13 Prediction method. The core of the prediction method is the creation of a set of predictions, combination of these predictions leads to the final prediction. in Section 3.1 of the main document. The technical diagram shows which equations and variables are needed for each part of the method.



**Input**

**Levee properties**

Crest width,  $B_c$   
Crest height,  $H$   
Slope angle,  $\phi$   
Anomalies( $x$ )

**Hydraulic loads**

WOS control list with  $N$  wave volumes,  $Wv$

Alternatively:

Control list with wave volumes, generated with Weibull distribution

**Hydraulic modelling**

**Empirical modelling**

using v/d Meer and Hoffmans

Input:  $Wv$

Output for each wave volume:

$T_0, u_0, h_0, Q_0$

**Analytical modelling**

using analytical flow velocity model

Input:  $Wv, D(x), f, \phi, u_0, Q_0$

Output for each wave volume:

Velocity profile as function of  $x, u(x)$   
 $U(x)$  holds all  $N$  number of  $u(x)$

**Erosion modelling**

**Cumulative Overload Method**

$$D(x) = \sum_{n=1}^N (\alpha_M(\alpha_a u_n)^2 - \alpha_S u_c^2)$$

if  $(\alpha_M(\alpha_a u_n)^2 - \alpha_S u_c^2) > 0$

When  $D \geq D_{critical} \rightarrow$  Break

Input:

representation of flow velocity,  $\alpha_{M+a+S}$  and  $U_c$

Output:

For each  $D \geq D_{critical}$  : respective location  $L(x)$  and #wave

Else : No damage,  $L(x)$  for  $D_{max}$

**Analytical Grass Erosion Model**

$$d(x) = (\omega(x)^2 U_n(x)^2 - U_c(x)^2) T_0 C_E$$

if  $\omega(x) U_n(x) \geq U_c(x)$

where  $\omega(x) = 1.5 + 5r_0(x)$

When  $d(x) \geq d_{critical} \rightarrow$  Break

Input:

$U(x), r_0, U_c, T_0,$

Output:

For each  $d(x) \geq d_{critical}$  : respective location  $L(x)$  and #wave

Else : No damage,  $L(x)$  for  $d_{max}$

**Dean Stream Power**

$$EWU(x) = \sum_{n=1}^N (u_n^3 - u_c^3) \Delta t \quad [m^3/s^2]$$

if  $u_n > u_c$

When  $EWU(x) \geq EWU_{critical} \rightarrow$  Break

Input:

representation of flow velocity and  $u_c$

Output:

For each  $EWU(x) \geq EWU_{critical}$  : respective location  $L(x)$  and #wave

Else : No damage,  $L(x)$  for  $EWU_{max}$

**Wave Impact Approach**

if flow detachment, then:

$$J_E(x) = \sum_{n=1}^N \int_t^T (\sigma_{zz,n}(X,t) - P_c) dt$$

if  $\sigma_{zz,n} \geq P_c$

when  $J_E \geq J_{critical} \rightarrow$  Break

Input:

$Wv, P_c, \phi$

Output:

For each  $J_E \geq J_{critical}$  : respective location  $L(x)$  and #wave

Else : No damage,  $L(x)$  for  $J_{E,max}$

**Combination**

**Set of predictions**

With  $M$  number of models and  $K$  number of calibrations.  
Number of predictions:  $P = M * K$

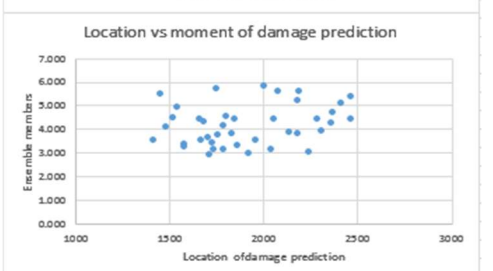
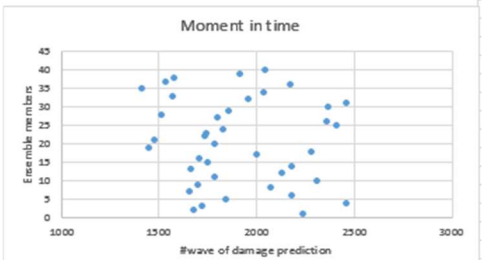
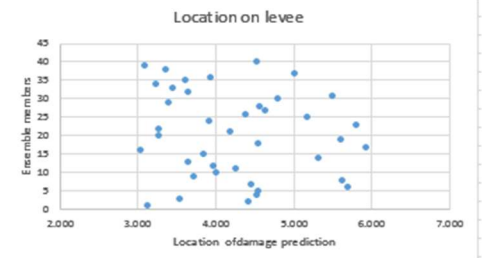
Each  $P$  has, either:

Prediction(s) of  $L$  and number of waves

or:

'no grass cover failure'

Example for  $P = 4 * 10$  predictions, random data



**Combination of predictions**

Combining all prediction to come to one final prediction, or a prediction per mode.

**Output**

Failure: No  $\rightarrow$  Prediction "No grass cover failure"  
Failure: Yes  $\rightarrow$  Prediction of location and moment-indication

**Miscellaneous**

**Calibration parameters**

For the hydraulic modelling:  
Bottom friction coefficient,  $f$

For the analytical grass erosion model  
Erosion strength parameter,  $C_E$

Turbulence intensity,  $r_0$

For the Cumulative Overload Method  
Influence factors,  $\alpha_{M+a+S}$

For predictor calibrations  
Critical velocities,  $U_c$

Critical pressure,  $P_c$

**Damage criterion**

Damage number,  $D_{critical}$

Maximum erosion depth,  $d_{critical}$

Erosion Work Unit limit,  $EWU_{critical}$

Critical load,  $J_{critical}$

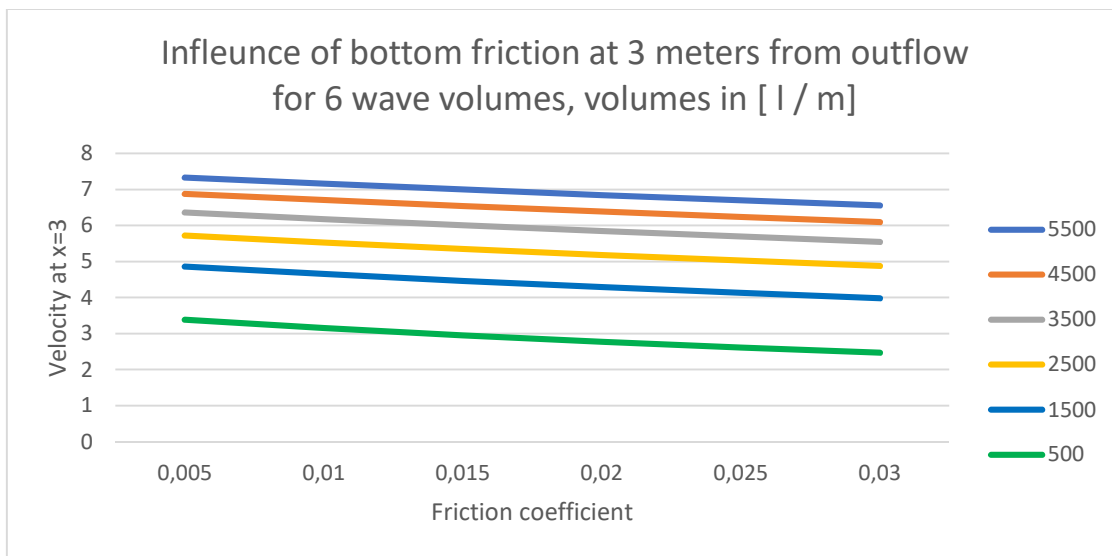
## Appendix D – Influence of wide crests and validity of the friction factor

### Influence of wide crests

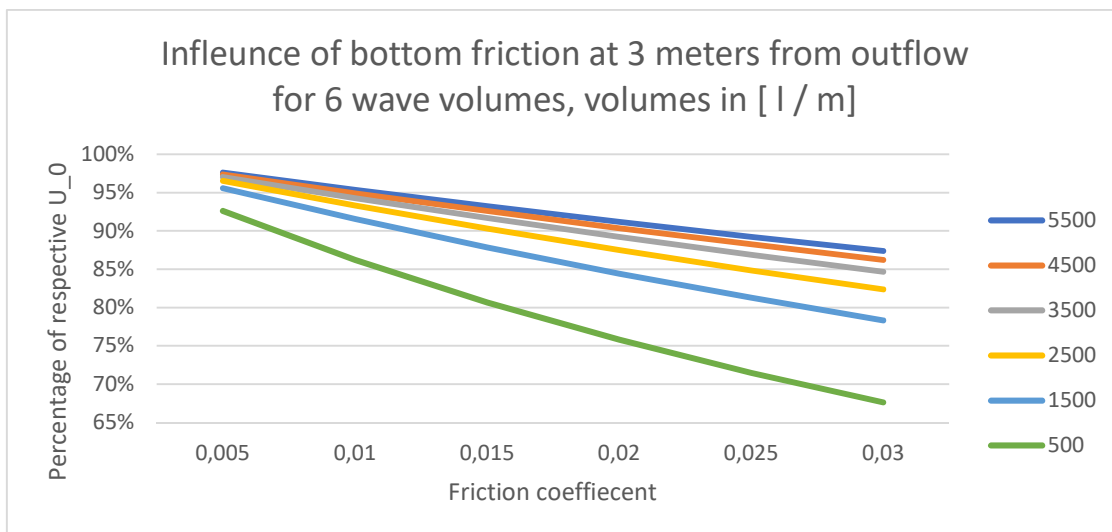
The sections where Wave Overtopping Simulator experiments are performed, are similar to some extent but the role of levee crest differs. In some cases, the levee crest is not tested, in other cases several meters of crest are incorporated in the tested cross-section. In the hydraulic model the influence of the crest is mainly governed by the bottom friction parameter  $f$ , next to the hydraulic boundary conditions and distance to the outflow. The flow on the crest is modelled as follows:

$$U_{horizontala}(x) = \left( \frac{f x}{2 Q} + \frac{1}{u_0} \right)^{-1} \quad [m/s]$$

Where  $f$  is the bottom friction parameter,  $Q$  is the discharge at the outflow of the simulator,  $u_0$  is the depth-averaged flow velocity at the outflow and  $x$  is the distance to the outflow. In the figure below, the depth-averaged flow velocity [m/s] is plotted against a varying bottom friction parameter [-] with the distance to the outflow fixed at three meters, for a simulated crest width of 3 meters. The lines represent different hydraulic boundary conditions in the form of wave volumes [l/m].



In the figure below, the ratio between the depth-averaged flow velocity at the outflow and the depth-averaged flow velocity at  $x=3$  meter is plotted for a range of wave volumes.



These plots show how the model incorporates crest width: for smaller wave volumes the influence of the crest width is larger, and for increasing bottom friction the influence increases.

### Validity of the friction factor

In the new method, the friction coefficient is assumed to be 0.01, which is representative for concrete or smooth earth according to the Manning-definitions of n and relation of n to the bottom friction f. But in fact, the bottom friction coefficient is a calibration parameter for the analytical hydrodynamic model and not a fixed material property as Manning's suggests. The table below shows some values of f, linked to specific definitions of n and a range over wave volumes. Where the wave volumes represent the hydraulic conditions. The cells marked in green indicates values of f which lay in between 0.01 +/- 0.005, red indicates <0.095 and yellow indicates >0.095.  $f_{lim} = \frac{g * Q * \sin(\phi)}{4 * U_{s,0}^3}$ ,  $x = x_{crest}$  &  $t = t_0$

The relation between n and f is:

Manning's (hydraulic manual)		Volumes [ l/ m ]				
Surface	n	5500	3000	2000	1000	500
glass	0.01	0.002991	0.003119	0.003299	0.003593	0.004314
concrete	0.014	0.005863	0.006114	0.006467	0.007041	0.008456
smooth earth	0.02	0.011966	0.012478	0.013197	0.01437	0.017258
grass	0.03	0.026923	0.028075	0.029694	0.032333	0.03883
high grass	0.05	0.074786	0.077985	0.082483	0.089813	0.10786

According to theory, the bottom friction coefficient has a certain lower limit. This limit is linked to the wave volume and slope, but this does not include horizontal (crest) sections. This limit is defined as:

$$f_{lim} = \frac{g * Q * \sin(\phi)}{4 * U_{s,0}^3}$$

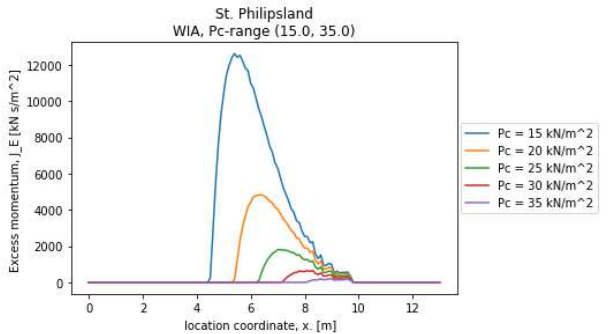
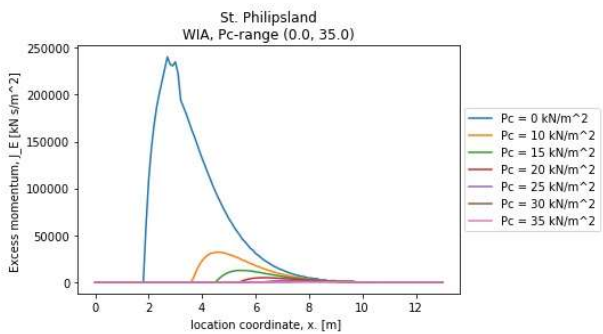
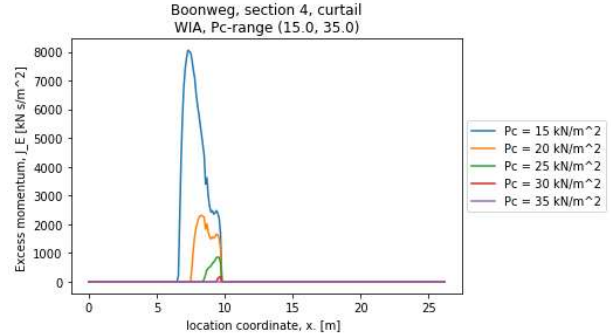
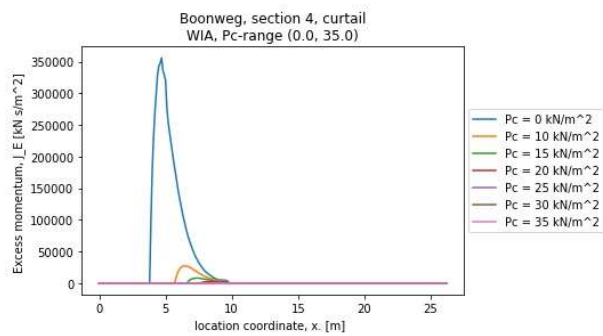
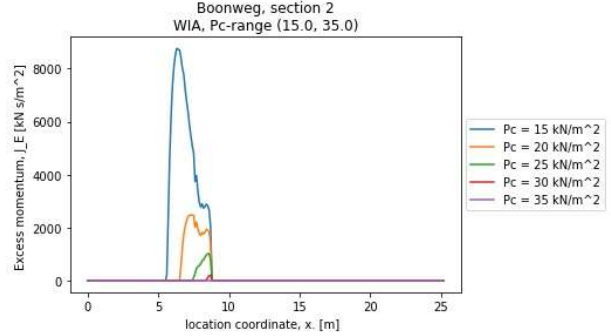
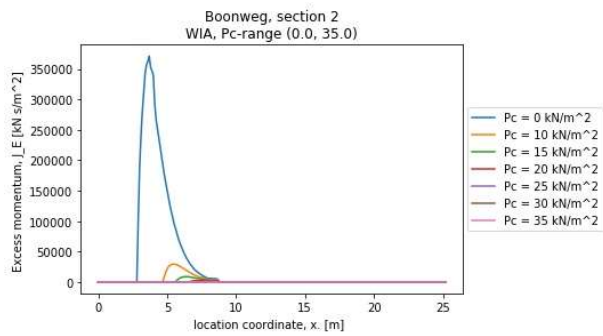
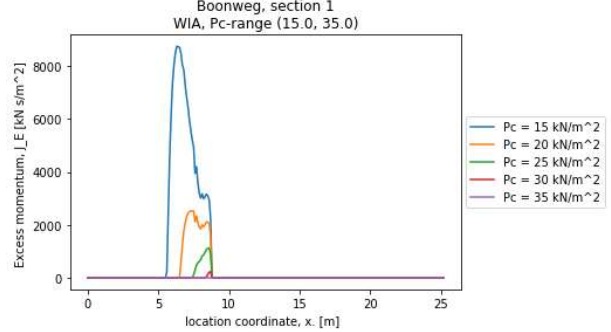
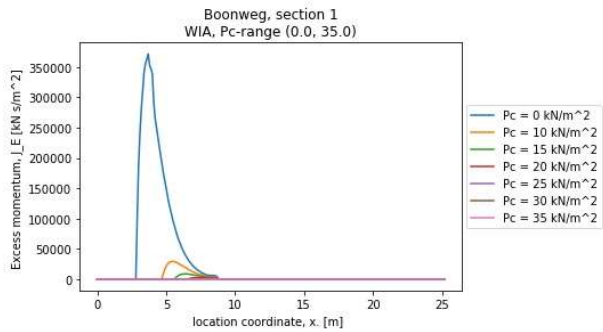
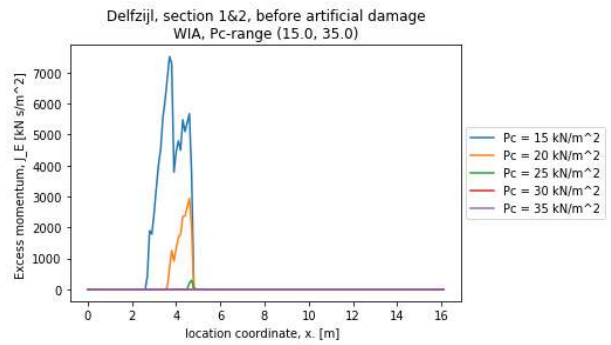
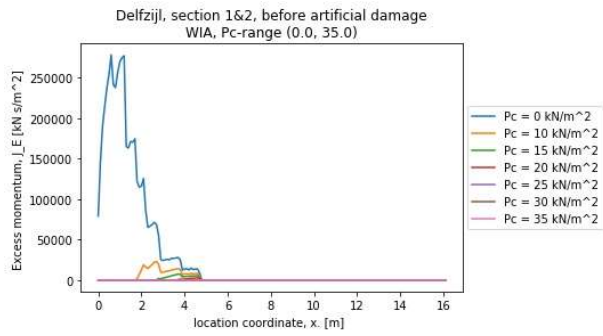
The table below shows the values of  $f_{lim}$  for varying slope steepness and wave volumes. All cells are green since all cells have shown  $f > f_{lim}$ , with  $f=0.01$ .

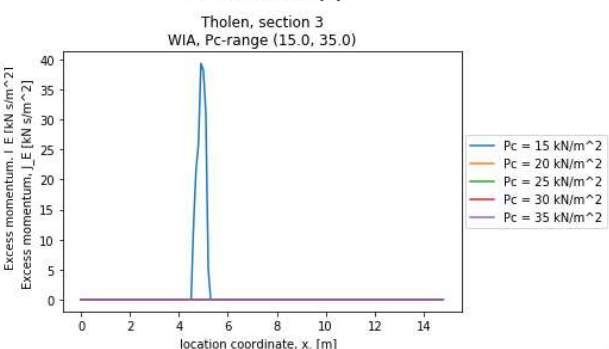
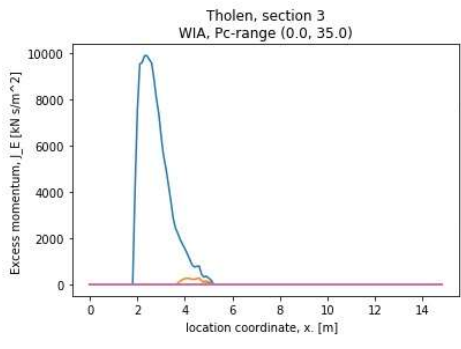
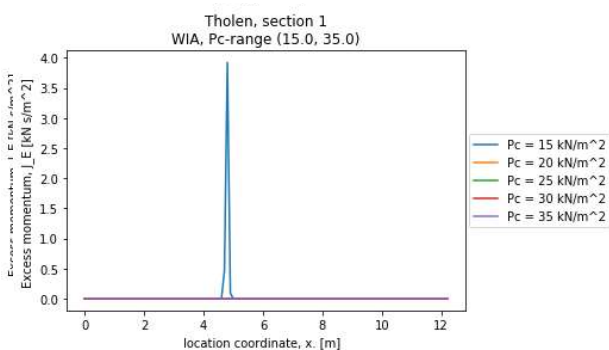
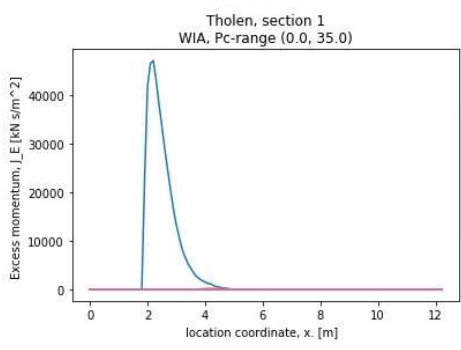
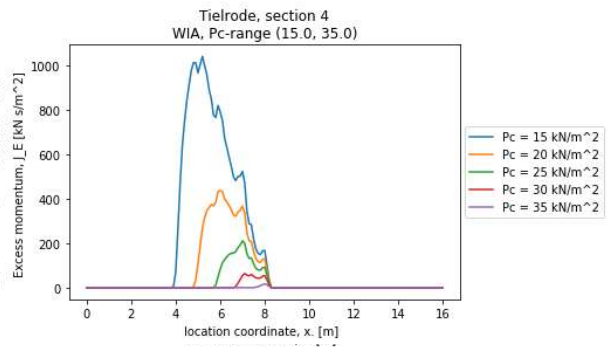
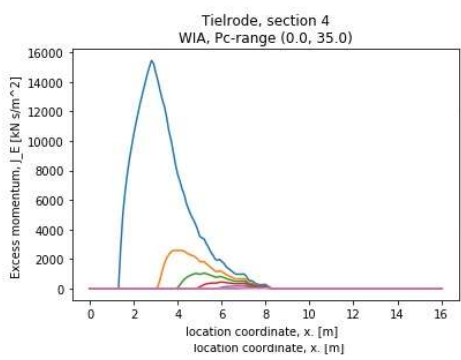
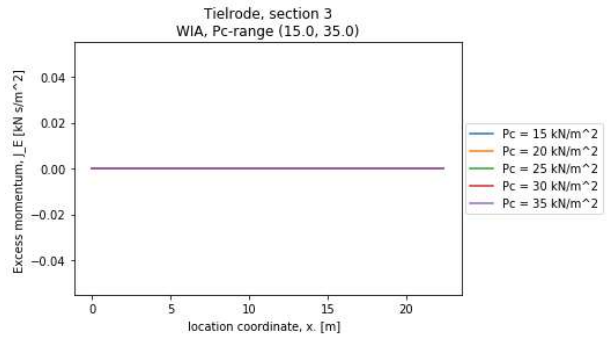
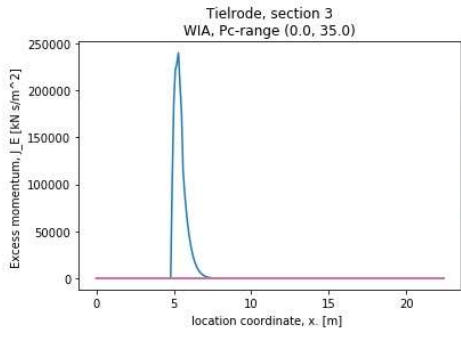
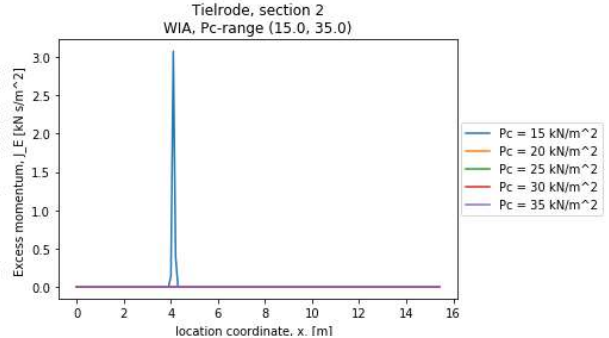
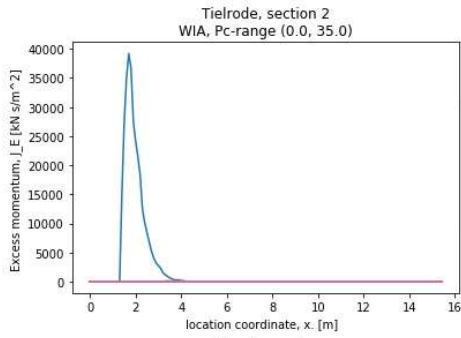
	cot	2	2.5	3	3.5	4
rad	0.463647609	0.380506	0.321751	0.2783	0.244979	
5500 l/m	0.006197683	0.005147	0.004382	0.003807	0.003361	
3000 l/m	0.006355414	0.005278	0.004494	0.003904	0.003447	
2000 l/m	0.006572894	0.005458	0.004648	0.004038	0.003565	
1000 l/m	0.006917378	0.005745	0.004891	0.004249	0.003751	
500 l/m	0.007720646	0.006412	0.005459	0.004743	0.004187	

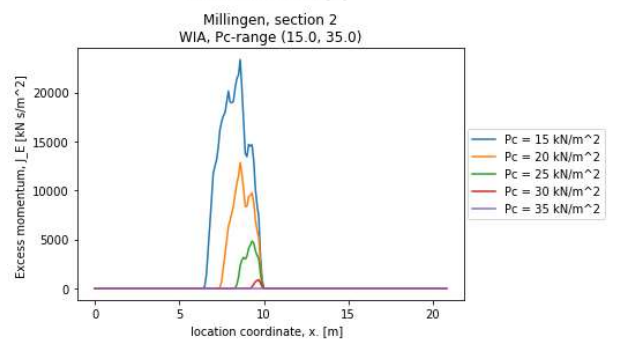
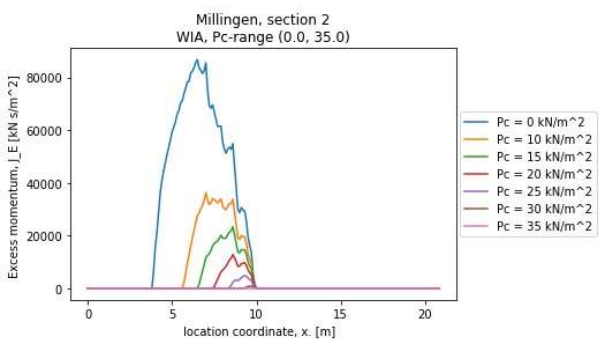
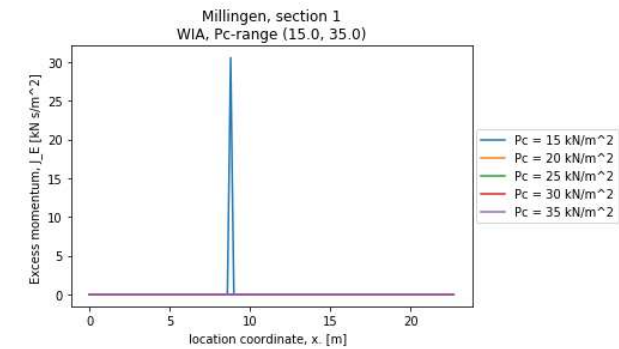
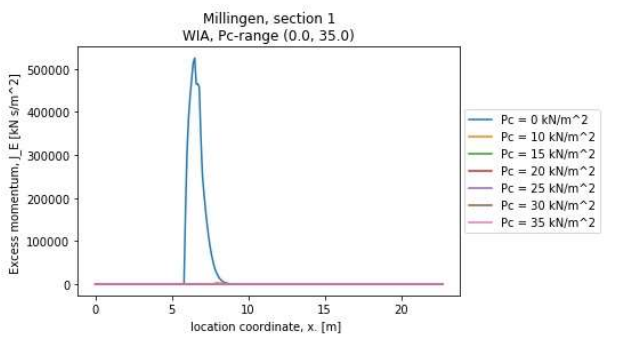
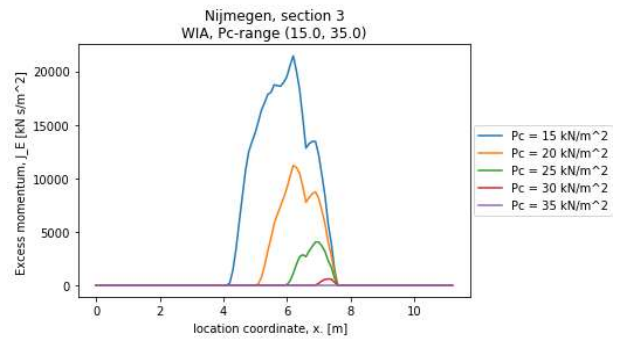
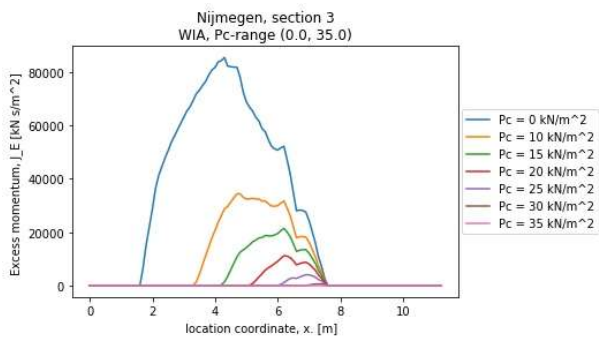
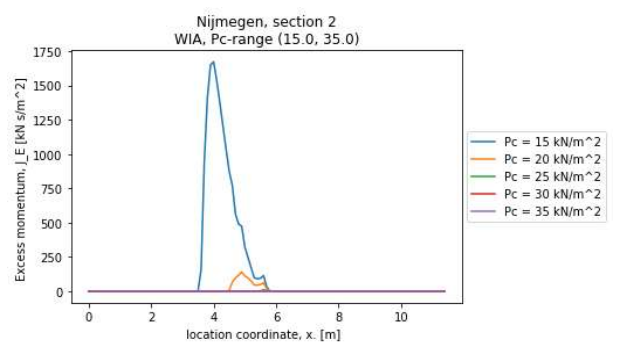
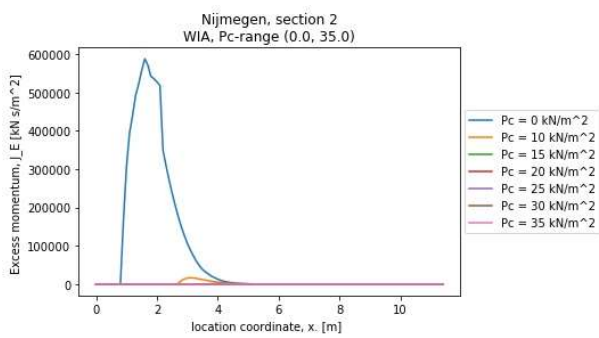
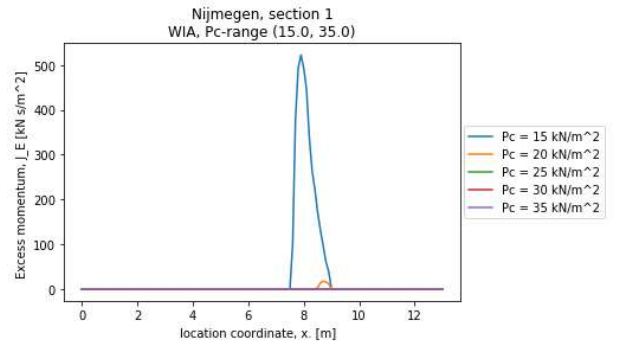
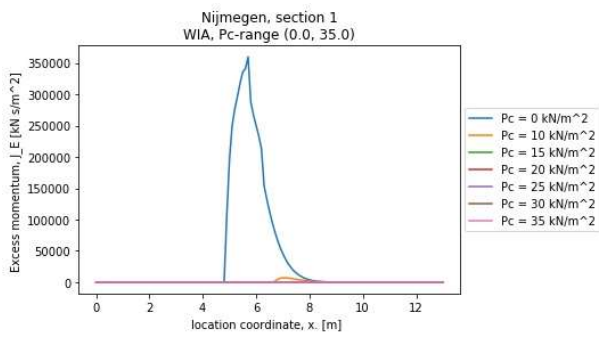
Especially for smaller wave volumes, the crest width has a significant influence, for larger waves this influence decreases. In the context of this thesis, the influence of the crest is incorporated but not fully elaborated. Further elaboration can be done in the form of calibrating to hydrodynamic model for each experiment, yielding calibrated bottom friction for each section. Knowing that mainly larger wave volumes cause erosion, the constant value for f is assumed to be sufficiently valid for the purpose.

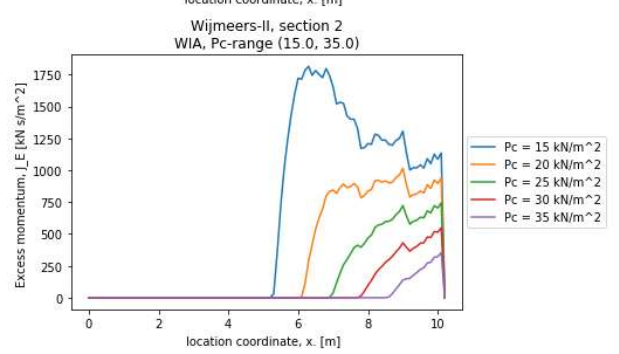
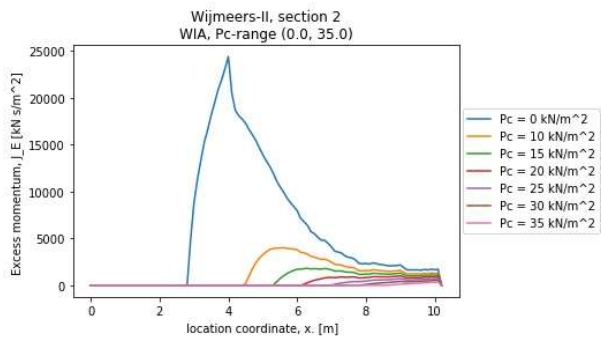
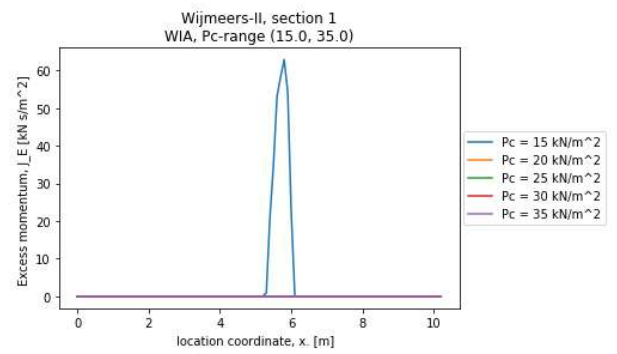
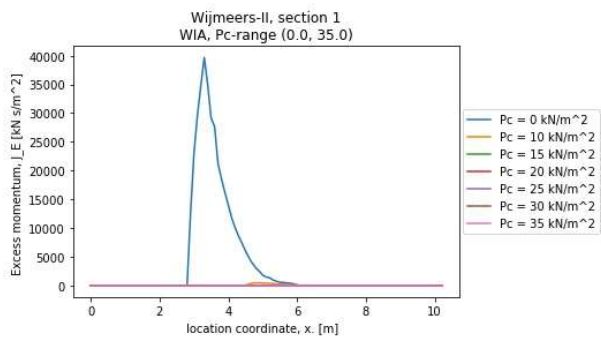
## Appendix E – WIA realizations

This appendix contains the realisations of the Wave Impact Approach (WIA) in the context of the thesis “Prediction method for grass erosion on levees by wave overtopping”. The WIA has been evaluated for each experiment in the test dataset. For each experiment two plots are given of the excess momentum [ $\text{kN s} / \text{m}^2$ ] of the entire deployed wave sequence as a function of the location on the surface. The left-hand side plots show a varying critical pressure from 0 till  $35 \text{ kN/m}^2$ , the right-hand side plots show a varying critical pressure from 15 till  $35 \text{ kN/m}^2$ .









## Appendix F – COM, AGEM & DSP calibrations

Three tables are given respectively linked to the COM, AGEM and DSP. Each table is filled with the calibrated critical velocities for each section for the respective model. Each row represents a section. In the first column a baseline calibration is given if applicable, in the other columns a calibration for a corresponding anomaly is given if applicable. Sections in the tables marked red are sections that are omitted from the research, sections marked grey with white font colour are sections used for validation. The calibrated velocities in the tables are the leading values. Indicative visualizations (plots) are added for each section, values in the tables are normative values.



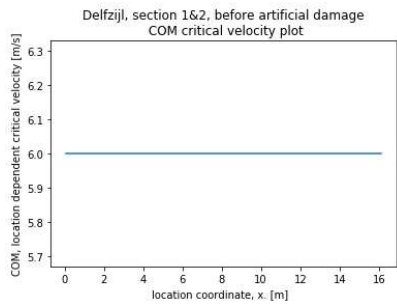
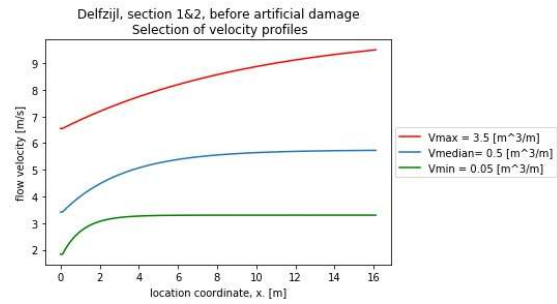
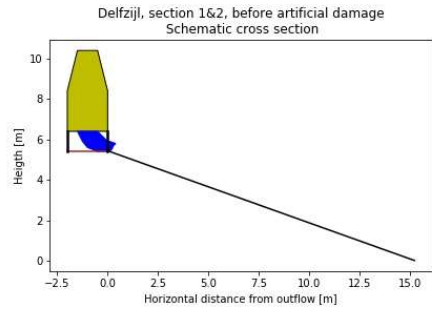




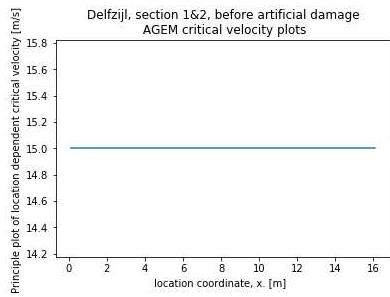
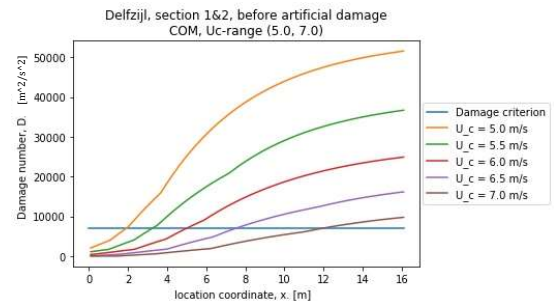
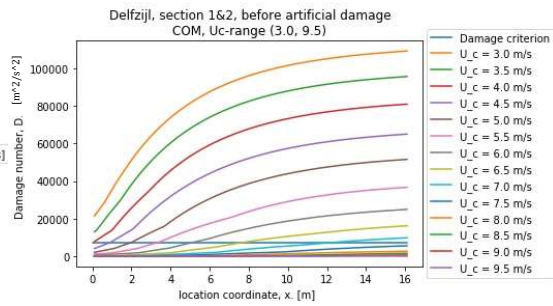




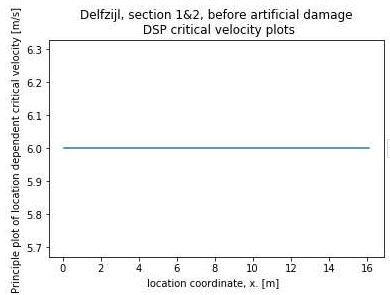
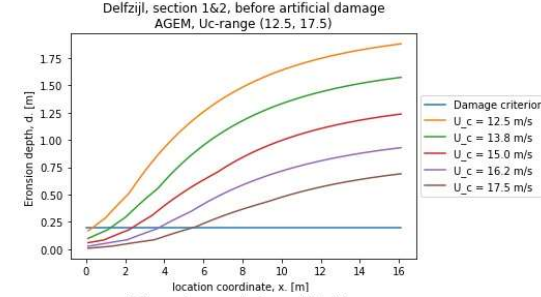
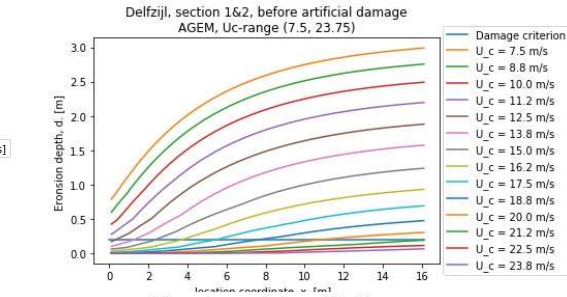




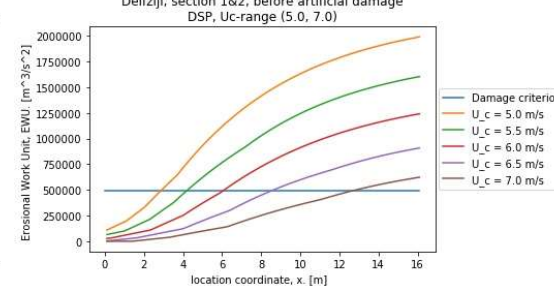
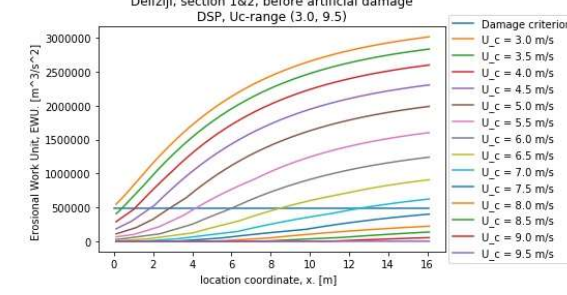
COM, baseline  $U_c = 6.0$  [m/s]

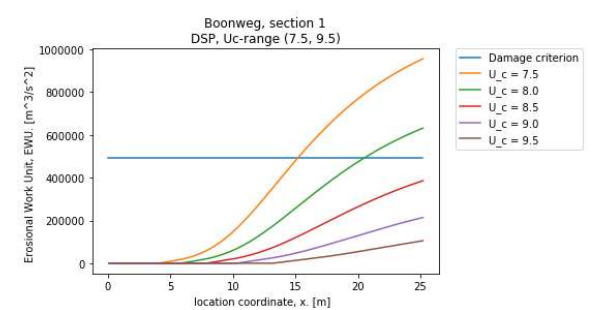
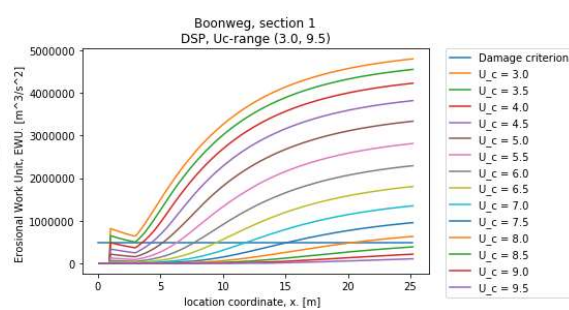
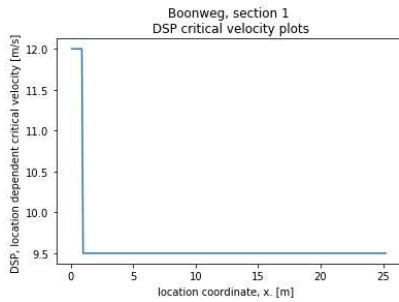
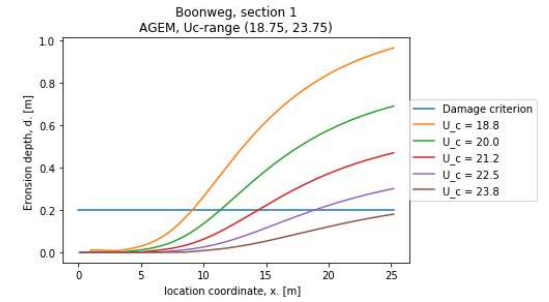
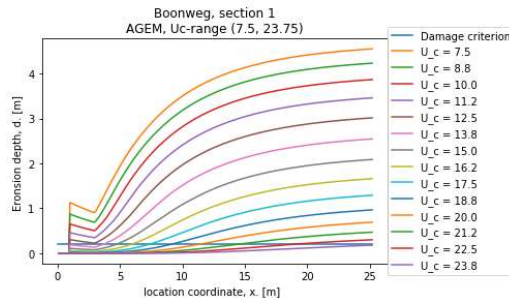
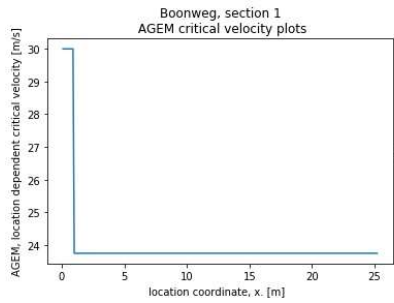
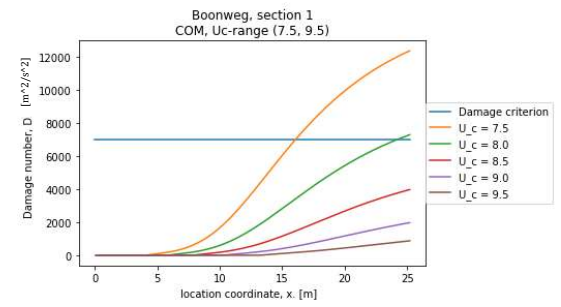
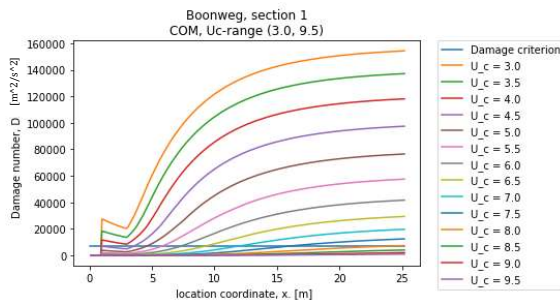
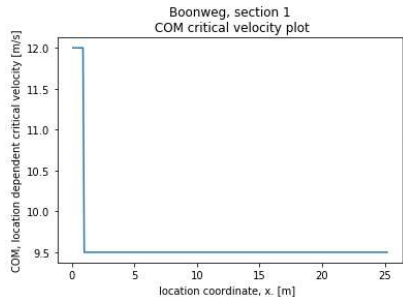
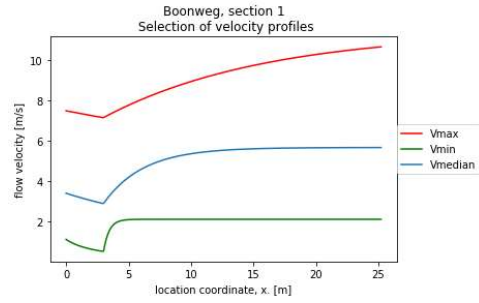
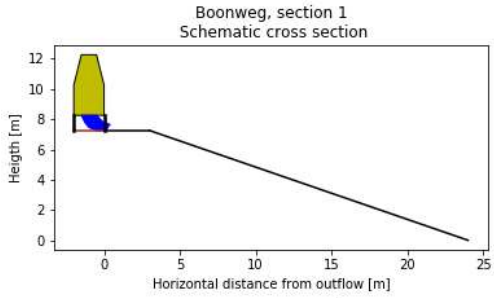


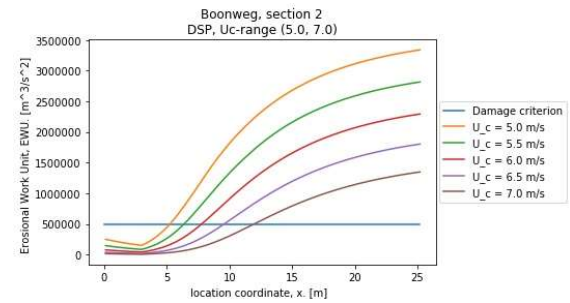
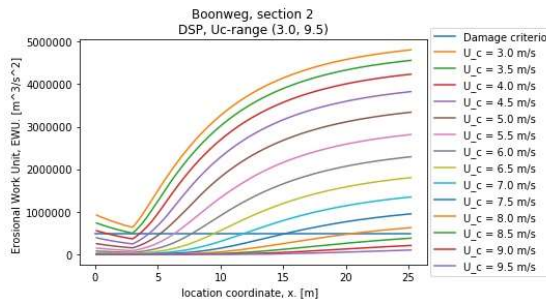
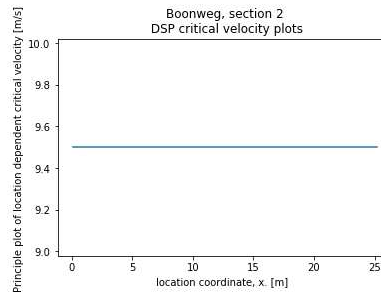
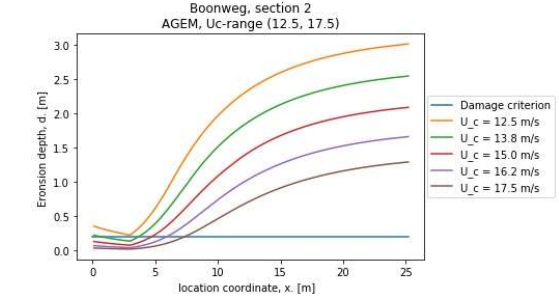
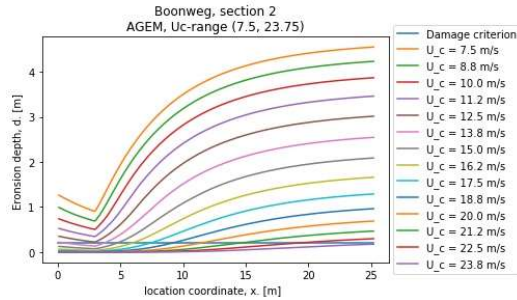
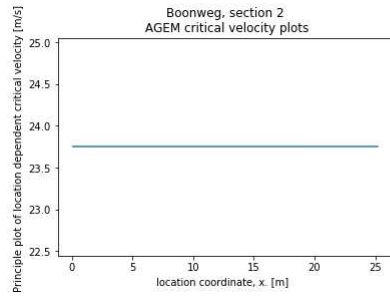
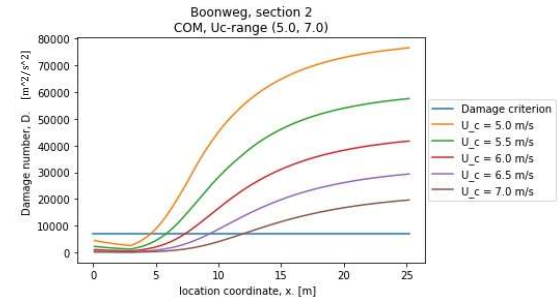
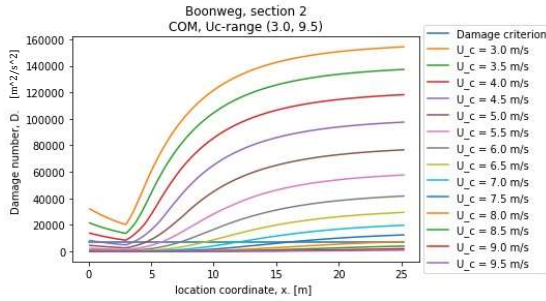
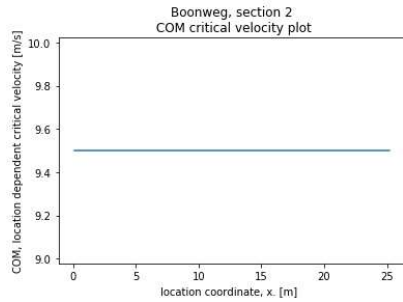
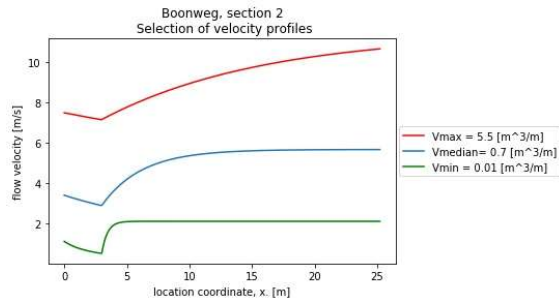
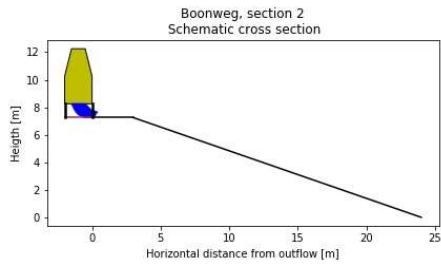
AGEM, baseline  $U_c = 15.0$  [m/s]

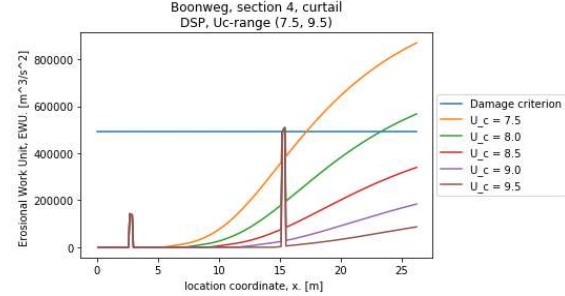
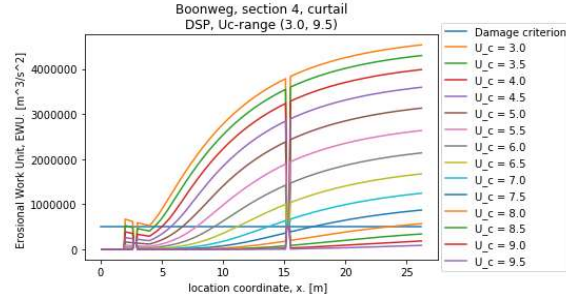
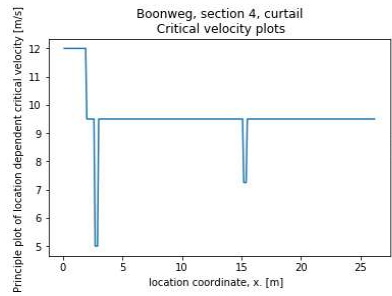
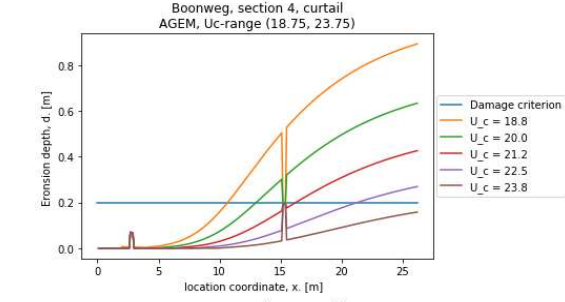
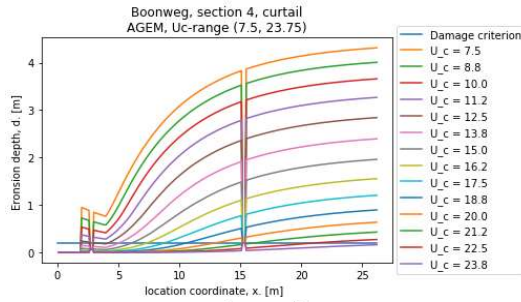
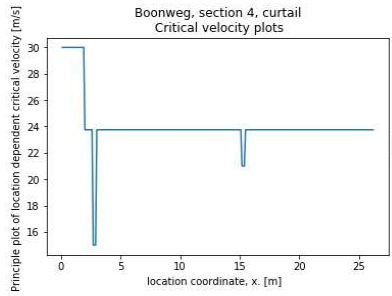
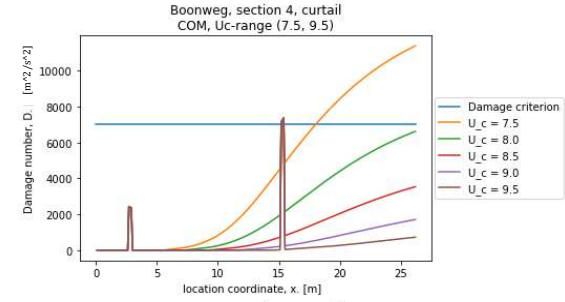
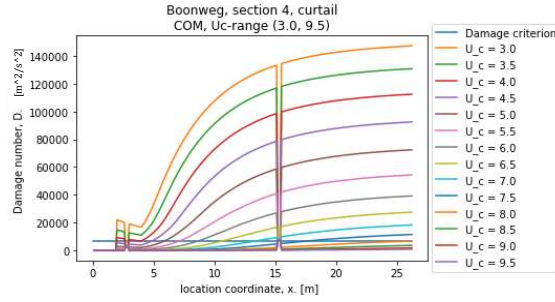
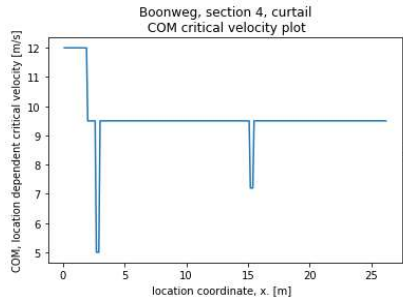
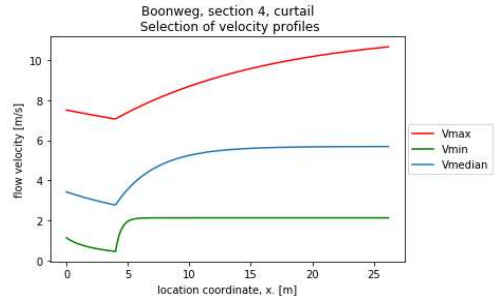
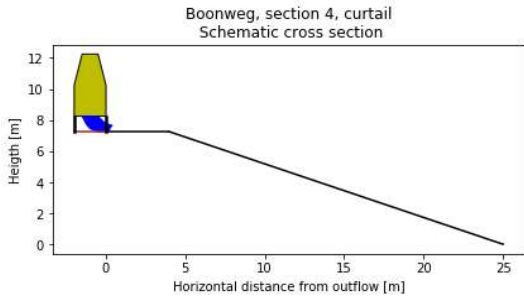


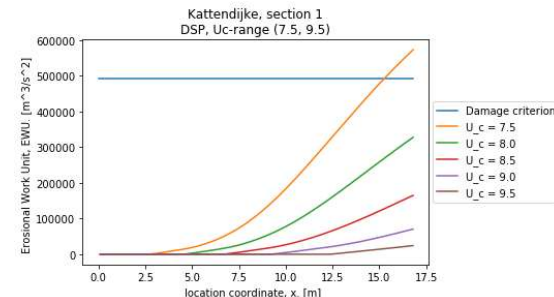
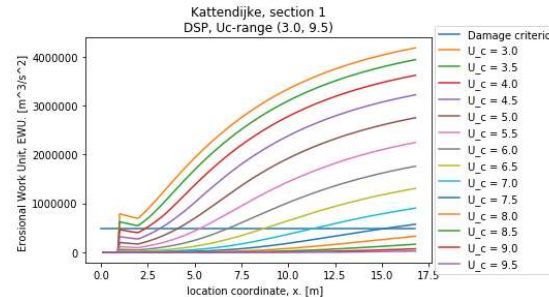
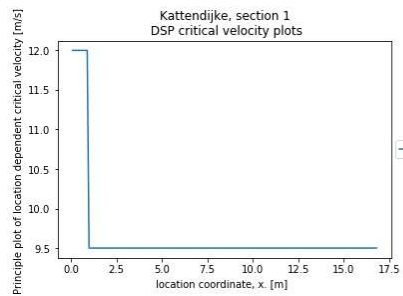
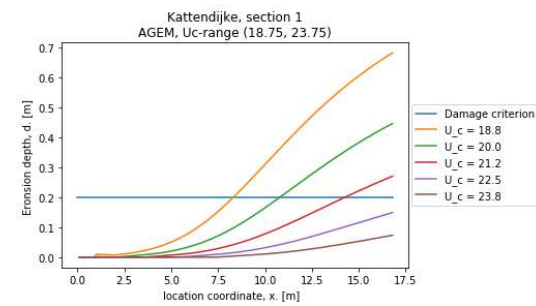
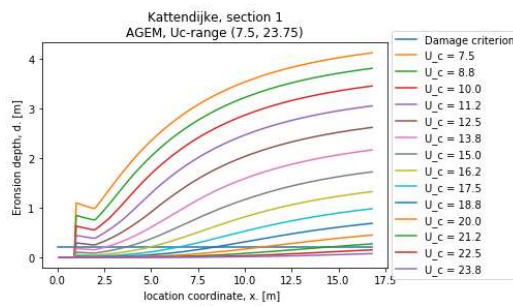
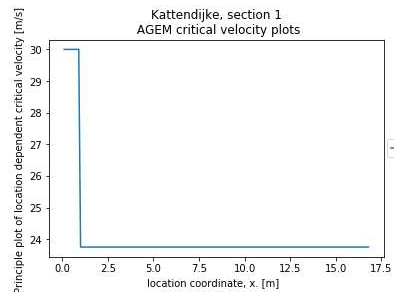
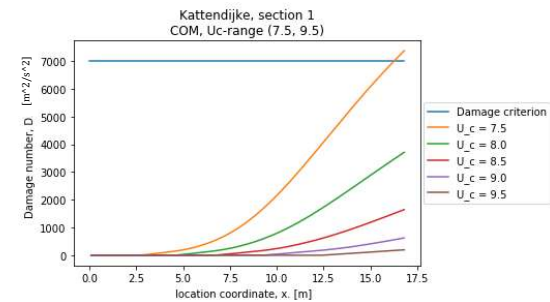
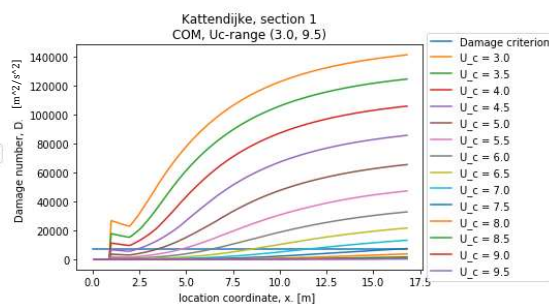
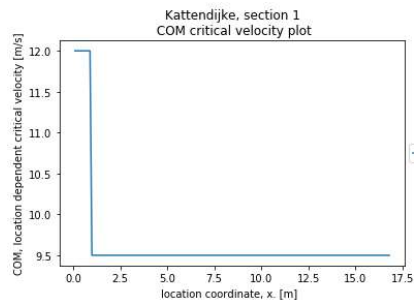
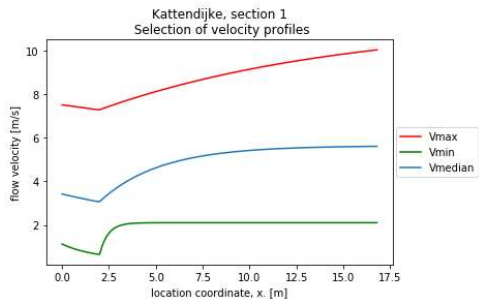
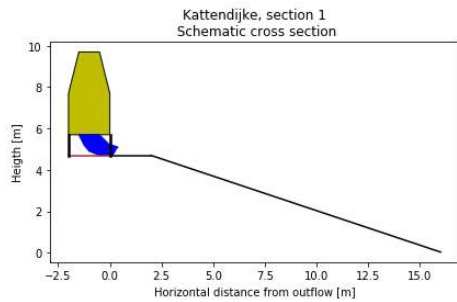
DSP, baseline  $U_c = 6.0$  [m/s]

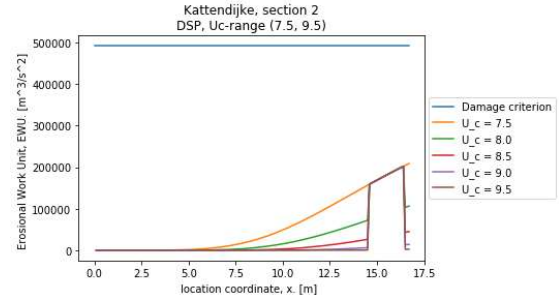
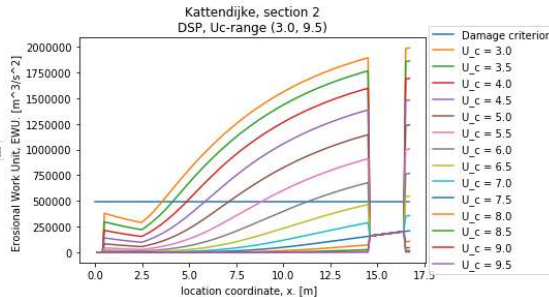
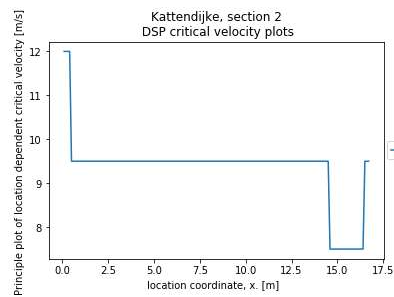
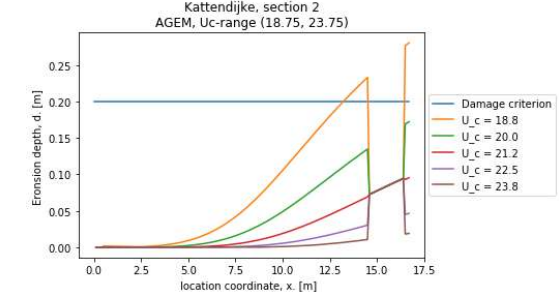
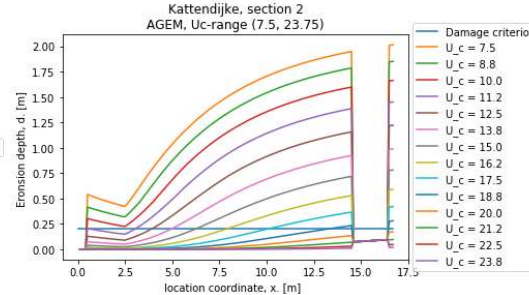
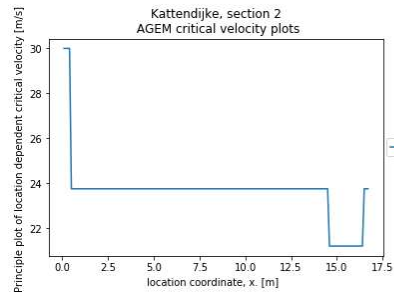
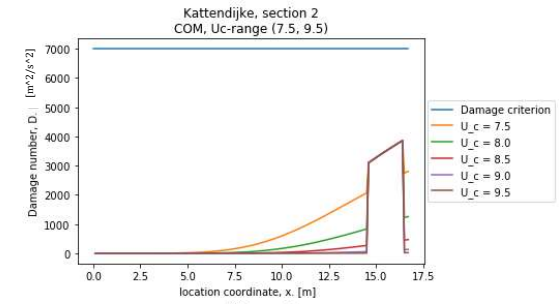
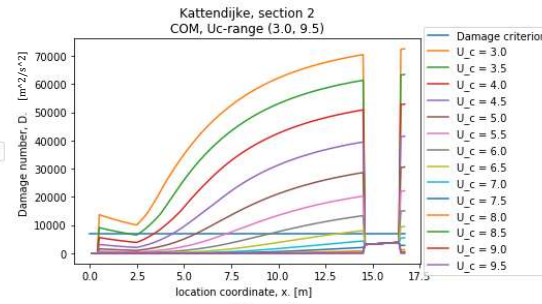
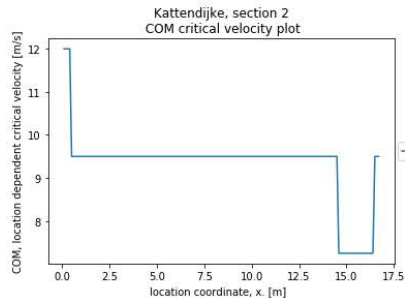
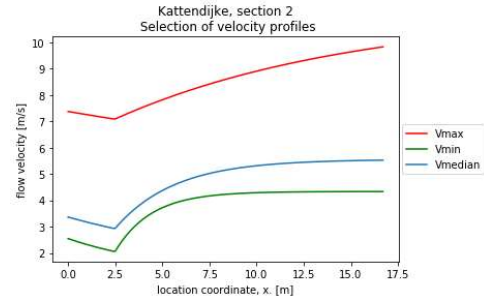
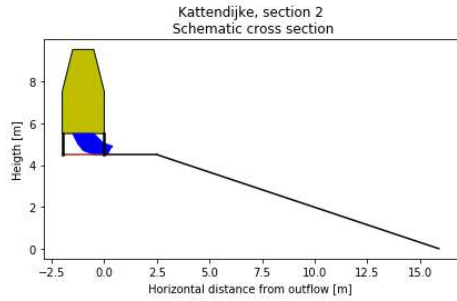


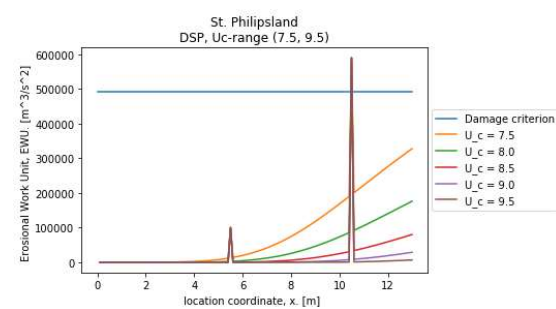
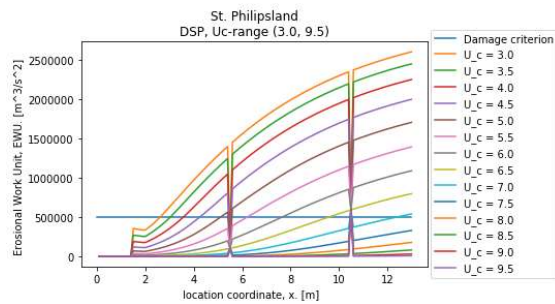
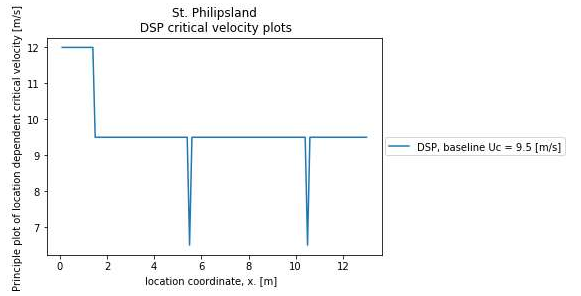
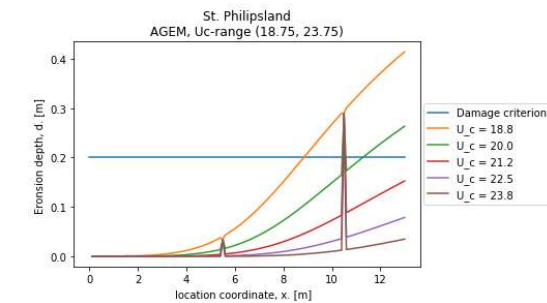
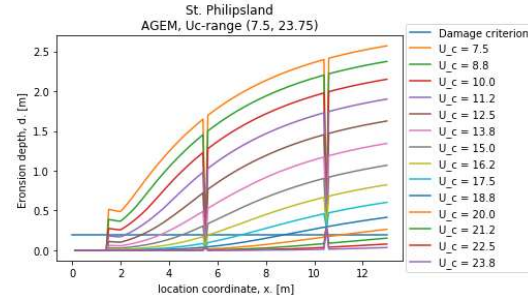
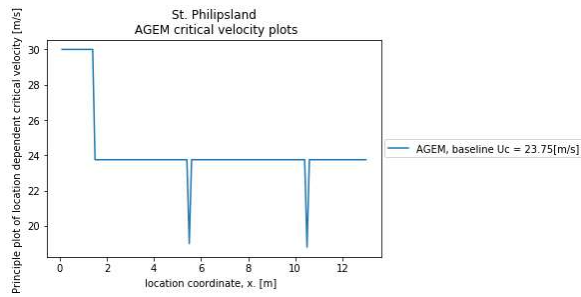
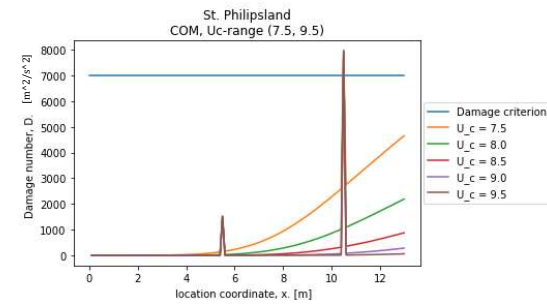
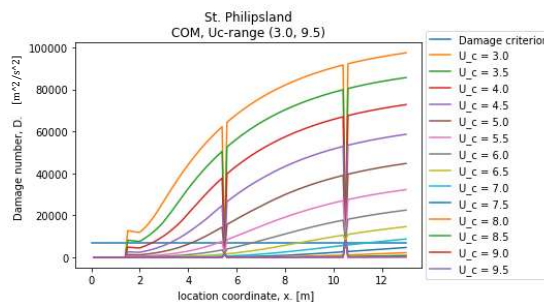
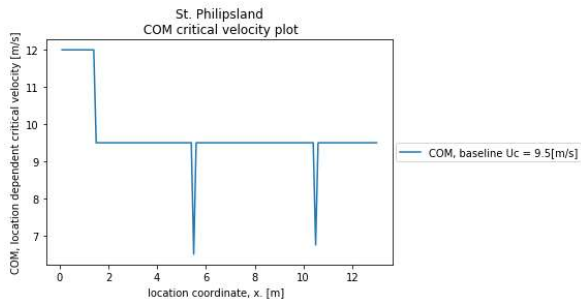
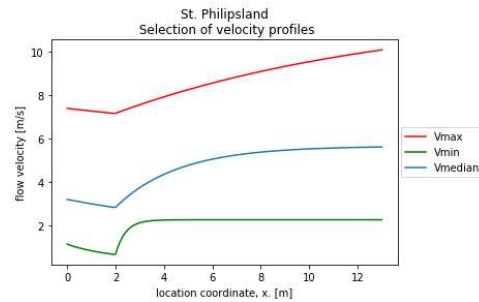
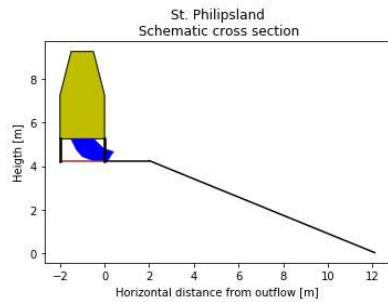


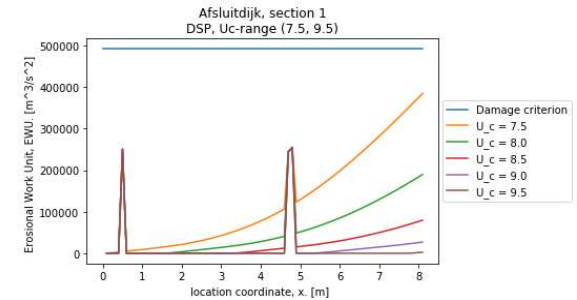
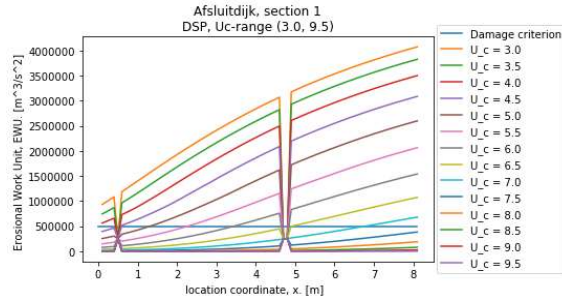
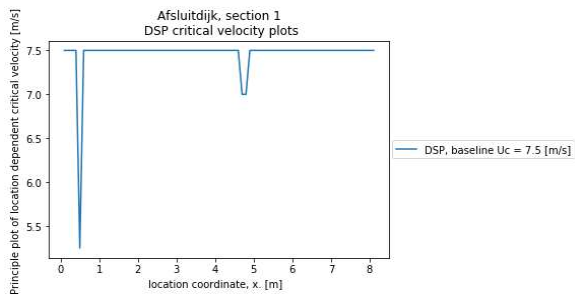
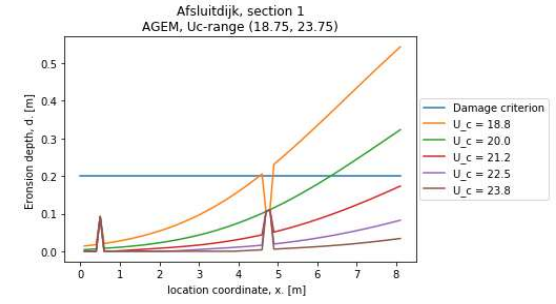
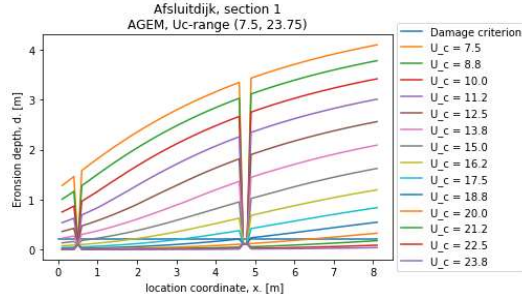
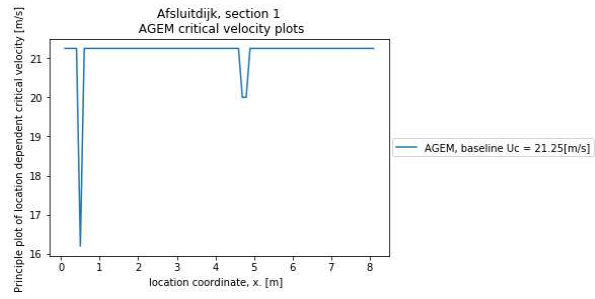
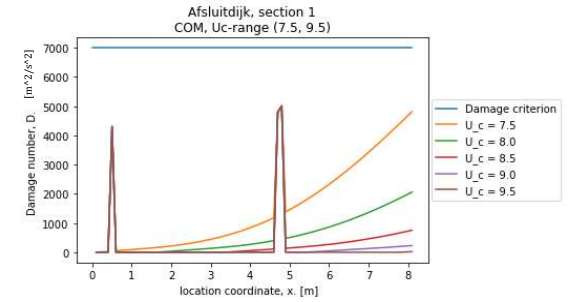
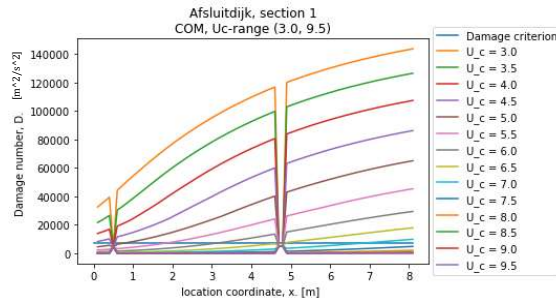
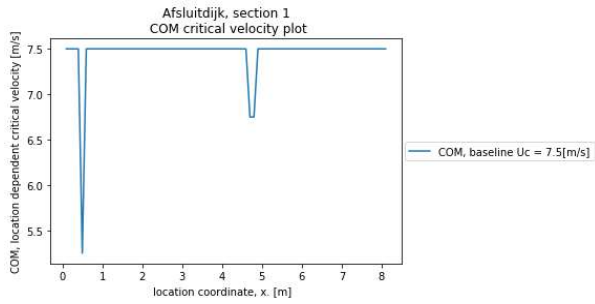
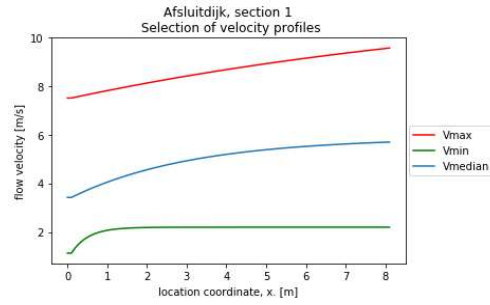
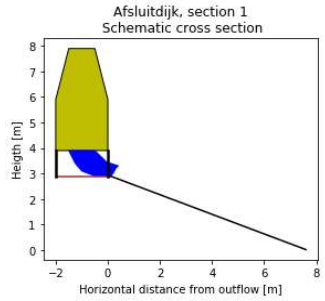


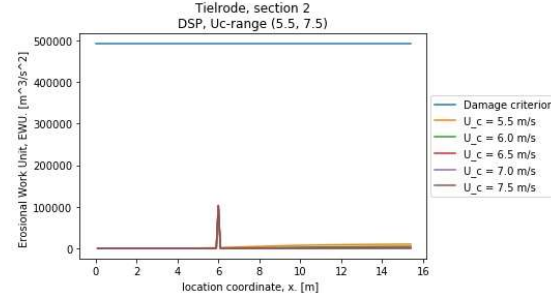
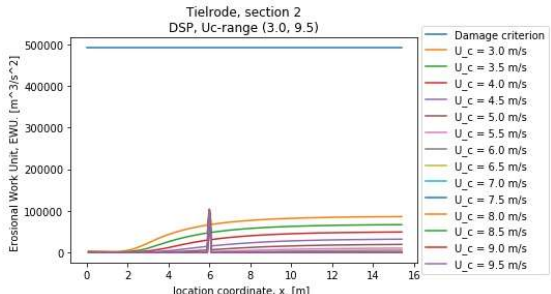
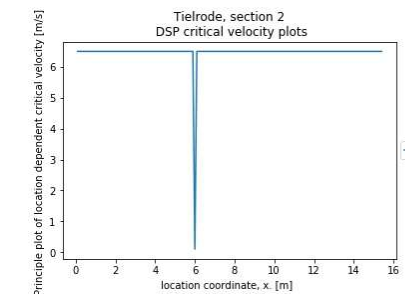
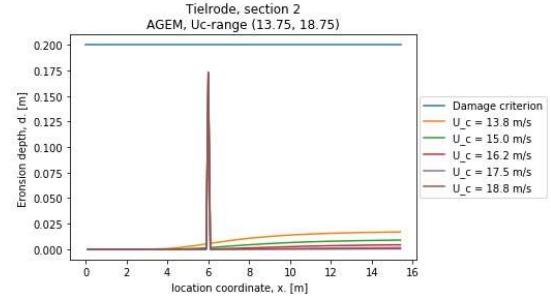
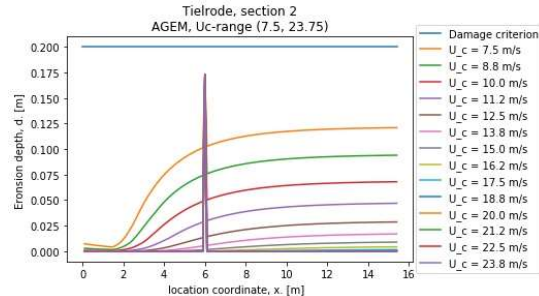
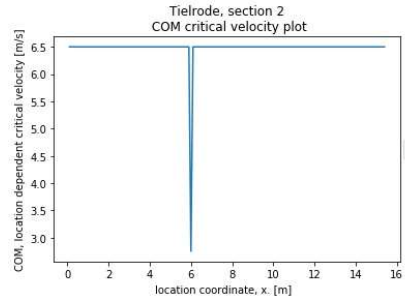
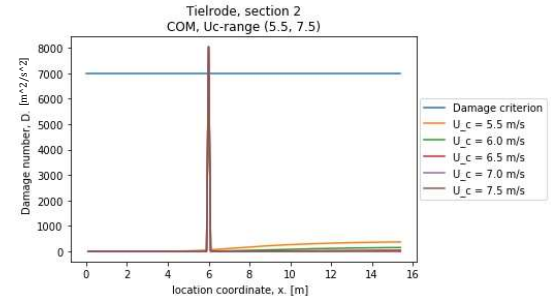
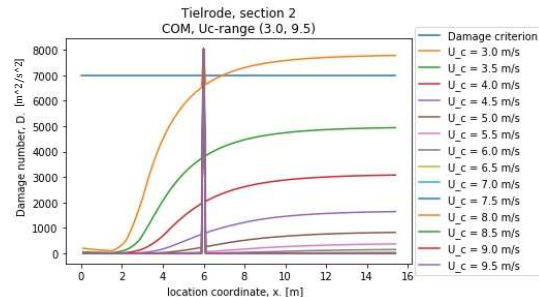
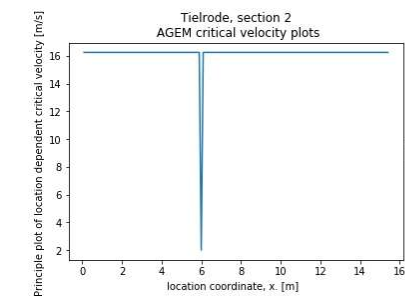
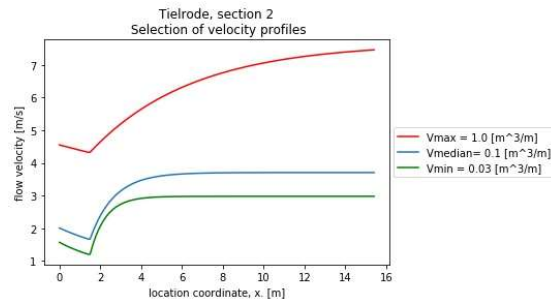
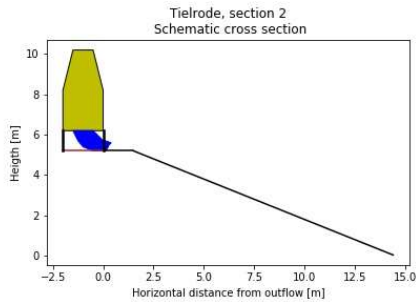


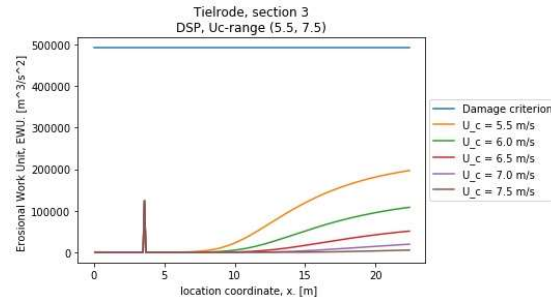
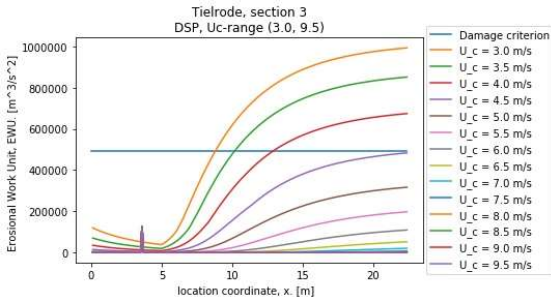
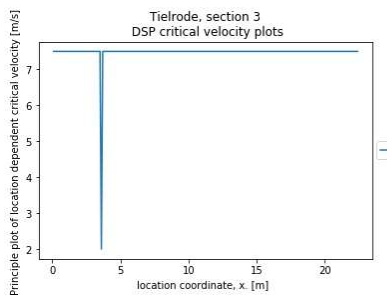
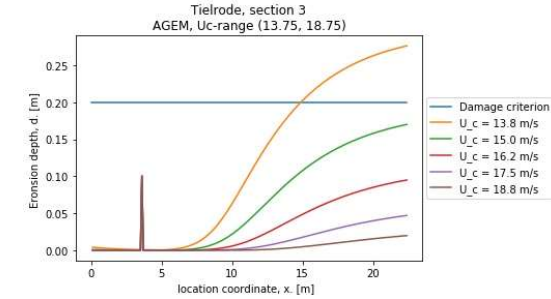
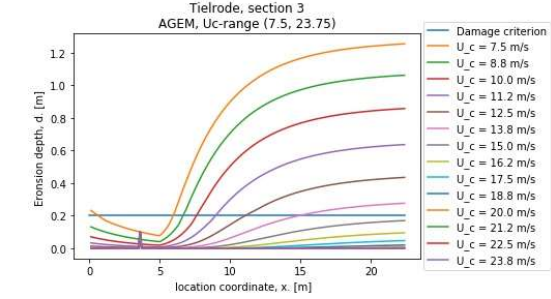
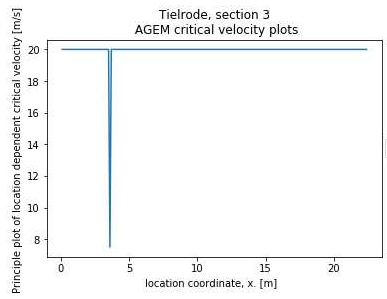
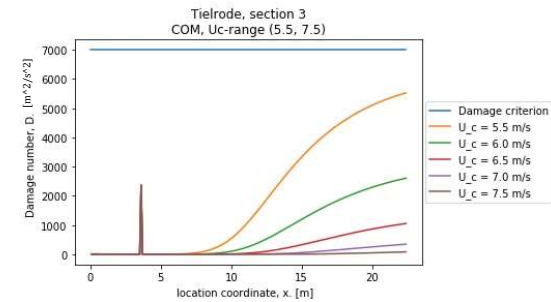
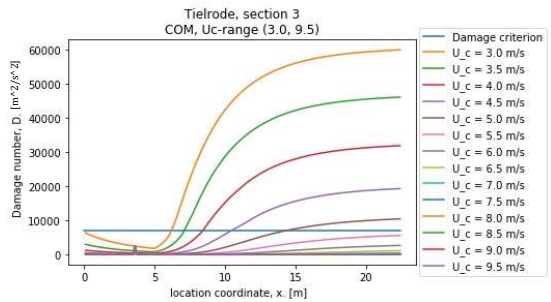
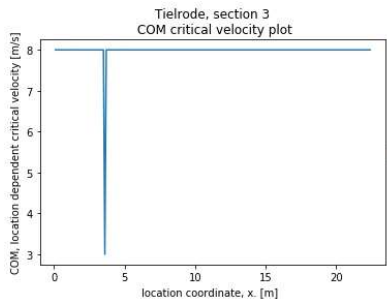
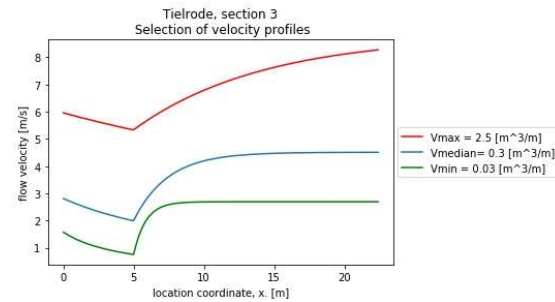
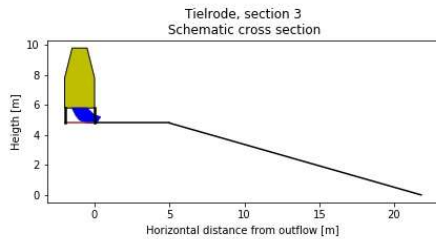


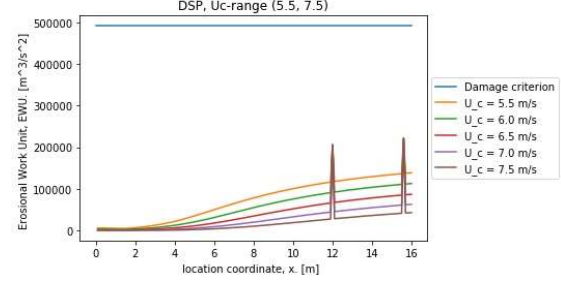
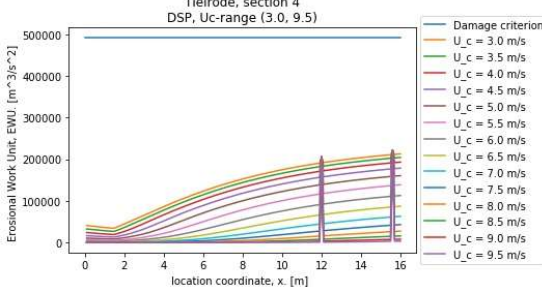
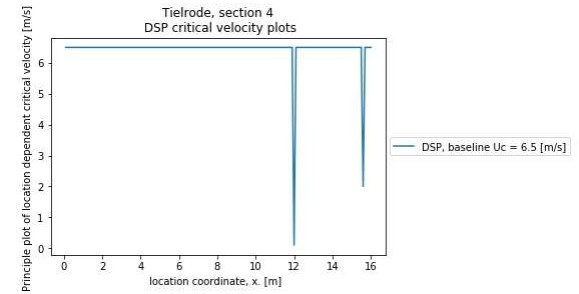
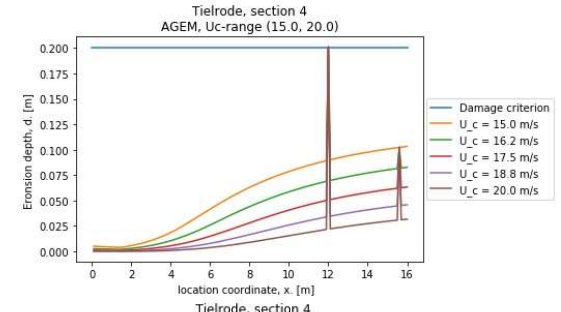
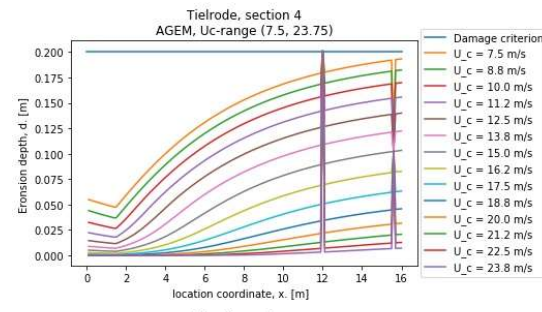
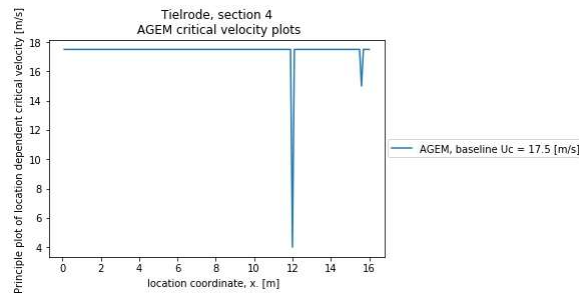
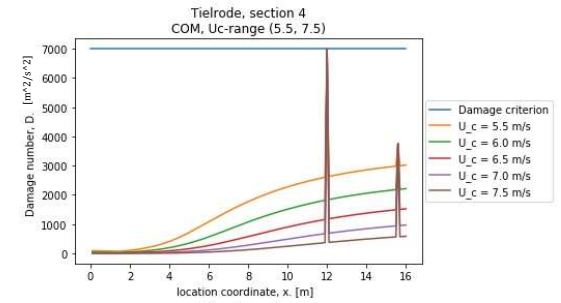
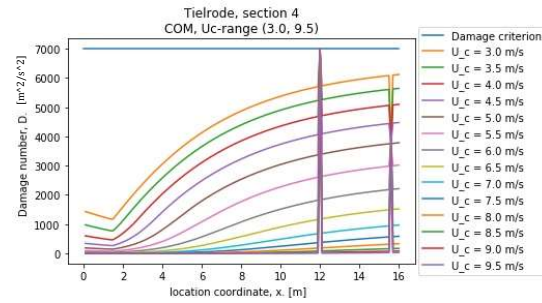
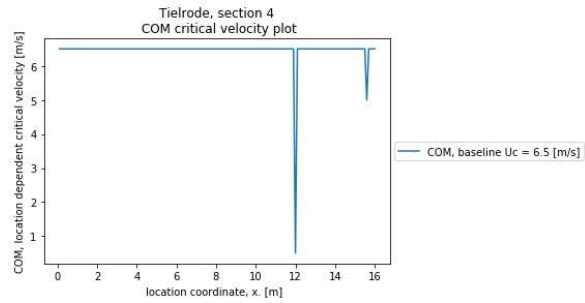
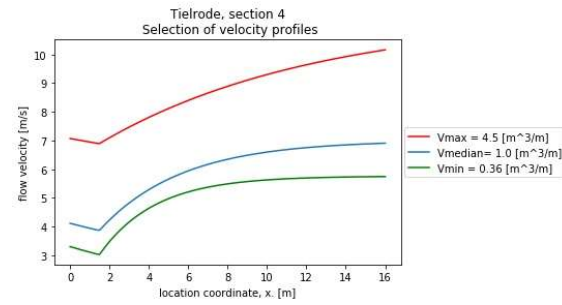
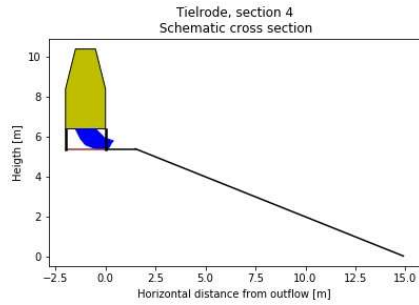


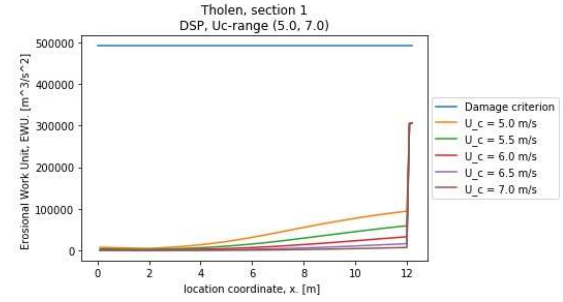
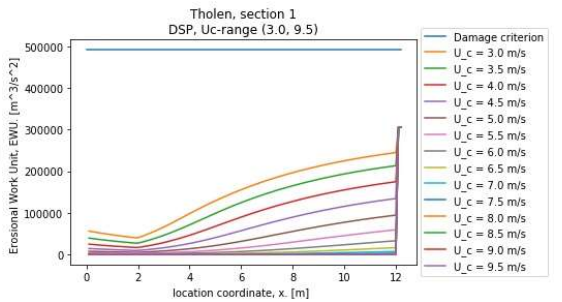
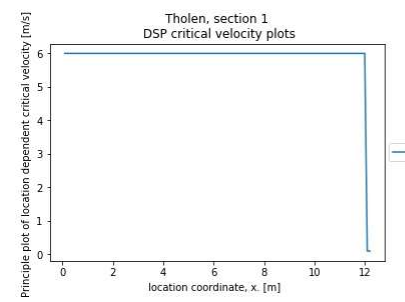
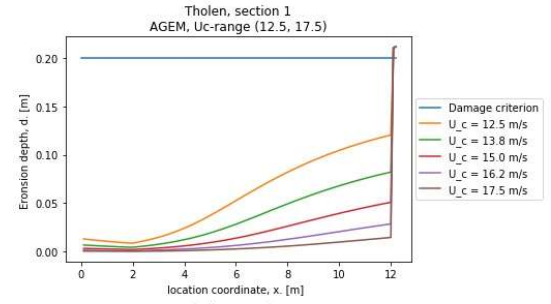
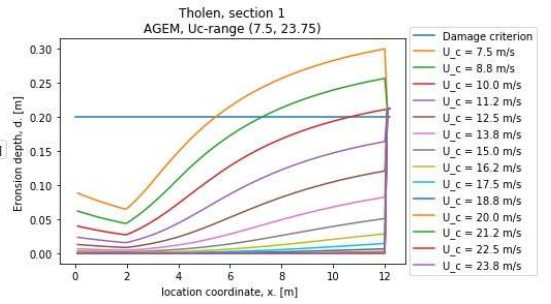
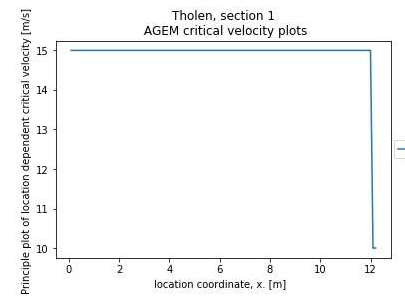
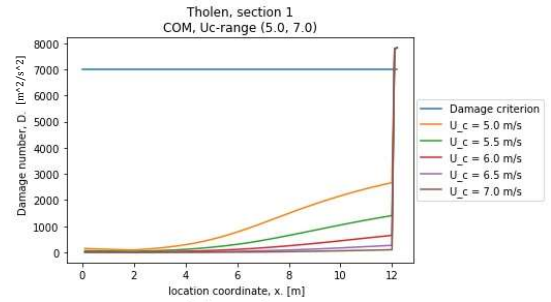
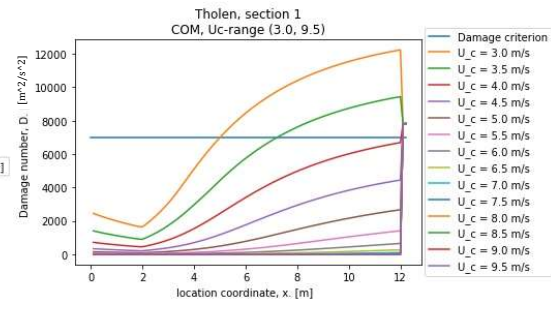
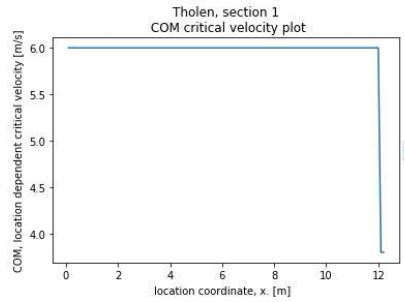
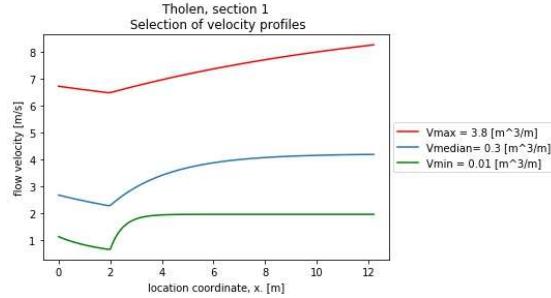
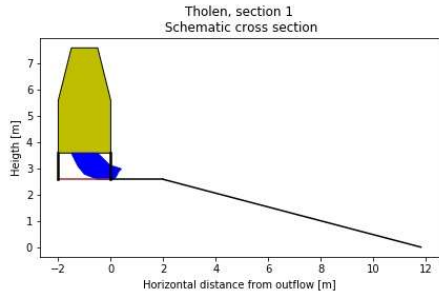


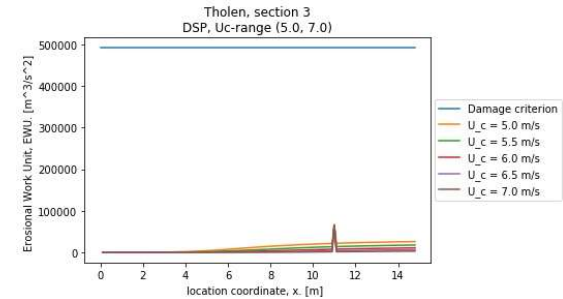
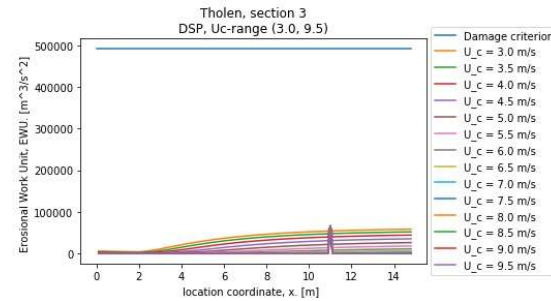
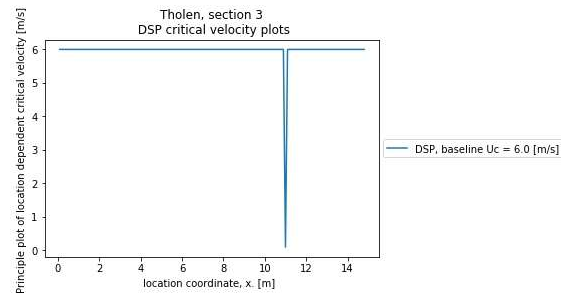
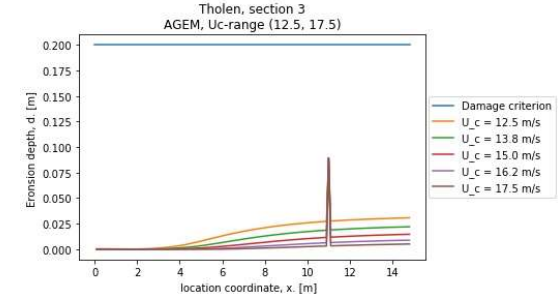
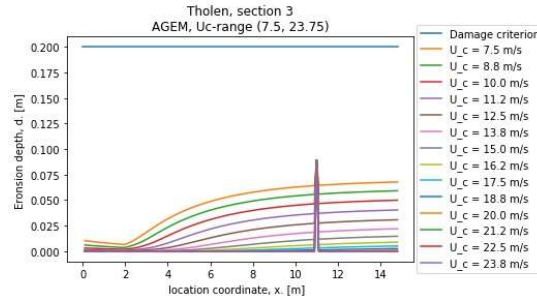
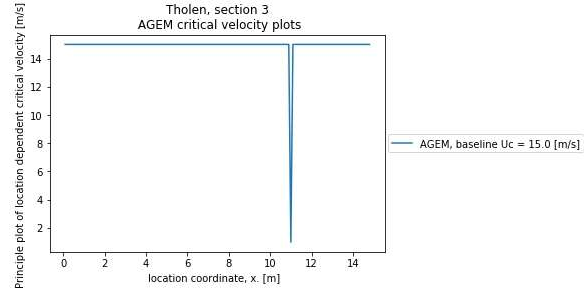
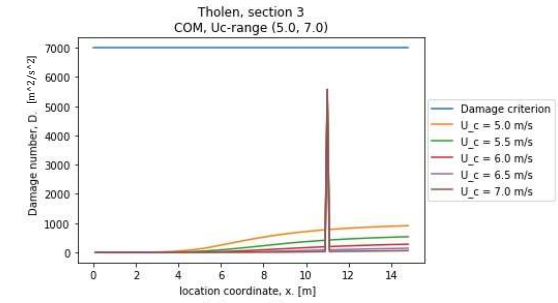
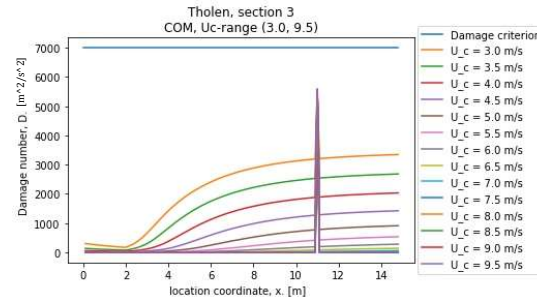
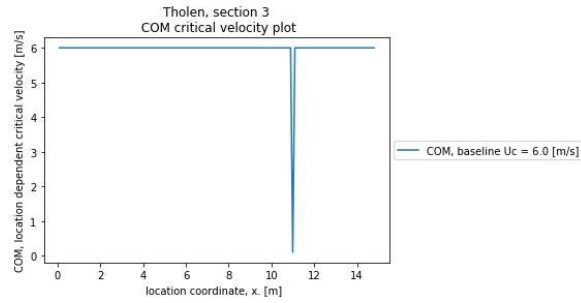
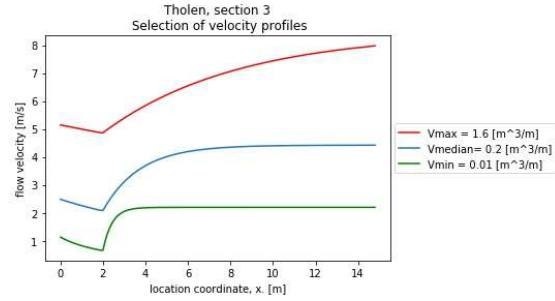
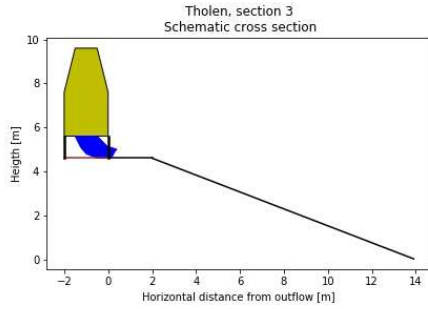


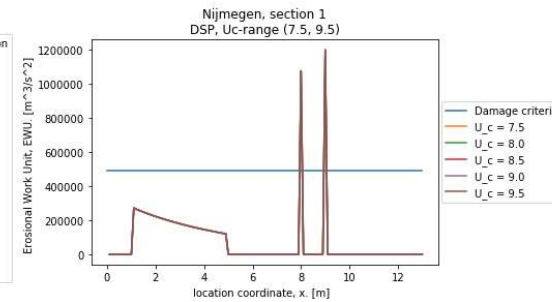
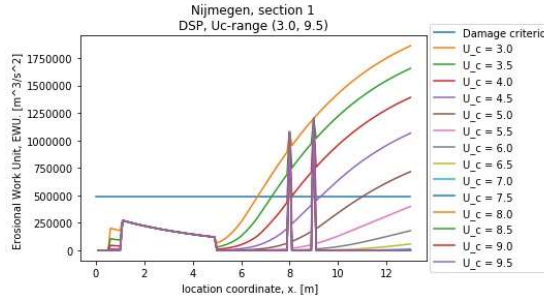
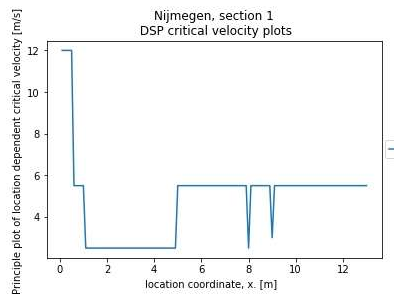
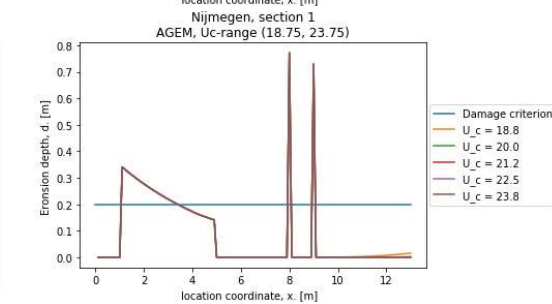
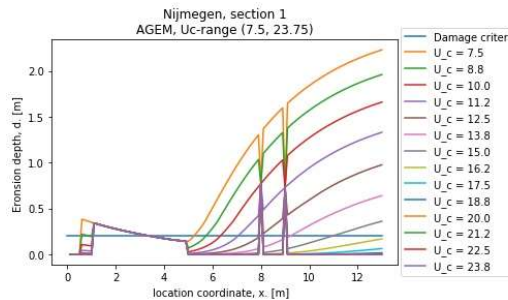
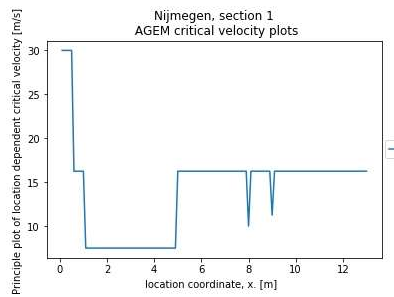
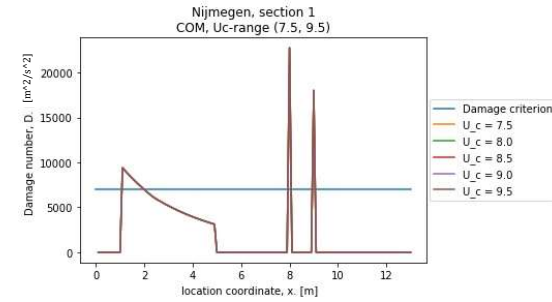
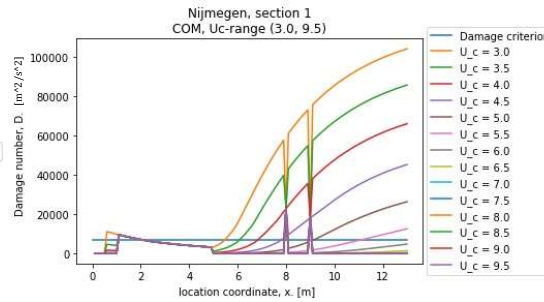
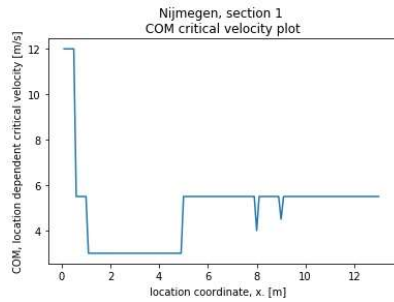
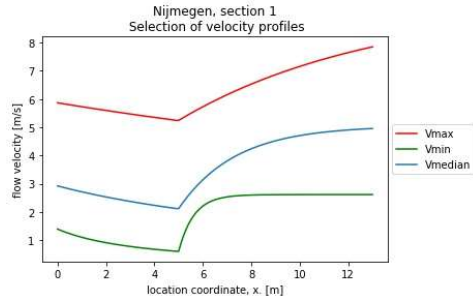
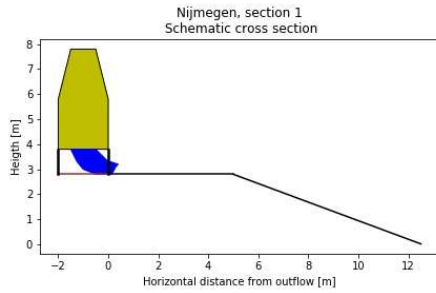


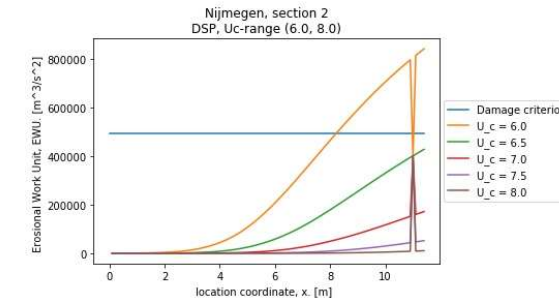
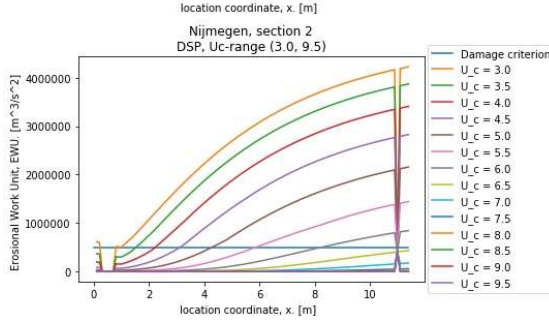
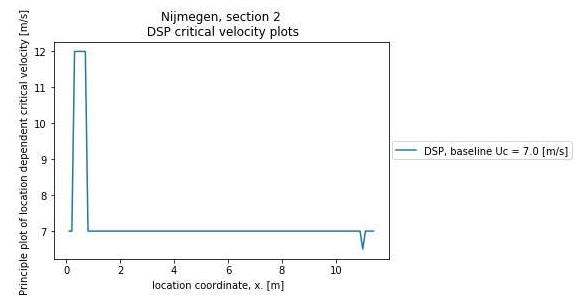
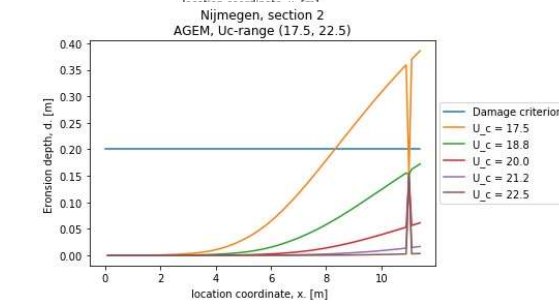
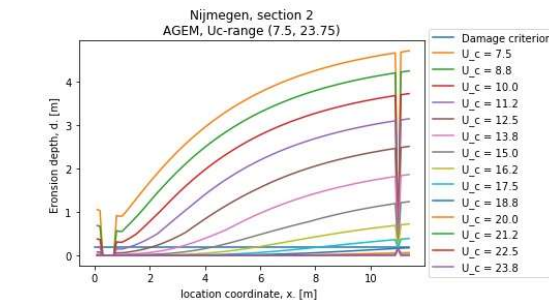
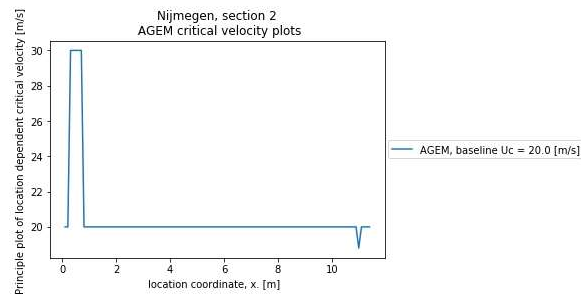
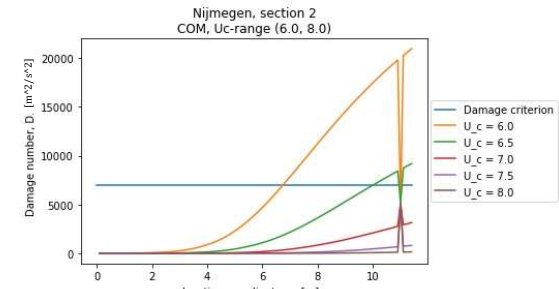
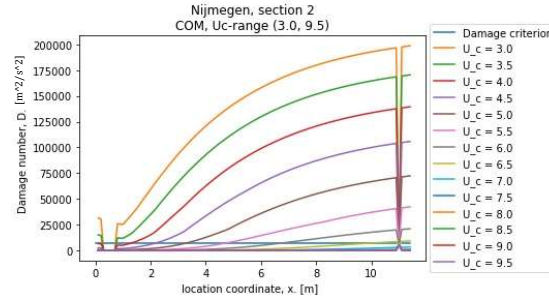
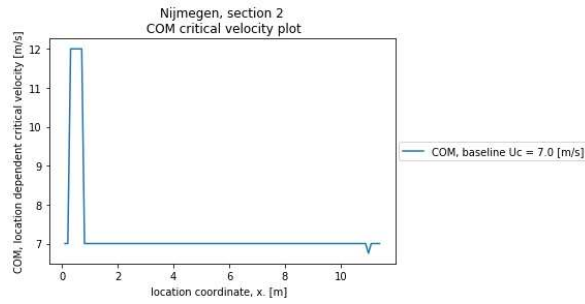
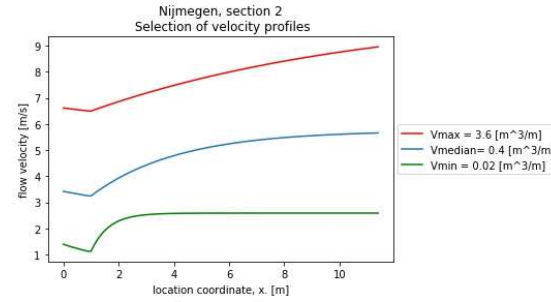
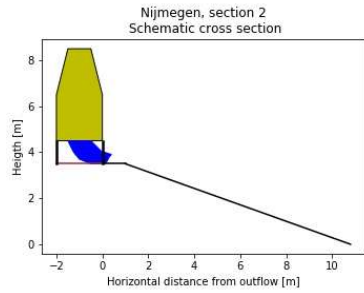


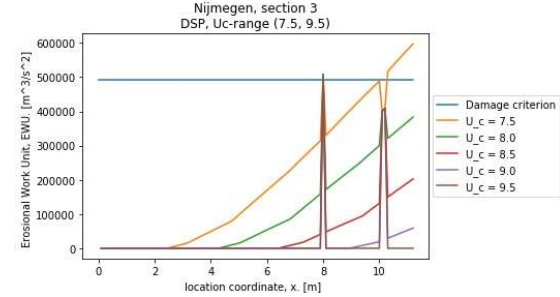
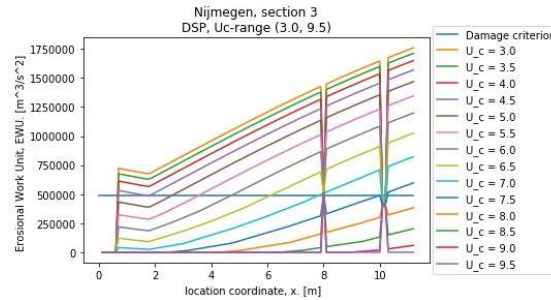
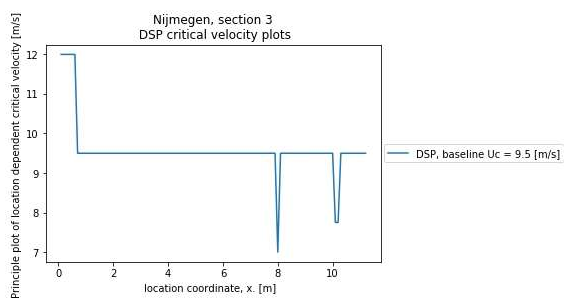
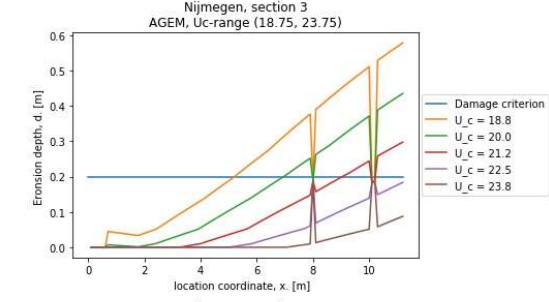
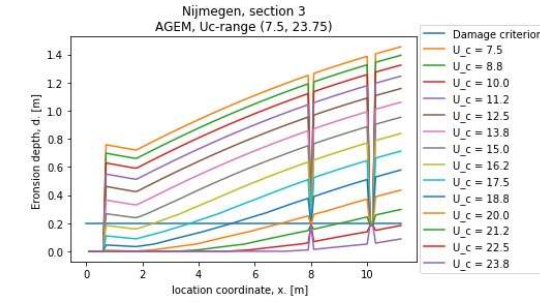
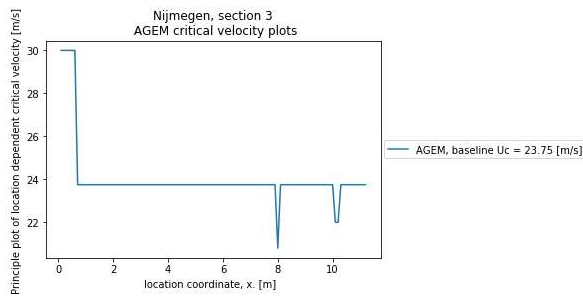
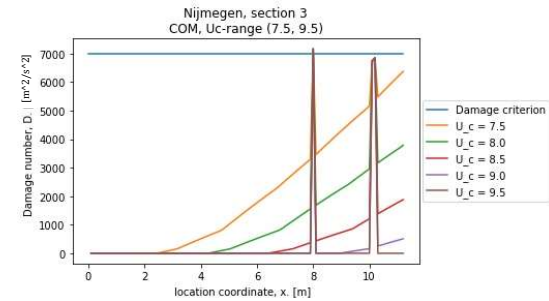
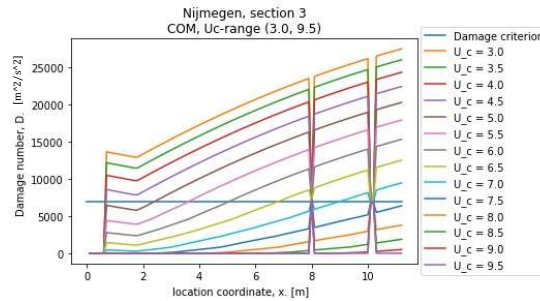
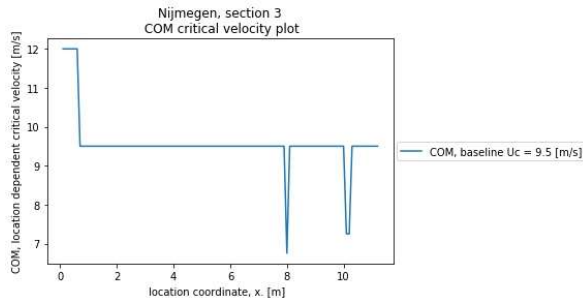
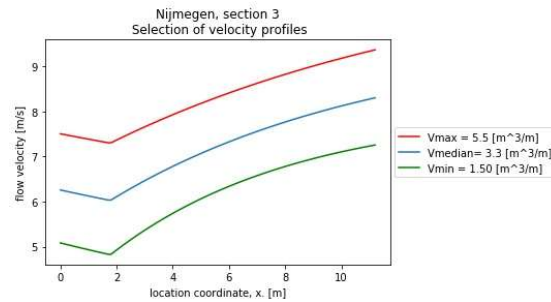
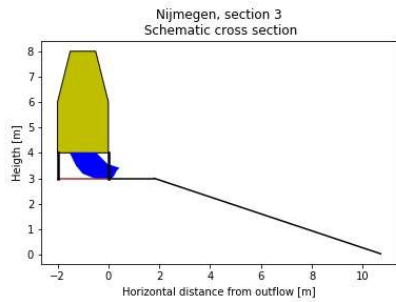


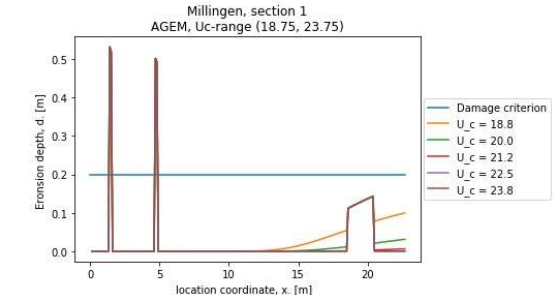
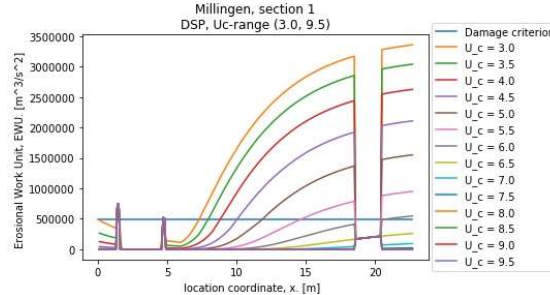
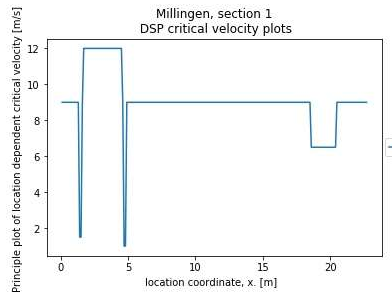
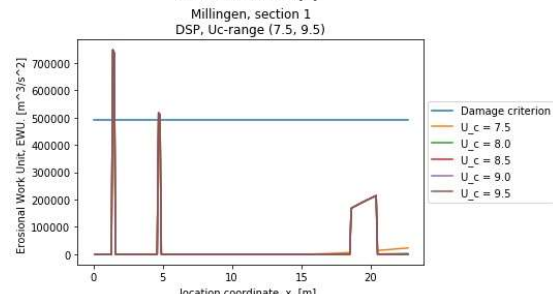
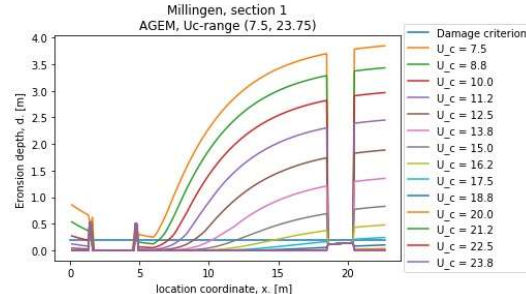
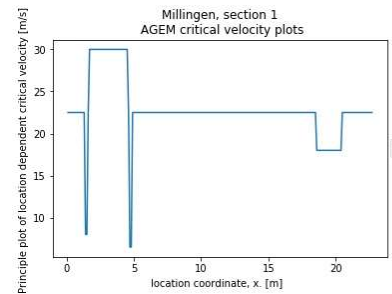
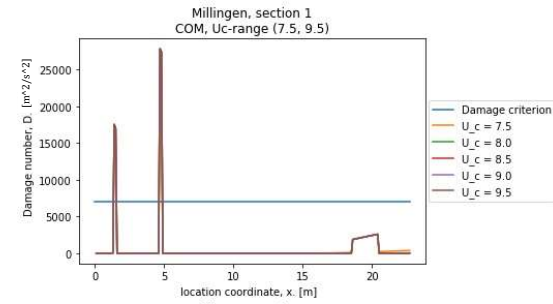
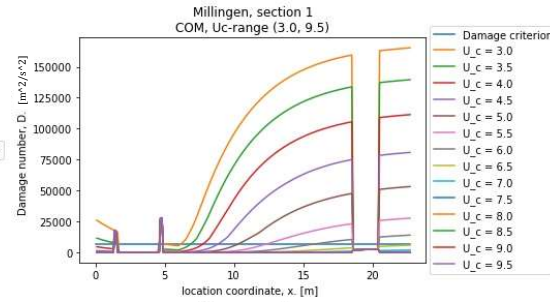
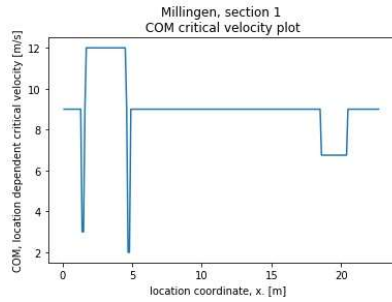
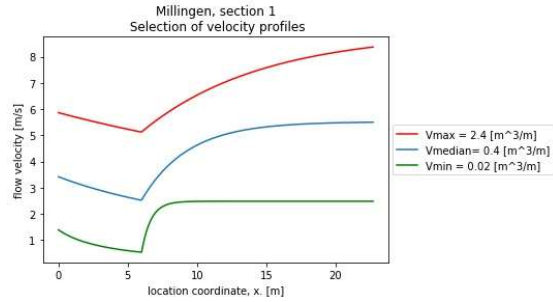
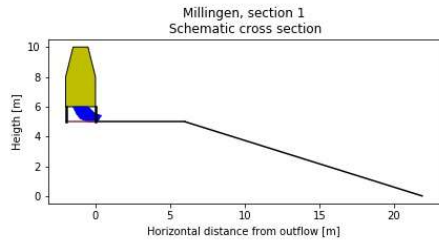


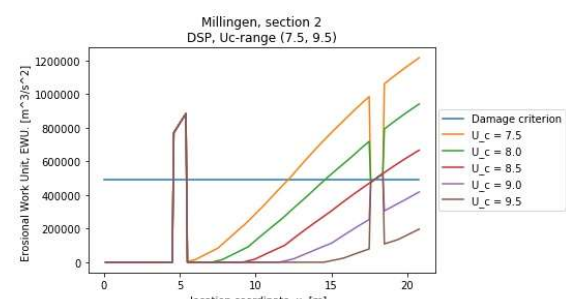
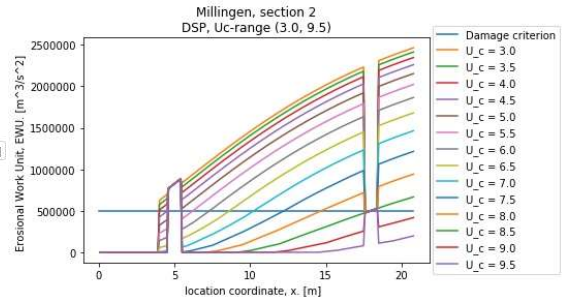
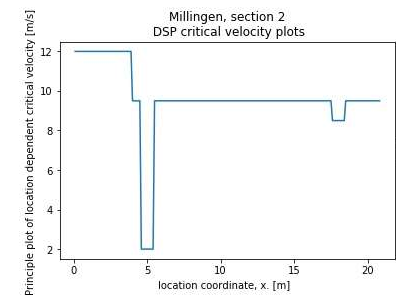
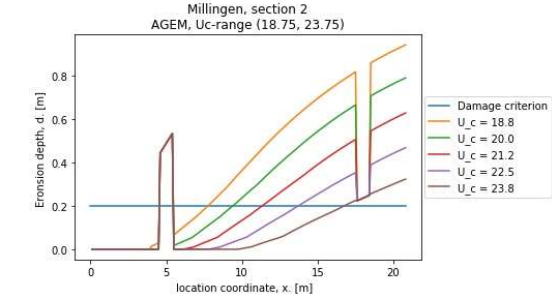
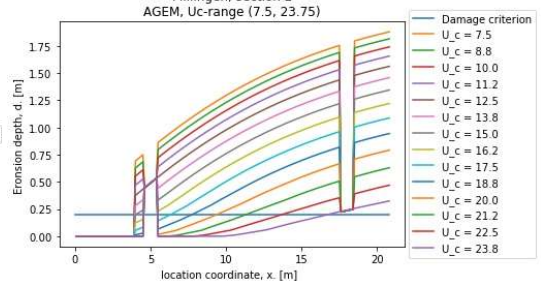
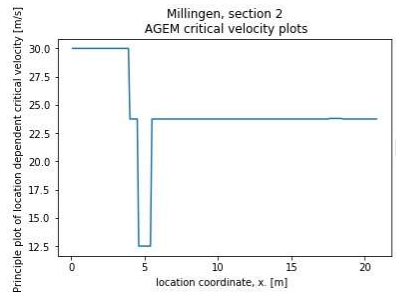
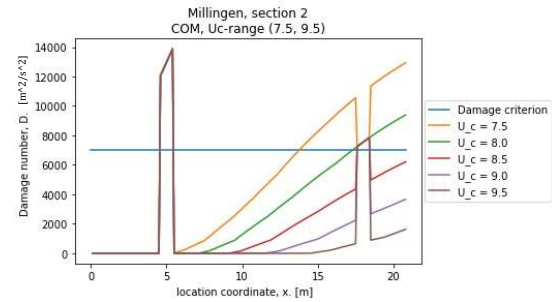
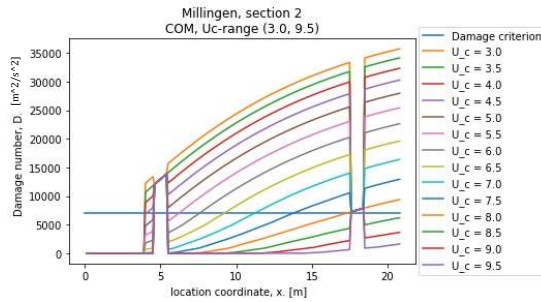
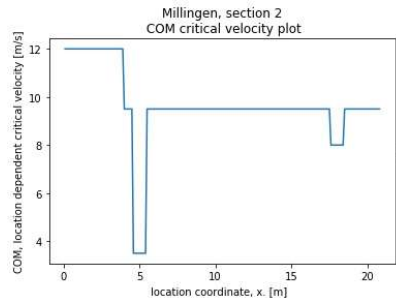
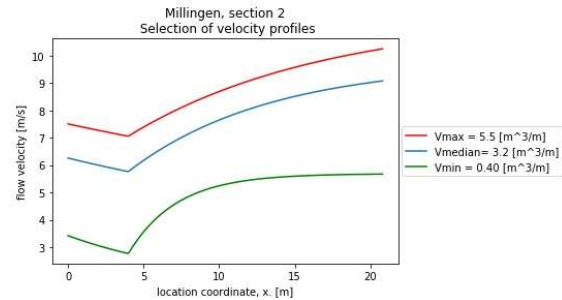
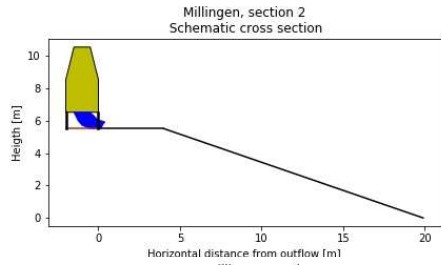


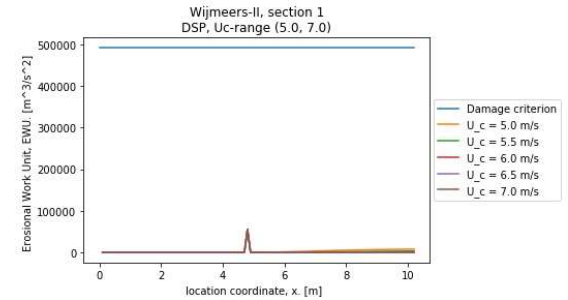
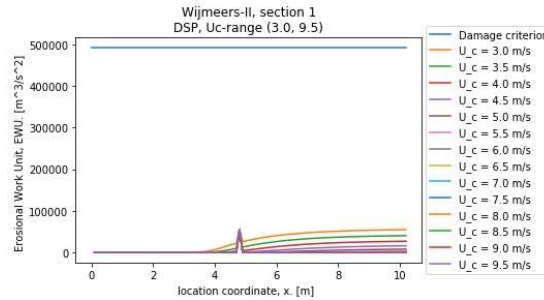
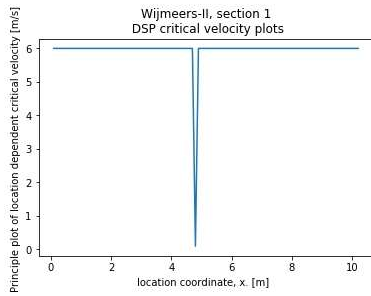
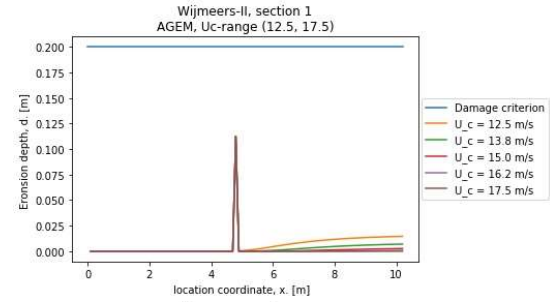
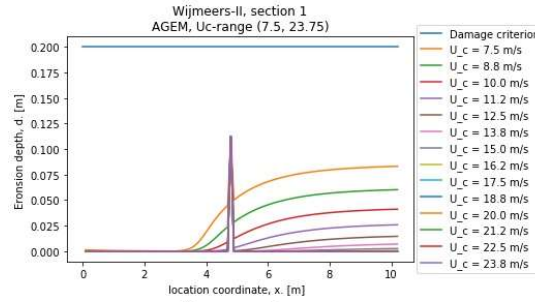
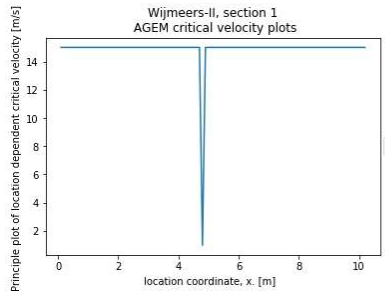
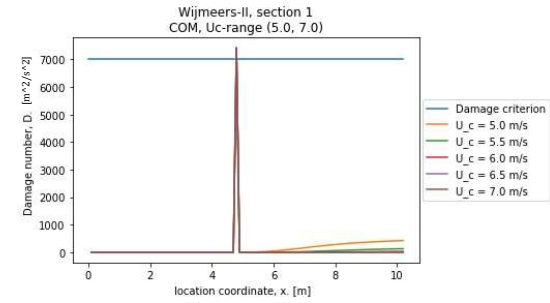
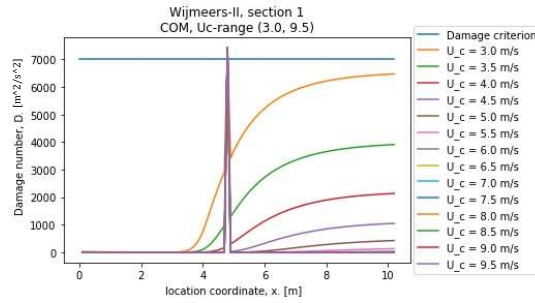
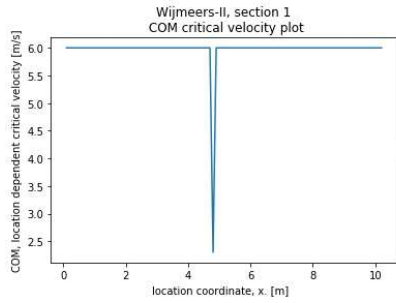
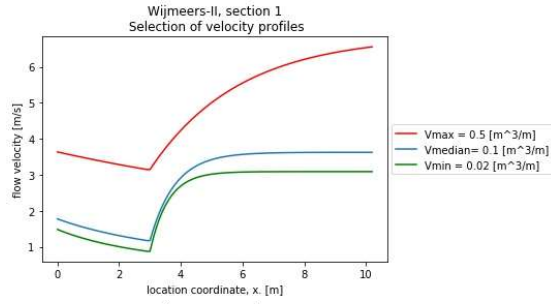
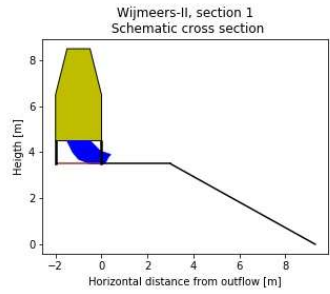


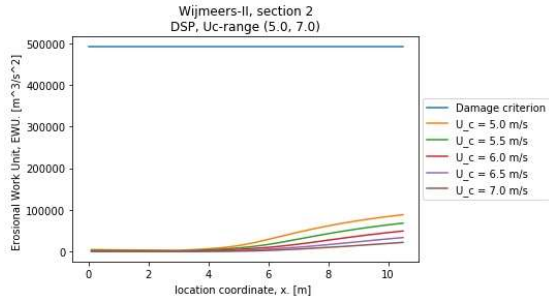
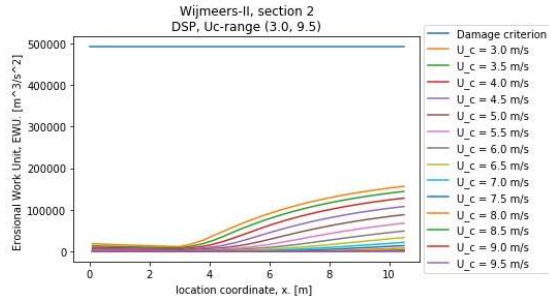
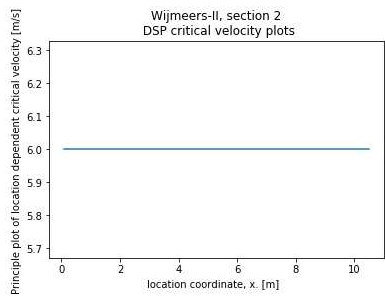
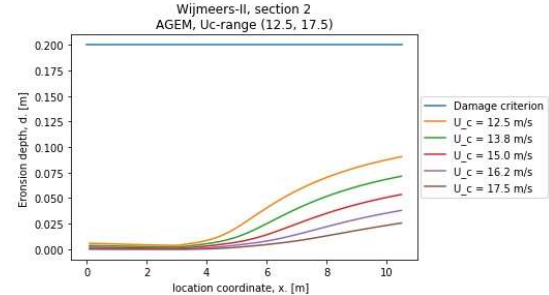
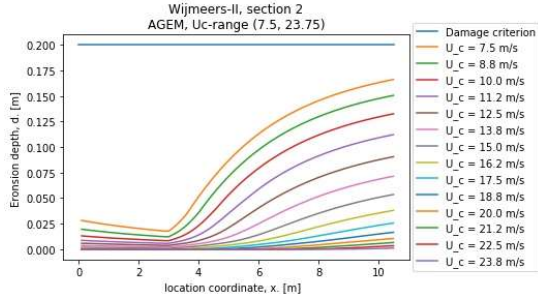
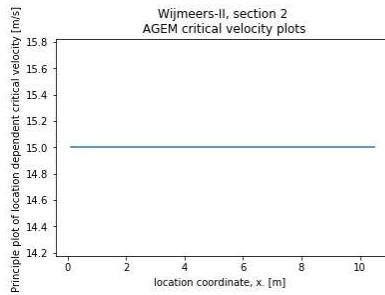
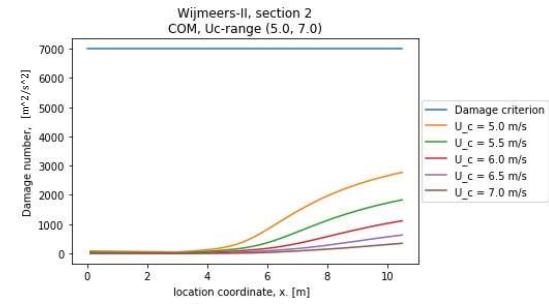
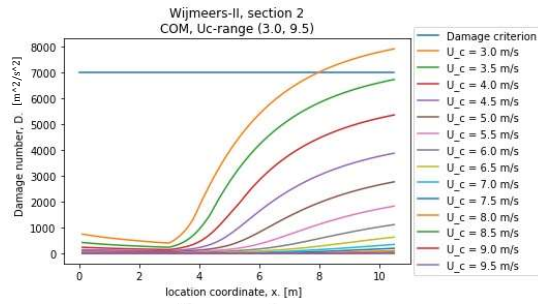
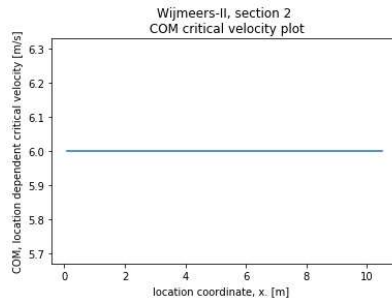
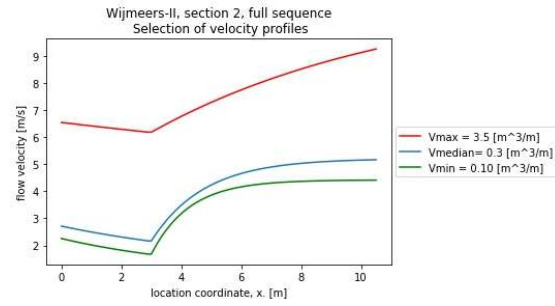
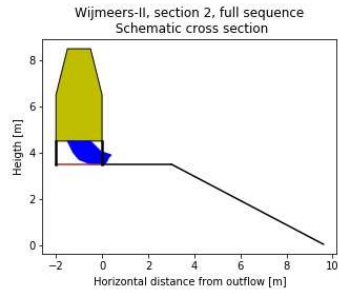










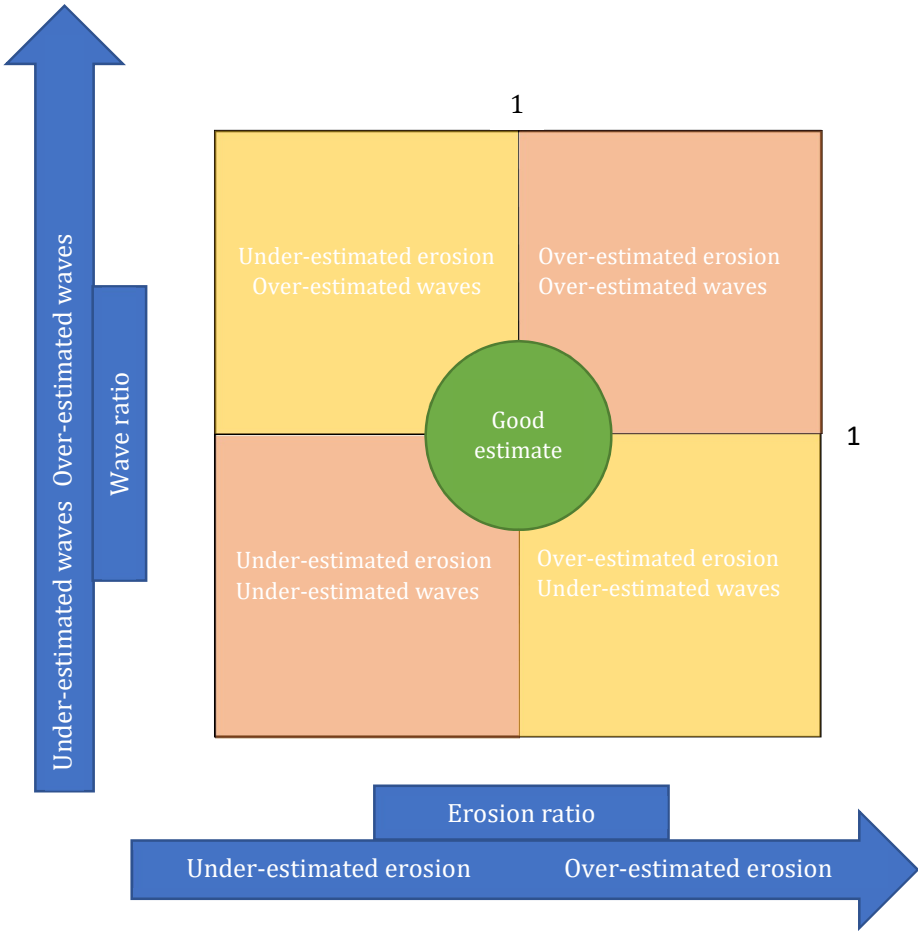


# Appendix G – Technical memo of validation predictions

The memo provides more insight in the predictions done for the validation in the master thesis “Prediction method for grass erosion on levees by wave overtopping”.

The performance is represented using two ratios, wave-ratio and the erosion-ratio. The ratios are between the model output and the experiment output. With a ratio of 1, the model exactly mimics the experiment outcome, a ratio larger than one indicates over-estimation and a ratio smaller than one indicates under-estimation. The wave-ratio is the ratio between the computed number of waves (model output) and the actual number of waves (experiment output). The erosion-ratio is the ratio between the computed erosion (model output) and the observed erosion in the factual reports (experiment output). The erosion is expressed in the definitions in table 4. Ratio-scores 1 +/- 0.40 are considered acceptable.

The principle of the performance metric is illustrated the figure below.

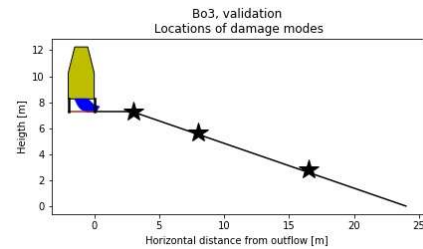


## Boonweg section 3 (Bo3)

### Input

#### Properties of the experiment

Crest width	3 meter
Crest height	7.25 meter
Slope	0.322 rad
Control list	2008 Boonweg
Discharges	0.1; 1; 10; 30; 50; 75 l/m/s
Number of waves	5369
Significant wave height	2 meter



#### Input from initial condition registration:

Damage type	Track	Track	Track
Location	3	8	16.5

### Output

#### Majority vote

	Baseline	Track at 3m	Track at 8m	Track at 16.5m
No failure	32	15	6	1
Failure	25	0	9	14
Verdict	No failure	No failure	Failure	Failure

Majority vote per model, if failure: lower limit/ mean/ upper limit. In between brackets the number of no-failure and failure predictions (No-failure / failure).

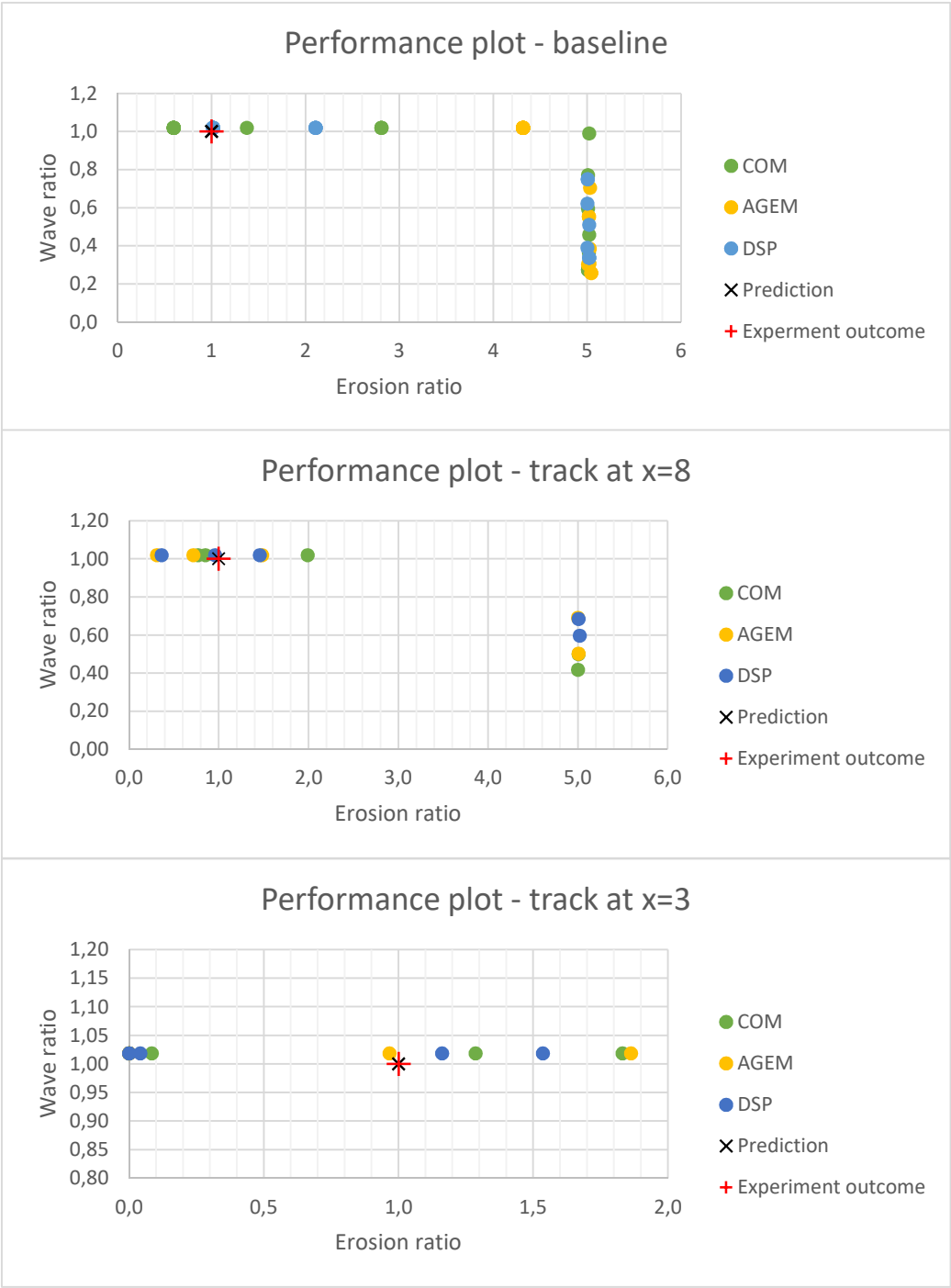
	Baseline	Track at 3m	Track at 8m	Track at 16.5m
COM	No Failure (11/8)	No failure (5/ 0)	No failure (3/ 2)	1246/ 2979/ 4500 (0/ 5)
AGEM	No Failure (10/9)	No failure (5/ 0)	No failure (3/ 2)	1488/ 2904/ 4472 (1/ 4)
DSP	No Failure (11/8)	No failure (5/ 0)	No failure (3/ 2)	1982/ 3161/ 4434 (1/ 4)
Overall	No Failure (32/25)	No failure (15/ 0)	No failure (9/ 6)	1246/ 3012/ 4500 (2/ 13)

Prediction: Grass cover failure at 16.5m from the outflow, situated at tracks, during the second half of the 50l/s per m loading step.

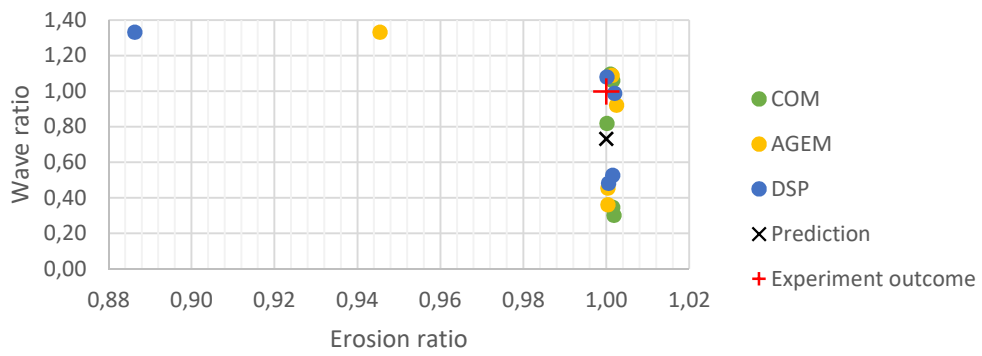
Experiment outcome: After the 30l/s per meter sessions (2159 waves), minor erosion is noted at 21meter from the outflow on a spot that is identified as weak spot before the experiment. After the 50 l/s per meter sessions (3683 waves) start of erosion at toe transition. Some minor surface erosion along the slope. No damage at service road after toe. During the first 75l/s per meter session, bulging of the grass cover occurred at the previously mentioned weak spot. After 1.5hr in this session, the grass-cover failed (4105 waves). Pavers emerged from below the grass cover, but these seemed not the be the cause of the erosion., the erosion appeared to migrate down from above. Around the location of the track at 16.5meter from the outflow, a second bulge formed and grass sods were washed away during the last few waves causing the grass cover to fail. The experiment was extended with 30minutes to see how this developed. No damage was noted at the service road.

Verdict: The baseline prediction is correct. The prediction of the lower two tracks was too conservative, at 8meter from the outflow no failure occurred and the failure at 16.5m occurred above the upper bound of number of waves prediction. The service road and pavers below the surface were not included in the nul-opname, therefore these were not taken into account and both were not the cause of damage development. The damage initiator, the weak spot with mice activity, could not be included in the prediction because this type of failure has not been observed in the test data.

Plots of the predictions. Non-failure predictions are represented by a value of 100 above the duration threshold. The predictions are linked to the section ID's trough the predictor ID's on the horizontal axis.



Performance plot - track at x=16.5

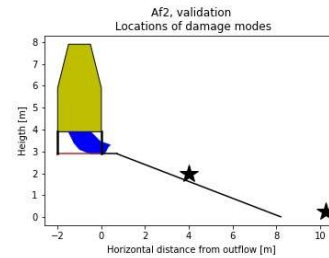


## Afsluitdijk section 2 (Af2)

### Input

Properties of the experiment

Crest width	0.7 meter
Crest height	2.9 meter
Slope	0.367 rad
Control list	2009 Afsluitdijk
Discharges	1; 10; 30; 50; 75 l/m/s
Number of waves	5360
Significant wave height	2 meter



Input from initial condition registration:

Damage type	Track	Toe
Location	4	After toe

### Output

Majority vote

	Baseline	Track at 4m	Toe
No failure	37	9	6
Failure	20	6	21
Verdict	No failure	No failure	Failure

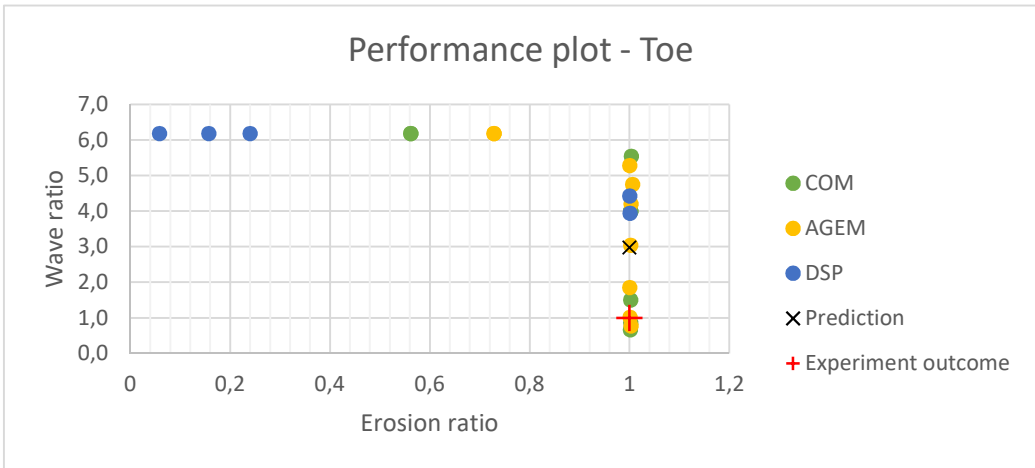
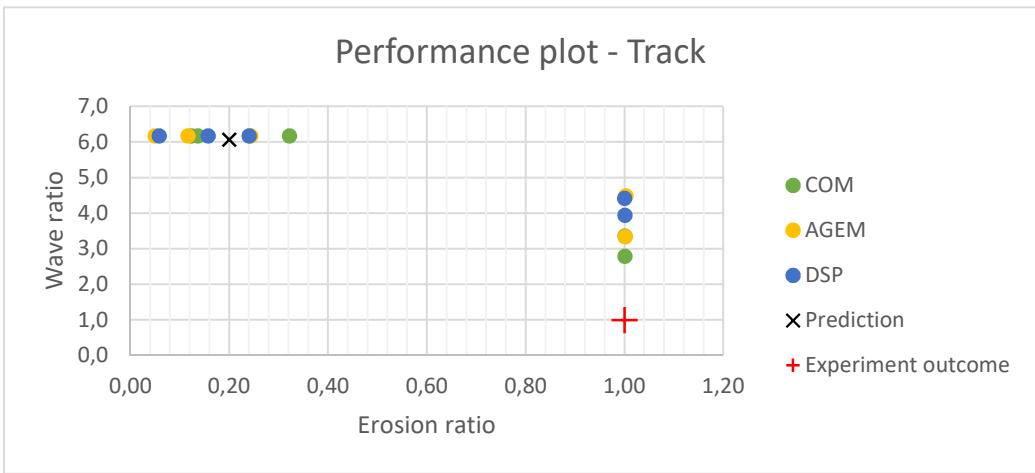
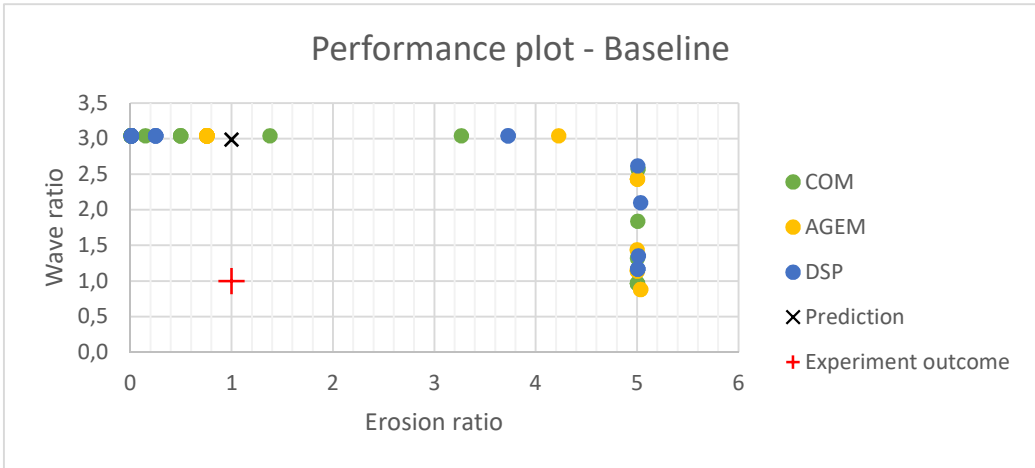
Majority vote per model, if failure: lower limit/ mean/ upper limit. In between brackets the number of no-failure and failure predictions (No-failure / failure).

	Baseline	Track at 4m	Toe
COM	No Failure (13/6)	No failure (3/ 2)	585/ 2594/ 4895 (2/ 7)
AGEM	No Failure (11/8)	No failure (3/ 2)	681/ 2538/ 4664 (2/ 7)
DSP	No Failure (13/6)	No failure (3/ 2)	1234/2650/3916 (2/ 7)
Overall	No Failure (37/20)	No failure (9/ 6)	585/ 2628/ 4895 (6/ 21)

Prediction: Failure after the toe at the pavement after 1700 waves and development of damage at the heavy track.

Experiment outcome: After 75min of 10l/s per meter (282 waves), the first damage developed at the location of the heavy track with the 13cm deep pit and after the toe. At the end of the 10l/s per meter sessions (884 waves) the grass cover has failed. Also erosion occurred just after the toe where the fence was removed and where the grass was trampled and muddy, the grass cover was removed at certain places. After 4hours and 20min of 30 l/s per meter (1795 waves), the experiment was stopped due to excessive erosion of the pavement elements.

Verdict: The erosion at the heavy track developed into failure in contrast with the prediction, only at a 13cm deep pit in this track. But only for the location with the 13cm deep pit, on other places no damage developed but this may be due to the premature termination. Failure at the toe occurred earlier than predicted.

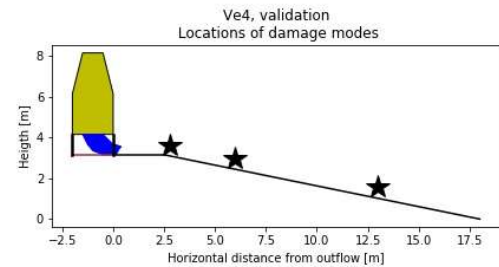


## Vechtdijk section 4 (Ve4)

### Input

Properties of the experiment

Crest width	2.5 meter
Crest height	3.2 meter
Slope	0.201 rad
Control list	2010 Vechtdijk
Discharges	0.1; 1; 5; 10; 30; 50 l/m/s
Number of waves	2487
Significant wave height	3 meter



Input from initial condition registration:

Damage type	Track	Mole	Mole
Meters from outflow	2.8	6	13

### Output

Majority vote

	Baseline	Track at 2.8m	Mole at 6m	Mole at 13m
No failure	44	15	15	15
Failure	13	0	27	27
Verdict	No failure	No failure	Failure	Failure

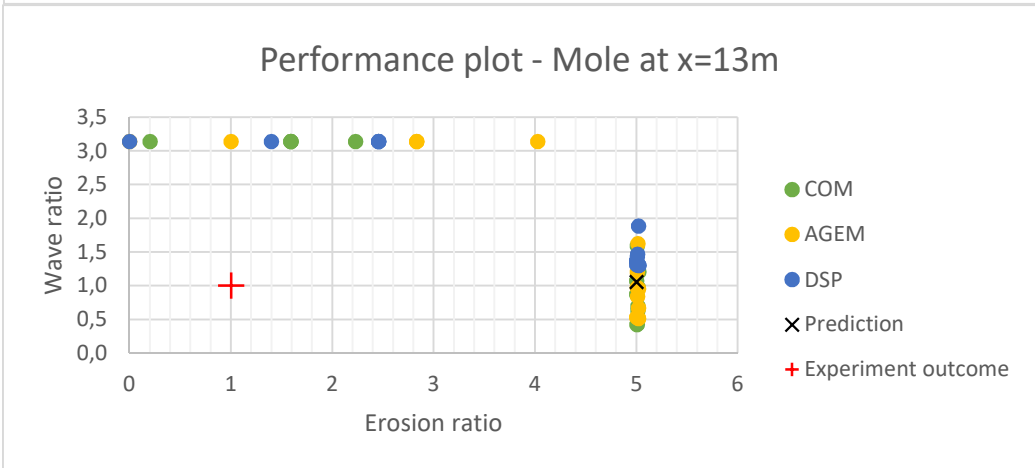
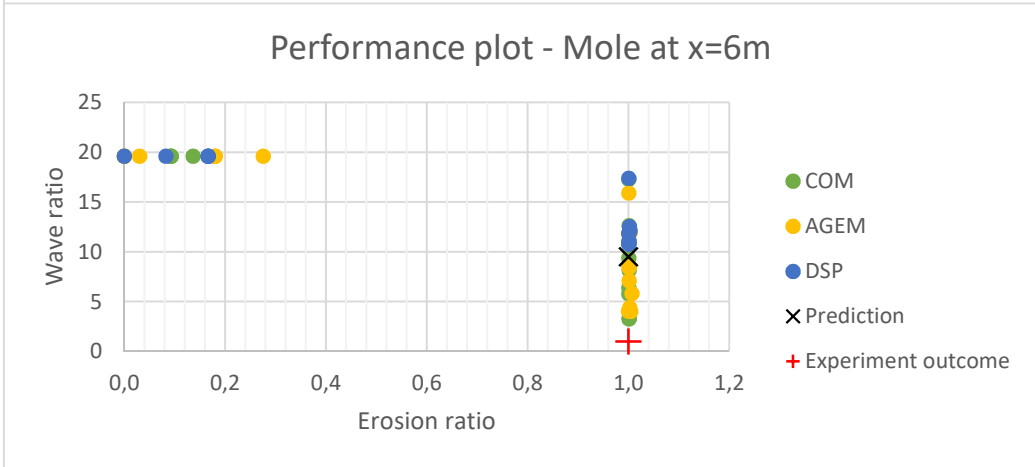
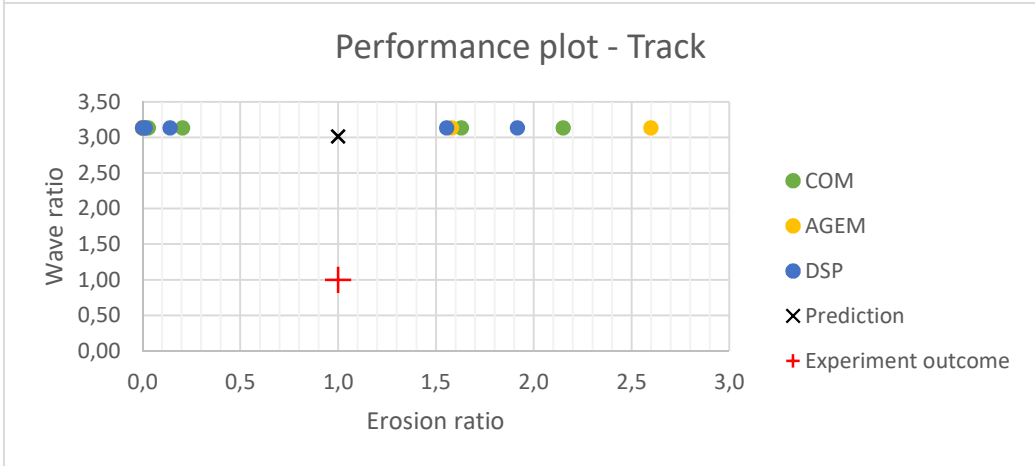
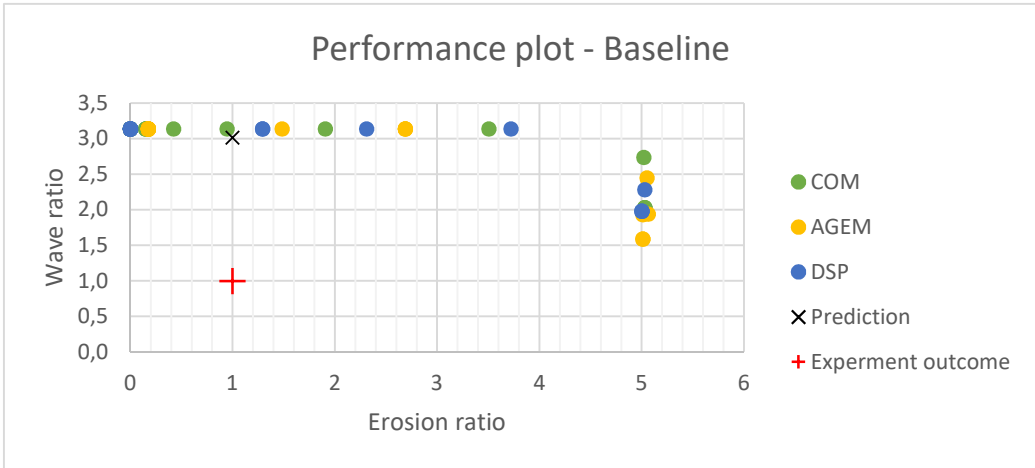
Majority vote per model, if failure: lower limit/ mean/ upper limit. In between brackets the number of no-failure and failure predictions (No-failure / failure).

	Baseline	Track at 2.8m	Mole at 6m	Mole at 13
COM	No Failure (15/4)	No failure (5/0)	431/ 1134/ 2283 (5/ 9)	347/ 723/ 1313 (5/ 9)
AGEM	No Failure (14/5)	No failure (5/0)	529/ 1030/ 2102 (5/9)	422/ 717/ 1339 (5/ 9)
DSP	No Failure (15/4)	No failure (5/0)	1426/1604/2296 (5/ 9)	1073/1166/1555 (5/ 9)
Overall	No Failure (45/12)	No failure (15/0)	431/ 1256/ 2283 (15/ 27)	347/ 869/ 1555 (15/ 27)

Prediction: Grass cover failure at 13m after 500 waves, which is during 10 l/s per meter. And grass cover failure at 6 meter after 774 waves (during 30 l/s per meter) if the test is continued.

Experiment outcome: During the first session of 5l/s per meter (53 till 132 waves), the grass cover failed at two locations around 6 to 7 meters from the outflow, where mole activity was present. At the end of the last 5l/s per meter session (290 waves), the erosion expanded down the slope but not in depth. During following session, the size of the erosion increased, but only marginally in depth. After one hour in the first 30 l/s per meter session, the stop criterion was reached and the experiment was terminated (825 waves).

Verdict: The prediction for the mole activity at 13 meters from the outflow was off. The grass cover did fail at a 6 meters from the outflow as indicated by the prediction, but the prediction was too optimistic. The final cause of termination was not foreseen.

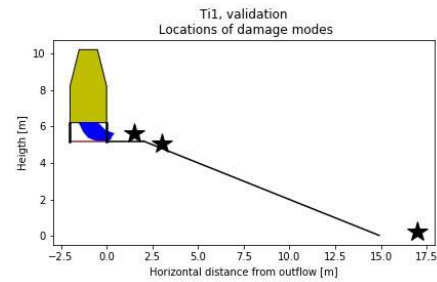


## Tielrode section 1 (Ti1)

### Input

#### Properties of the experiment

Crest width	2 meter
Crest height	5.2 meter
Slope	0.381 rad
Control list	2010 Antwerpen
Discharges	1; 10; 30; 50 l/m/s
Number of waves	2558
Significant wave height	0.75/ 1 meter



Input from initial condition registration:

In the nul-opname a straight edge has been identified, this damage mode is not included in the prediction method. As a test this is included as mole activity at 3 meters from the outflow, following from the experience with the validation for Boonweg section 3.

Damage type	Track	Mole	Toe
Meters from outflow	1.5	3	After toe

### Output

Majority vote

	Baseline	Track at 1.5m	Mole at 3m	Toe
No failure	57	15	29	19
Failure	0	0	13	8
Verdict	No failure	No failure	No failure	No failure

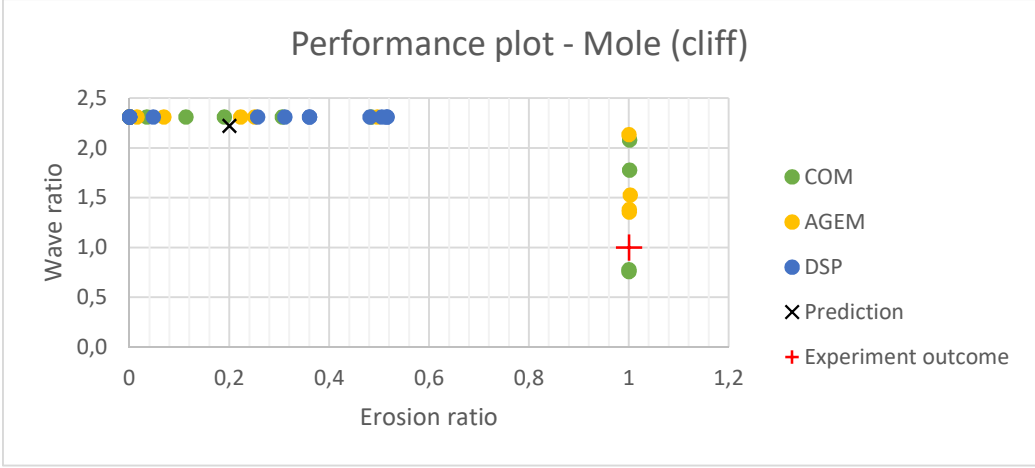
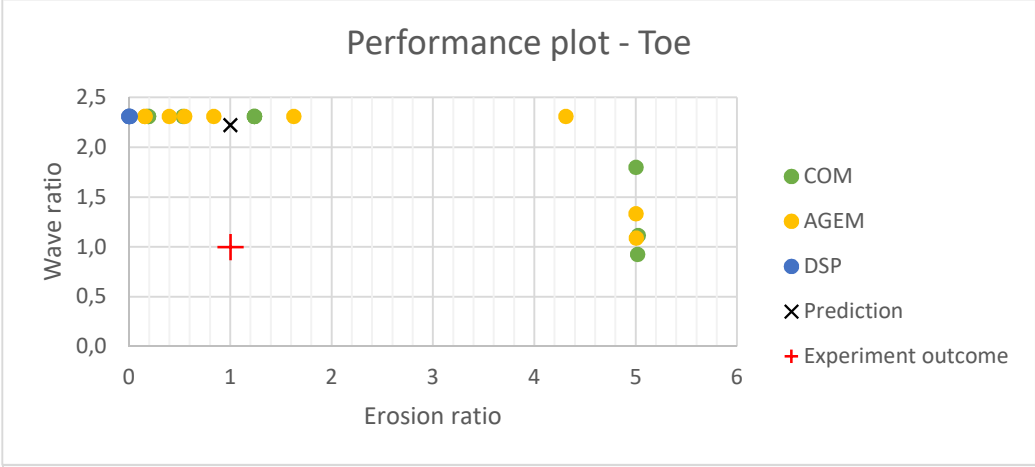
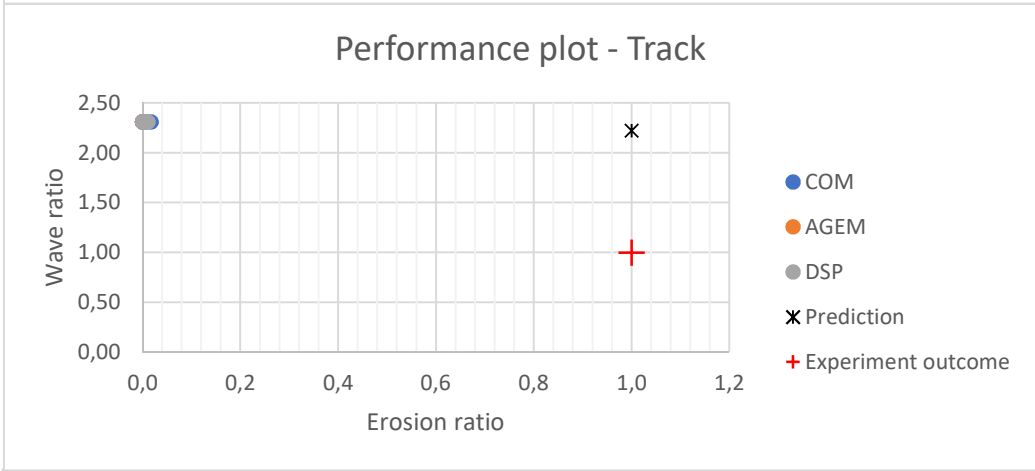
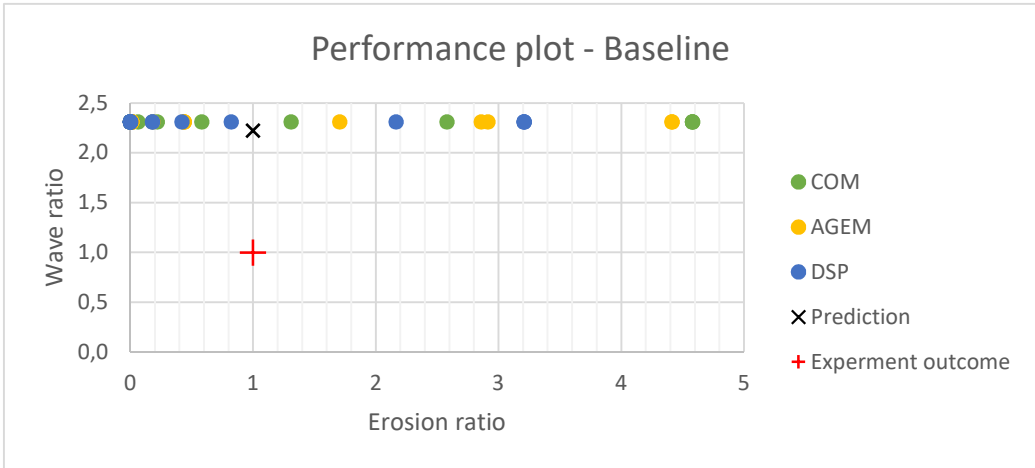
Majority vote per model, if failure: lower limit/ mean/ upper limit. In between brackets the number of no-failure and failure predictions (No-failure / failure).

	Baseline	Track at 2.8m	Mole at 3m	Toe
COM	No Failure (19/0)	No failure (5/0)	No failure (10/4)	No failure (6/3)
AGEM	No Failure (19/0)	No failure (5/0)	No failure (10/4)	No failure (7/2)
DSP	No Failure (19/0)	431/ 884/ 1555 (5/0)	No failure (9/5)	No failure (6/3)
Overall	No Failure (57/0)	No failure (15/0)	No failure (29/13)	No failure (19/8)

Prediction: No failure.

Experiment outcome: After 36 minutes in the 30 l/s per meter session (1120 waves), the grass cover was washed away initiated by the straight edge. No erosion at the toe is noted.

Verdict: The slope failed at the location of an anomaly that is not incorporated in the method. Modelling of the straight edge by mole-activity showed not to be representative.

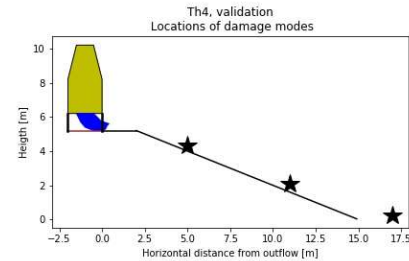


## Tholen section 4 (Th4)

### Input

#### Properties of the experiment

Crest width	2 meter
Crest height	5 meter
Slope	0.395 rad
Control list	2011 Tholen
Discharges	1; 5; 10; 30; 50; 75 l/m/s
Number of waves	5806
Significant wave height	2 meter



#### Input from initial condition registration:

Damage type	Mole	Mole	Toe
Meters from outflow	5	11	After toe

### Output

#### Majority vote

	Baseline	Mole at 5m	Mole at 11m	Toe
No failure	32	15	3	0
Failure	25	27	39	27
Verdict	No failure	Failure	Failure	Failure

Majority vote per model, if failure: lower limit/ mean/ upper limit. In between brackets the number of no-failure and failure predictions (No-failure / failure).

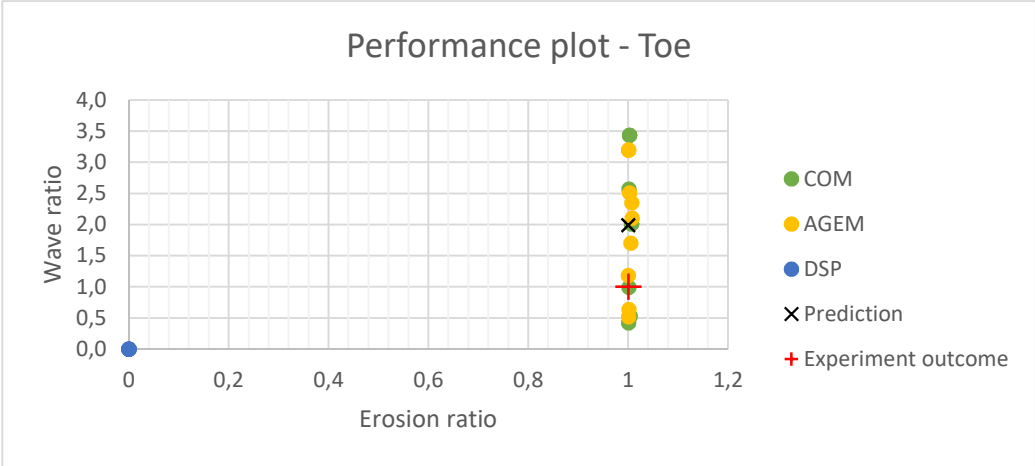
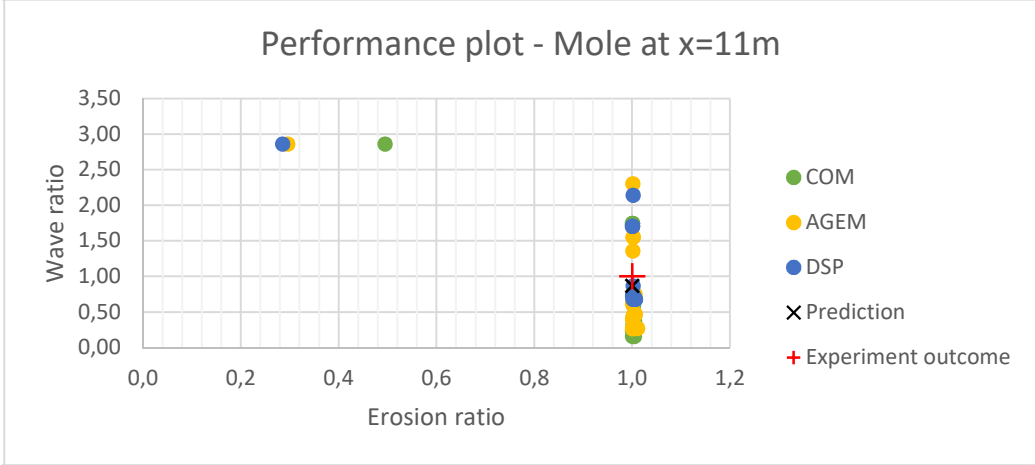
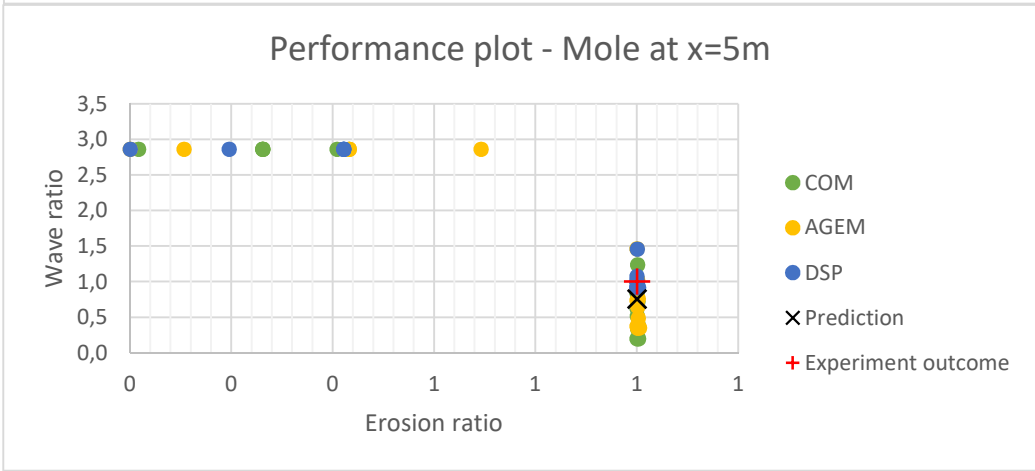
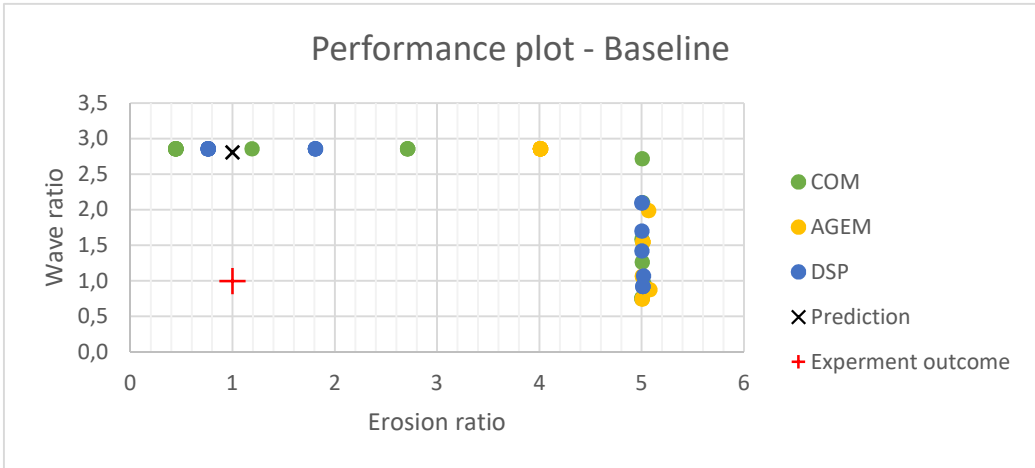
	Baseline	Mole at 5m	Mole at 11m	Toe
COM	No Failure (11/8)	402/ 1155/ 2551 (5/ 9)	319/ 1525/ 3604 (1/ 13)	554/ 2558/ 4534 (0/ 9)
AGEM	No Failure (10/9)	713/ 1418/ 3021 (5/ 9)	547/ 1683/ 4755 (1/ 13)	684/ 2554/ 4225 (0/ 9)
DSP	No Failure (11/8)	1891/2113/3007 (5/ 9)	319/ 1795/ 4419 (1/ 13)	1363/2775/4506 (0/ 9)
Overall	No Failure (32/25)	402/ 1562/ 3021 (15/ 27)	29/ 1209/ 5023 (3/ 39)	544/ 2629/ 4534 (0/ 27)

Prediction: Grass cover failure at 5m and 11m after respectively 1127 and 1209 waves, both in the third 10 l/s per meter session. Toe failure after 1772 waves if the experiment is continued.

Experiment outcome: During the 5l/s per meter sessions erosion was developing just after the toe where a track and mole activity was present. At the end of the last session (1321 waves) the grass cover failed at the toe. After four hours in of 10 l/s per meter almost the entire toe has failed, after 4hr and 45min the session was paused. The damage was mitigated to finish the 10 l/s per meter was continued. While the first 30 l/s per meter session did not change much. One and a half hour into the second session (2065 waves), the experiment was terminated due to large amounts of expelled sand. This showed moments later when a large section of the slope subsided.

#### Verdict:

The failure of due to the mole activity at 11 meter from the outflow did not emerge after 1209 waves, but after 2065 waves when the surrounding slope subsided. The toe strength is predicted too optimistic, since it failed earlier than predicted. In both instances, the method was correct as for locating the failures.



## Appendix H – Critical velocity registration

In the factual report of the tests at the Vechtdijk in 2010, a remark was made during the test on section 3 (Ve3): “Op het talud werden de al aanwezige gaten steeds groter (zie foto 5.12). Opvallend was dat er alleen iets gebeurde bij golven > 1000 l/m en vooral bij golven > 1500 l/m. Met name de erosie in vak 6D versnelde.” Translation: “Present holes on the slope grew (picture 5.12). It was striking that only for large wave volumes things happened, for wave volumes > 1000l/m and especially for > 1500l/m.”

Illustrated in the figure below are the flow velocities computed by the hydrodynamic model, results are shown for the smallest, median a largest waves and additional for a wave volume of 1100 l/m and 1500l/m. Registrations quoted previously give extra insight on which wave volumes and possibly which velocities have the most influence in the erosional process.

